AALBORG UNIVERSITY

Radio Access Technology Section
Department of Electronic Systems

Radio Link Modelling for Relay Deployment in Urban Macro-cells

Ignacio Rodríguez Larrad

Master Thesis / 2010-2011

Long Master Thesis Information

TITLE:
Radio Link Modelling for Relay Deployment in Urban Macro-cells

PROJECT PERIOD:
September 2010 – May 2011

PROJECT GROUP:
Mobile Communication - group 1207

AUTHOR:
Ignacio Rodríguez Larrad

SUPERVISORS:
Troels B. Sørensen
Claudio Coletti
Hung T. Nguyen

Number of pages in report: 73

Number of pages in appendix: 46

Total number of pages: 119

Number of copies printed: 5

ABSTRACT

Relaying is a potential solution to **improve coverage and capacity at cell edge** in **LTE-Advanced**. To achieve this objectives, it is critical to have a **very good connection** in the **backhaul link** between the relay node and the base station. When this is possible, the **overall SINR and throughput** in the network **improve**.

To study this link, a **measurement campaign** was performed in the **urban area** of Aalborg. Based on the results obtained, this study concludes that the use of **relay nodes** is **beneficial** under specific conditions (relay antenna height and type, environment).

Path loss models play an **important role** in the design of cellular systems and **different models can be applied** to characterize the different links in a relayed network so a **comparative with the measurements** was done.

Preface

This Long Master Thesis has been written by Ignacio Rodríguez Larrad (group1207, Mobile Communication) from September 2010 to May 2011 at Aalborg University. It has been possible to execute this project thanks to the collaboration between Radio Access Technology Section (Aalborg University), Nokia Siemens Networks and Telenor.

It has been written in LaTeX and consists of the following chapters: Introduction, Path loss models, Measurement campaign, Data processing, Path loss analysis and Conclusions. All the technical details in the report are supported with different appendixes.

MATLAB has been used to create graphics and give support to the different calculations performed.

Literature references follow IEEE recommendations. Texts, figures and tables are referenced using a number in brackets which indicates the position in the reference list:

Quoted text [Reference Number]
Figure (number): Figure Description [Reference Number]
Table (number): Table Description [Reference Number]

Ignacio Rodríguez Larrad - Mobile Communication
Aalborg University, 31st May, 2011

Acknowledgments

First of all, the author would like to acknowledge Aalborg University, and especially Radio Access Technology Section for the scholarship and the opportunity of participating in a challenging and interesting project.

Secondly, the author would like to thank his supervisors Troels B. Sørensen, Claudio Coletti, Hung T. Nguyen for their continuous assistance effort and guidance during the whole project and specially for their help with the measurement campaign.

Thanks to Nokia Siemens Networks and Telenor for their collaboration, which made this project possible.

Thanks to Kim Olesen and Kristian Bank from the laboratory, for their initial help with the scanner and the nice setup on the van for the measurements.

Thanks to Niels Jørgensen from Nokia Siemens Networks for his help during the hard measurement campaign in February with negative temperatures and snow covering the streets.

The author would like to make a special mention to Lucas Alados, Javier Gallardo and Carlos Yáñez for all the good moments lived at room A6-127. Also Sara Meseguer, Marta Pérez-Regadera, Francisco Galvañ and Mario Muñoz should be included in this special mention for their continuous visits in the room.

Finally, but not less important, the author would like to thank to all his family and friends for their continuous support along all this years.

Contents

List of Figures

List of Tables

Abbreviation List

ART	Above-Roof-Tops
BRT	Below-Roof-Tops
BS	Base Station
BP	Break-point
COST	Europen Cooperation in Science and Technology
CPICH	Common Pilot Channel
dB	Decibel
dBi	Decibel-Isotropic
dBm	Decibel-mili-Watt
dec	Decade
deg	Degree
E-UTRA	Evolved Universal Terrestrial Radio Access
FS	Free Space
FDD	Frequency Division Duplex
GPS	Global Positioning System
GSM	Global System for Mobile Communications
Hz	Hertz
h	Hour
IEEE	Institute of Electrical and Electronic Engineers
IN-BB	In-between buildings
ISD	Inter-Site distance
LOS	Line-of-Sight
LTE	Long Term Evolution
m	Meter
NLOS	Non-Line-of-Sight
prob	Probability
RF	Radio Frequency
RN	Relay Node
RX	Receiver
SF	Spreading Factor
STL	Street-Level
s	Second
TX	Transmitter
UARFCN	UTRA Absolute Radio Frequency Channel Number
UE	User Equipment

UMTS	Universal Mobile Telecommunications System
UTRA	Universal Terrestrial Radio Access
WCDMA	Wideband Code Division Multiple Access
WI	Walfisch-Ikegami
WiMAX	Worldwide Interoperability for Microwave Access
WINNER	Wireless World Initiative New Radio
3GPP	Third Generation Partnership Project
$^\circ$	Degree

Symbol List

BW	Bandwidth [Hz]
c	Speed of Light [$3 \cdot 10^8$ m/s]
d	Distance [m]
f	Frequency [Hz]
f_c	Carrier Frequency [Hz]
$FSPL$	Free Space Path Loss [dB]
G	Gain [dB]
h	Heigth [m]
IHG	Interference Height Gain [dB]
ITG	Interference Type Gain [dB]
$ISCP$	Interference Signal Code Power [dBm]
L	Loss [dB]
$MPLHG$	Measured Path Loss Height Gain [dB]
NF	Noise Figure [dB]
P	Power [dBm]
P_{rx}	Received Power [dBm]
P_{tx}	Transmitted Power [dBm]
PHG	Power Height Gain [dB]
PL	Path Loss [dB]
PTG	Power Type Gain [dB]
PSD	Power Spectral Density [dBm/Hz]
$RSCP$	Received Signal Code Power [dBm]
$RSSI$	Received Signal Strength Indicator [dBm]
$SINR$	Signal to Interference-Noise Ratio [dB]
SIR	Signal to Interference Ratio [dB]
$SIRHG$	Signal to Interference Height Gain [dB]
$SIRTG$	Signal to Interference Type Gain [dB]
SNR	Signal to Noise Ratio [dB]
t	Time [s]
TP	Throughput [bps]
TP_{eff}	Effective Throughput [bps]
λ	Wavelength [m]

"There are two possible outcomes: if the result confirms the hypothesis, then you've made a measurement. If the result is contrary to the hypothesis, then you've made a discovery."

Enrico Fermi (Physicist)

Chapter 1

INTRODUCTION

1.1 Motivation

Over last years, the number of users in cellular networks has increased considerably. Also the demand for higher mobile broadband data traffic make these networks to need to be updated. Considering that network coverage is a crucial issue when higher frequencies are used for transmission, the deployment of low-cost and low-power Relay Node [1] can be considered as an interesting solution to improve network coverage at the cell edge and in severely shadowed environments. [2] [3]

By deploying relay nodes, the distance between base stations and user equipment is split into two (or more) hops, as can be seen in Figure 1.1. With this setup, the overall path loss over the link is reduced.

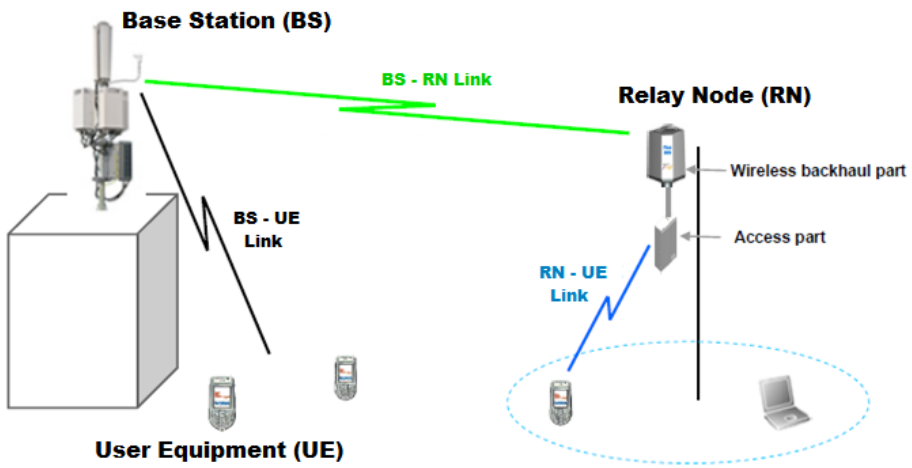

Figure 1.1: Different transmission links considered in a Relay Enhanced Cellular Network.

Often the link model in deployment studies is simplified so that only the link between the relay node and the user equipment is actually modelled with confidence. Existing propagation models for below rooftop base station can often be applied on this link, given that relay nodes are typically positioned close to street level (i.e. lamp post height).
The problem comes out when modelling the link between the relay node and the base station (BS - RN Link in Figure 1.1). It is especially difficult to apply jointly consistent models for the two links (BS-RN Link and RN-UE Link) and towards different base stations for accurate signal to interference modelling.

Some of the issues complicating the modelling are the use or assumption of planned relay node positions and/or directional characteristics on the link between base station and relay node. In fact, site planning is generally needed to boost the performance of this link so that it does not act as a bottleneck for the relay access link transmission.

1.2 Background

High data rates and spectral efficiency, in addition to a suitable coverage are main objectives of future wireless and mobile communication systems. To simultaneously satisfy this requirements, LTE-Advanced expects to offer peak data rates of 1 Gbps in downlink and 500 Mbps in uplink, as well as bandwidth scalability up to 100 MHz and improved cell edge performance among other objectives. [4]

To solve the propagation issues over high frequencies explained before, accomplishing the different objectives planned in LTE-Advanced, there are several possible solutions:

- Increase transmitted power in base stations and user equipment: more transmitted power will lead int a higher interference, decreased battery lifetime in user equipment and an increase of the cost. Apart from this, introducing more power could be difficult due to the RF limitations in the base station.
- Macro base station intensification: by introducing more base stations in the network, deployment and maintenance costs increases, there will be more interference so there is no cell edge performance enhancement.
- Relay nodes (RN): relay nodes located at cell edge can improve the low SINR experienced by users and minimize the cell outage.

Relay nodes should be a feasible solution since they are low cost and low power nodes reducing the overall path loss as explained before. LTE-Advanced implements OFDMA in the downlink which is flexible enough for resource allocation.

On the other hand, they introduce extra delay and overhead in the communication so it is really important to manage interference and resource partitioning.

According to their operation mode it is possible to distinguish different types of relays. The most reliable thought right now is to think that relay nodes will work as inband, decode and forward, one-way relays. This means relay nodes with a single parent base station performing half-duplex transmission assuming that all base stations transmit at the same time, frequency, and power. Each relay decodes the information from the base station, and recodes it for sending to the user equipment. Inband means that the access link works on the same frequency as the backhaul link. [1]

1.3 Objectives

Since the main objective in this project is to study the different links explained in Section 1.1, focusing on the backhaul link between base station and a potential relay node, many questions came out.

It is necessary to study a potential relay deployment in order to obtain the best performance. It will be investigated if the analyzed link is better at lower heights or at higher heights, or the different behavior of the link in terms of signal to interference ratio (signal quality) when using a directional or an omnidirectional antenna at the relay part.

Based on measurements it would be possible to extract some conclusions about the most favorable position for the relay node in a real urban macro-cell network and get an idea of the path loss introduced in the link.

To cover all this aspects, the following steps are covered in this report:

- Research on existing path loss models (specific and non-specific for relay deployment).
- Analysis of the impact of the different path loss models on typical network parameters. System level simulation.
- Measurement campaign.
- Statistical analysis of measured data: signal quality and most favorable relay node location.
- Path loss estimation and comparison with the actual models.

1.4 Guidelines

This report is divided in 6 chapters as following:

Chapter 1: Introduction.

Chapter 2: Path Loss Models: introduces the different existing path loss models. A comparison between them is done for the different links and completed with an evaluation of their impact on system level parameters such as SINR or throughput.

Chapter 3: Measurement Campaign: summarizes the most important facts related with the campaign conducted in the urban area of Aalborg.

Chapter 4: Data Processing: analyzes different backhaul characteristics comparing measured signals at different heights and different types of antennas. Also some guidelines about most favorable relay location are given.

Chapter 5: Path Loss Analysis: explains how it is possible to extract path loss values from the measured samples.

Chapter 6: Conclusions and Future work: summarizes the main results obtained. Some guidelines for future measurement campaigns are also given.

Different appendixes give support to the chapters in the main text:

Appendix A: System Level Simulation: shows the results obtained in a network simulation performed in MATLAB. It takes into account different path loss models and calculate important network performance parameters.It is related to Chapter 2.

Appendix B: Equipment Information: collects all the details of the setup performed to run the measurement campaign. It is straightly related to Chapter 3.

Appendix C: Measured Signal: gives an idea of the measured signal. Some basics on UMTS are included and differences with LTE are explained. It gives support to Chapter and Chapter 4.

Appendix D: Processing Details: gives support to Chapter 4 and Chapter 5 calculations. It gathers some plots explaining the analysis performed.

Appendix E: Vertical Gain Correction: gives support to Chapter 6 calculations introducing a correction factor applicable in particular urban macro-cell environments.

Chapter 2

PATH LOSS MODELS

Propagation path loss models play an important role in the design of cellular systems as they are used in the typical initial network design to determine the number of sites necessary to provide enough coverage and predict possible interference problems.

As relays are relatively new elements, it is not clear yet which model is suitable to predict its place inside the network. Path loss models are proposed for cellular systems operating in different environments (urban, suburban, rural, indoor, outdoor) and many of them impose their own conditions which is also a problem considering new technologies as 3GPP LTE-Advanced working at frequencies over 2 GHz where only a few models are available.

In this chapter, a definition of path loss is given and some different existing models are explained and used to characterize the links in a relayed network. At the end, a comparison between these models and its influence on network system level design is performed.

2.1 Path Loss

Path loss (PL) is also know as path attenuation. It is a reduction in power density of an electromagnetic wave propagating in space. Focusing on a wireless communication system it can be defined as a dimensionless parameter which represents the difference between transmitted power (P_{tx}) and received power (P_{rx}).

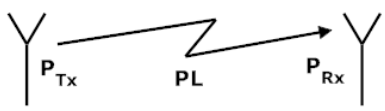

Figure 2.1: Path Loss definition.

$$PL = P_{tx} - P_{rx} \tag{2.1}$$

Path loss can be predicted by using models which take into account specific system parameters such as frequency, antenna heights, ... Some of the existing models were derived in an statistical manner based on field measurements while other are developed analytically based on diffraction effects. [5]

Equation 2.2 can be defined as a first approach to an empirical Path Loss model: [6]

$$PL = PL(d_0) + 10 \cdot n \cdot log_{10}\left(\frac{d}{d_0}\right) + d + X_\sigma \tag{2.2}$$

In this equation, $PL(d_0)$ is the measured or predicted Path Loss at distance d_0 (normally, calculated with Equation 2.3 in free space conditions), n is the Path loss exponent (indicates how quickly the signal attenuates as function of distance). c is an offset correction factor (constant offset between the reference model and the measurements) and X_σ is a random variable describing the shadow fading deviation from the mean Path loss value.

$$PL(d_0) = FSPL(d_0) = 20\, log_{10}\left(\frac{4\pi\, d_0}{\lambda}\right) \tag{2.3}$$

Free space conditions are taking into account line of sight path through free space (usually air) with no obstacles nearby to cause reflection or diffraction.

2.2 Model description

As it can be seen in Equation 2.2, path loss is highly dependent on distance. Long distance prediction models intended for macrocell systems use base station and mobile station antenna heights and frequency while short distance prediction models (for microcells) uses also other parameters such as building heights, streets width and orientation, ... describing the environment. For really small distances (in the range of 10 to 100 m), deterministic models based on Ray-Tracing tools are used (depending on processing power and availability of GIS (Geographic Information System) data). [5]

This report will focus on some different macrocell and microcell models which, in principle, could be used to characterize the links in a relayed network detailed in Section 1.1. Shadow fading will not be taken into account, the analysis will just focus on mean path loss values.

Models are described in the following sections [1].

2.2.1 COST-HATA

Hata's model is an overal statistic model based on Okumura's correction functions [7]. It was designed to predictpPath loss where land cover is known roughly. In principle, it is valid in large and small macrocells but not in microcells. This model does not capture the geometrical properties of the environment (see the parameters contained in the Okumura-Hata in Table 2.1) and it is not recommended for base station below rooftops. [8]

PARAMETER	DESCRIPTION
f	Frequency [MHz]
d	Distance [km]
h_{BS}	BS height [m]
h_{UE}	UE height [m]
C_m	Clutter correction factor [dB]

Table 2.1: Parameters in COST-HATA model.

The restrictions to the Okumura-Hata model are:

$$150\,MHz \leq f \leq 1500\,MHz$$
$$1\,km \leq d \leq 20\,km$$
$$30\,m \leq h_{BS} \leq 200\,m$$
$$1\,m \leq h_{UE} \leq 10\,m$$

So, according to the previous factors and conditions, path loss in an urban area is calculated as follows:

$$\begin{aligned} PL &= 69.55 + 26.16\,log_{10}\left(\frac{f}{MHz}\right) - 13.82\,log_{10}\left(\frac{h_{BS}}{m}\right) - a(h_{UE}) + \\ &+ \left\{44.9 - 6.55\,log_{10}\left(\frac{h_{BS}}{m}\right)\right\} log_{10}\left(\frac{d}{km}\right) \end{aligned} \tag{2.4}$$

[1] Each model uses its own notation. To keep it clear, a table explaining all the different parameters is included at the beginning of the description of each model.

$$a(h_{UE}) = \left\{1.1\,log_{10}\left(\frac{f}{MHz}\right) - 0.7\right\}\left(\frac{h_{UE}}{m}\right) - \left\{1.56\,log_{10}\left(\frac{f}{MHz}\right) - 0.8\right\} \quad (2.5)$$

As the inital Okumura-Hata model was valid only in the range between 150 MHz and 1500 MHz, COST 231 proposed an extension for higher frequencies up to 2000 MHz [8]. The rest of conditions in this COST-Hata model remain as stated before.

$$1500\,MHz \leq f \leq 2000\,MHz$$

$$\begin{aligned} PL &= 46.3 + 33.9\,log_{10}\left(\frac{f}{MHz}\right) - 13.82\,log_{10}\left(\frac{h_{BS}}{m}\right) - a(h_{UE}) + \\ &+ \left\{44.9 - 6.55\,log_{10}\left(\frac{h_{BS}}{m}\right)\right\} log_{10}\left(\frac{d}{km}\right) + C_m \end{aligned} \quad (2.6)$$

$$C_m = \begin{Bmatrix} 0dB & \text{medium sized cities / suburban centres} \\ 3dB & \text{metropolitan centres} \end{Bmatrix} \quad (2.7)$$

2.2.2 COST-WALFISCH-IKEGAMI

COST 231 proposed a combination of Walfisch and Ikegami models including more parameters to characterize the urban environment (they can be seen in Table 2.2). It is a non deterministic statistical model (as COST-Hata, it only uses characteristic values, no topographical data is considered). It does not take into account multipath and it is reliable for homogeneous land cover. [8]

PARAMETER	DESCRIPTION
f	Frequency [MHz]
d	Distance [km]
h_{BS}	BS height [m]
h_{UE}	UE height [m]
h_{roof}	UE height [m]
w	Road width [m]
b	Building separation [m]
φ	Road orientation respect to the direct radio path [°]

Table 2.2: Parameters in COST-WI model.

The restrictions to the COST-Walfisch-Ikegami model are:

$$800\,MHz \leq f \leq 2000\,MHz$$
$$20\,m \leq d \leq 5\,km$$
$$4\,m \leq h_{BS} \leq 50\,m$$
$$1\,m \leq h_{UE} \leq 3\,m$$

The model distinguishes between Line-of-Sight and Non-Line-of-Sight situations:

LOS

LOS situations between the base station and the user equipment are described in this model as simple propagation along a street canyon. Path loss is based on measurements taken in the city of Stockholm:

$$PL_{LOS} = 42.6 + 26\,log_{10}\left(\frac{d}{km}\right) + 20\,log_{10}\left(\frac{f}{MHz}\right) \tag{2.8}$$

NLOS

NLOS situations are modeled as diffraction over multiple screens (buildings). In this case, free space loss (L_0), multiple screen diffraction loss (L_{msd}) and rooftop to street level diffraction and scatter loss are considered (L_{rts}):

$$PL_{NLOS} = \begin{Bmatrix} L_0 + L_{rts} + L_{msd} & L_{rts} + L_{msd} > 0 \\ L_0 & L_{rts} + L_{msd} \leq 0 \end{Bmatrix} \tag{2.9}$$

$$L_0 = 32.4 + 20\,log_{10}\left(\frac{d}{km}\right) + 20\,log_{10}\left(\frac{f}{MHz}\right) \tag{2.10}$$

L_{msd} and L_{rts} are taking into account environment parameters (w, b, h_{roof}) and street orientation (φ) as indicated in Figures 2.2 and 2.3.

$$\begin{aligned} L_{rts} = & -16.9 - 10\,log_{10}\left(\frac{w}{m}\right) + 10\,log_{10}\left(\frac{f}{MHz}\right) + \\ & +20\,log_{10}\left(\frac{\Delta h_{UE}}{m}\right) + L_{ori} \end{aligned} \tag{2.11}$$

$$L_{ori} = \begin{Bmatrix} -10 + 0.354\left(\frac{\varphi}{deg}\right) & 0^\circ \leq \varphi < 35^\circ \\ 2.5 + 0.075\left(\frac{\varphi}{deg} - 35\right) & 35^\circ \leq \varphi < 55^\circ \\ 4 - 0.114\left(\frac{\varphi}{deg} - 55\right) & 55^\circ \leq \varphi < 95^\circ \end{Bmatrix} \tag{2.12}$$

$$\Delta h_{UE} = h_{roof} - h_{UE} \tag{2.13}$$

$$\Delta h_{BS} = h_{BS} - h_{roof} \tag{2.14}$$

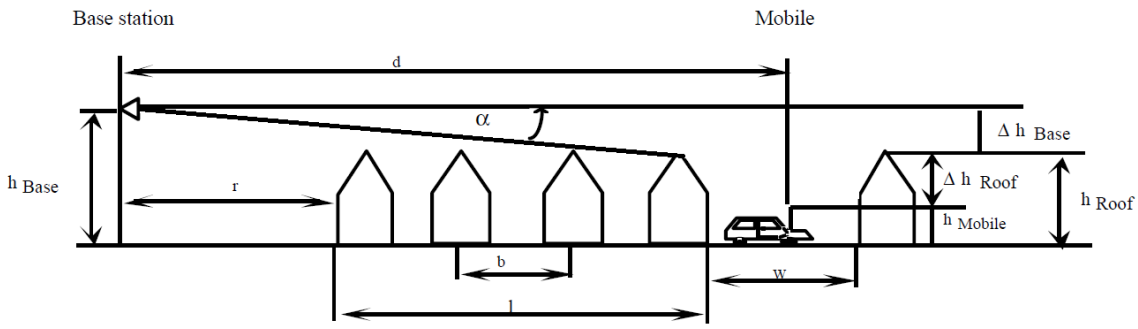

Figure 2.2: Typical propagation situation and parameter definition in COST-WI model. [8]

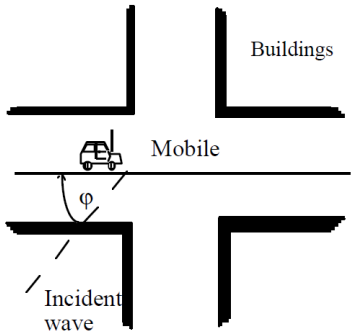

Figure 2.3: Street orientation definition in COST-WI model. [8]

Originally, Walfisch and Bertoni approximated the solution for multi-screen diffraction for base station antennas above rooftops, but COST extended the model to below rooftops based on measurements:

$$L_{msds} = L_{bsh} + K_a + K_d \cdot 10\,log_{10}\left(\frac{d}{km}\right) + K_f \cdot 10\,log_{10}\left(\frac{f}{MHz}\right) + \\ -9\,log_{10}\left(\frac{b}{m}\right) + L_{ori} \tag{2.15}$$

$$L_{bsh} = \begin{Bmatrix} -18log_{10}\left(1 + \frac{\Delta h_{BS}}{m}\right) & h_{BS} > h_{roof} \\ 0 & h_{BS} \leq h_{roof} \end{Bmatrix} \tag{2.16}$$

$$K_a = \begin{Bmatrix} 54 & h_{BS} > h_{roof} \\ 54 - 0.8\left(\frac{\Delta h_{BS}}{m}\right) & d \geq 0.5km, h_{BS} \leq h_{roof} \\ 54 - 0.8\left(\frac{\Delta h_{BS}}{m}\right)\left(\frac{d/km}{0.5}\right) & d < 0.5km, h_{BS} \leq h_{roof} \end{Bmatrix} \tag{2.17}$$

$$K_d = \begin{Bmatrix} 18 & h_{BS} > h_{roof} \\ 18 - 15\left(\frac{\Delta h_{BS}}{h_{roof}}\right) & h_{BS} \leq h_{roof} \end{Bmatrix} \tag{2.18}$$

$$K_f = \begin{Bmatrix} -4 + 0.7\left(\frac{f/MHz}{925} - 1\right) & \text{medium sized cities, suburban centres} \\ 1.5\left(\frac{f/MHz}{925} - 1\right) & \text{metropolitan centres} \end{Bmatrix} \tag{2.19}$$

$$h_{roof} = 3\,m \times \text{number of floors} + \begin{Bmatrix} 3\,m & \text{pitched} \\ 0 & \text{flat} \end{Bmatrix} \tag{2.20}$$

LOS/NLOS

In other studies, single snapshots of LOS or NLOS are considered; however, in this report, to keep a general overview on path loss models, it is considered necessary to specify a joint model between LOS and NLOS model following Equation 2.21. This will be done also for some of the other LOS/NLOS models later on.

$$\begin{aligned} PL &= prob(LOS) \cdot PL_{LOS} + prob(NLOS) \cdot PL_{NLOS} \\ &= prob(LOS) \cdot PL_{LOS} + (1 - prob(LOS))\,PL_{NLOS} \end{aligned} \tag{2.21}$$

Normally, the joint LOS/NLOS Path Loss model is considering a specific LOS probability in function of the distance to the base station (see Figure 2.4). In this case, the probability is defined as a step jumping from the LOS model to the NLOS model at a certain distance related to the heights of the buildings surrounding the base station. [9]

$$prob(LOS) = \left\{ \begin{array}{ll} \frac{h_{BS}-h_{roof}}{h_{BS}} \frac{d_{c0}-d}{d_{c0}} & d < d_{c0}, h_{BS} > h_{roof} \\ 0 & d \geq d_{c0}, h_{BS} \leq h_{roof} \end{array} \right\} \tag{2.22}$$

$$d_{c0} = 500\,m \tag{2.23}$$

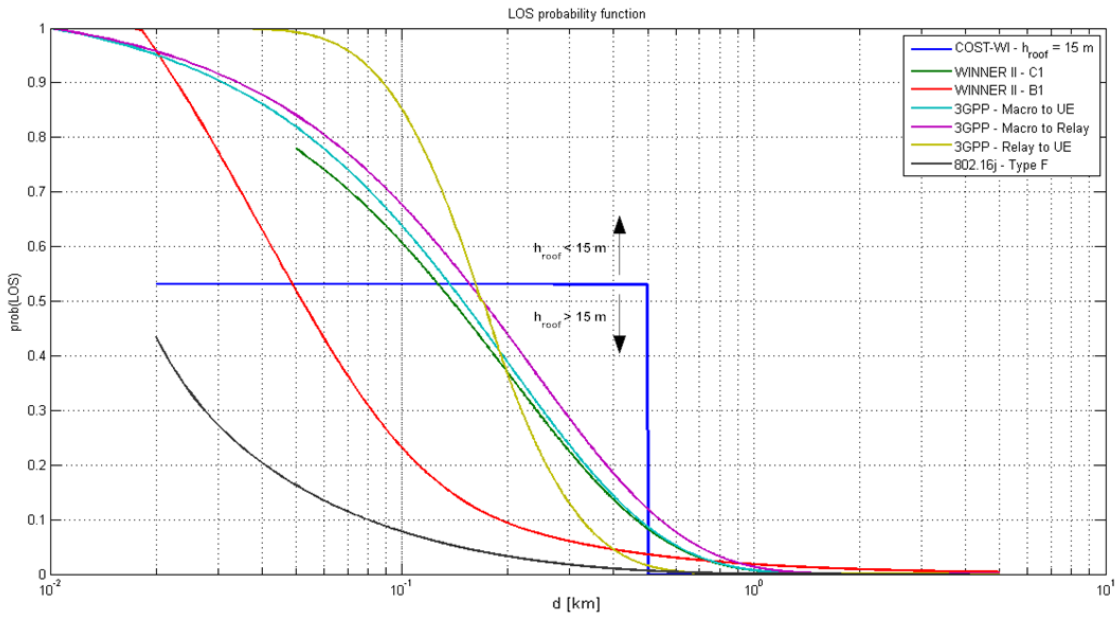

Figure 2.4: LOS Probability in terms of distance for some of the models under analysis.

COST-Walfisch-Ikegami is a good model for above rooftops and $h_{BS} >> h_{roof}$. As h_{roof} increases, a large error is obtained.

2.2.3 WINNER II D1.1.2

This section tries to gather some of the channel models for link and system level simulations described in WINNER II. These models describe different propagation scenarios (indoor, office, indoor-to-outdoor, outdoor-to-indoor, urban macrocell, urban microcell, stationary feeder, suburban macrocell,...) and follow a geometry-based stochastic channel modelling

approach. They are based on measurements and different results from literature. [10]

These models can be applied in the frequency range from 2 GHz to 6 GHz and are defined in some specific conditions.

PARAMETER	DESCRIPTION
f	Frequency [GHz]
d	Distance [m]
h_{BS}	BS height [m]
h_{RN}	RN height [m]
h_{UE}	UE height [m]

Table 2.3: Parameters in WINNER II models.

Model C1

This model is valid for suburban macrocells with base station antenna above rooftops and user equipment placed at street level. Buildings are typically low residential blocks of flats with a few floors. [10]

It is defined for LOS, NLOS and combined LOS/NLOS conditions.

These are the restrictions to this WINNER II - C1 model:

$$2\,GHz \leq f \leq 6\,GHz$$
$$10\,m < d < 5\,km$$
$$h_{BS} = 25\,m$$
$$h_{UE} = 1.5\,m$$

LOS

In LOS conditions, the model is defined as a two-slope model based on the two-ray ground reflection model with a certain slope (path loss exponent) for points nearby the base station until the breakpoint distance defined in Equation 2.24 (around 1 km, where Hata model does not apply) and other for larger distances when LOS is less present.

$$d_{BP} = 4\,h_{BS}\,h_{UE}\frac{f}{c} \tag{2.24}$$

So according to this, for shorter distances ($10\,m < d < d_{BP}$):

$$PL_{LOS} = 23.8\,log_{10}\left(\frac{d}{m}\right) + 41.2 + 20\,log_{10}\left(\frac{f/GHz}{5}\right) \tag{2.25}$$

And for longer distances ($d_{BP} \leq d < 5\,km$):

$$\begin{aligned} PL_{LOS} &= 40.0\,log_{10}\left(\frac{d}{m}\right) + 11.65 - 16.2\,log_{10}\left(\frac{h_{BS}}{m}\right) - 16.2\,log_{10}\left(\frac{h_{UE}}{m}\right) + \\ &+3.8\,log_{10}\left(\frac{f/GHz}{5}\right) \end{aligned} \tag{2.26}$$

NLOS

For NLOS conditions, the model is defined as a single-slope model but restricted to distances longer than 50 m:

$$50\,m \leq d < 5\,km$$

$$\begin{aligned} PL_{NLOS} &= \left(44.9 - 6.55\,log_{10}\left(\frac{h_{BS}}{m}\right)\right) log_{10}\left(\frac{d}{m}\right) + 31.46 + 5.83\,log_{10}\left(\frac{h_{UE}}{m}\right) + \\ &+23\,log_{10}\left(\frac{f/GHz}{5}\right) \end{aligned} \tag{2.27}$$

LOS/NLOS

To define a combined LOS/NLOS model, it is possible to proceed in the same way as before in COST-WI model. LOS probability is defined in terms of distance. This probability function can be seen in Figure 2.4.

$$prob(LOS) = e^{-\frac{d/m}{200}} \tag{2.28}$$

Model B5c

WINNER II - B5c in an actual relay model. It defines a LOS situation for a stationary feeder in a macro-cellular case, from below rooftop to street level [10]. It is only valid for specific heights of the base station and the relay node. It is similar to WINNER II - B1 model LOS (two-slope model with breakpoint distance definition) that will be defined later.

These are the restrictions to this model:

$$2\,GHz \leq f \leq 6\,GHz$$
$$10\,m < d < 5\,km$$
$$h_{BS} = 10\,m$$
$$h_{RN} = 5\,m$$

LOS

This is also a breakpoint two-slope model, and it is defined as follows:

$$d'_{BP} = 4\,h'_{BS}\,h'_{RN}\frac{f}{c} \tag{2.29}$$

$$h'_{BS} = h_{BS} - 1.0\,m \tag{2.30}$$

$$h'_{RN} = h_{RN} - 1.0\,m \tag{2.31}$$

For distances shorter than the breakpoint distance ($10\,m < d < d'_{BP}$):

$$PL_{LOS} = 22.7\,log_{10}\left(\frac{d}{m}\right) + 41.0 + 20\,log_{10}\left(\frac{f/GHz}{5}\right) \tag{2.32}$$

For distance longer than the breakpoint distance ($d'_{BP} \leq d < 5\,km$):

$$PL_{LOS} = 40.0\,log_{10}\left(\frac{d}{m}\right) + 9.45 - 17.3\,log_{10}\left(\frac{h'_{BS}}{m}\right) - 17.3\,log_{10}\left(\frac{h'_{RN}}{m}\right) + \\ +2.7\,log_{10}\left(\frac{f/_{GHz}}{5}\right) \tag{2.33}$$

Model B1

This model represents a typical urban microcell, where both antennas (from the relay node and the user equipment) are placed below rooftops. It is assumed for this definition, that the streets are laid out in a Manhattan-like grid. LOS conditions are referred for the main street and NLOS is considered in perpendicular streets and specific cases where LOS is blocked in the main street. [10]

LOS

These are the restrictions in LOS conditions along the main street:

$$2\,GHz \leq f \leq 6\,GHz$$
$$10\,m < d < 5\,km$$
$$h_{RN} = 10\,m$$
$$h_{UE} = 1.5\,m$$

$$d''_{BP} = 4\,h''_{RN}\,h''_{UE}\frac{f}{c} \tag{2.34}$$

$$h''_{RN} = h_{RN} - 1.0\,m \tag{2.35}$$

$$h''_{UE} = h_{UE} - 1.0\,m \tag{2.36}$$

For distances shorter than the breakpoint distance ($10\,m < d < d''_{BP}$):

$$PL_{LOS} = 22.7\,log_{10}\left(\frac{d}{m}\right) + 41.0 + 20\,log_{10}\left(\frac{f/_{GHz}}{5}\right) \tag{2.37}$$

For distance longer than the breakpoint distance ($d''_{BP} \leq d < 5\,km$):

$$PL_{LOS} = 40.0\,log_{10}\left(\frac{d}{m}\right) + 9.45 - 17.3\,log_{10}\left(\frac{h''_{RN}}{m}\right) - 17.3\,log_{10}\left(\frac{h''_{UE}}{m}\right) + \\ +2.7\,log_{10}\left(\frac{f/GHz}{5}\right) \tag{2.38}$$

NLOS

The NLOS in this model has different application conditions, as different distances ($d1$, $d2$) along the main and the perpendicular streets are taken into account (see Figure 2.5). As in COST-WI model, w is defining the width of the roads.

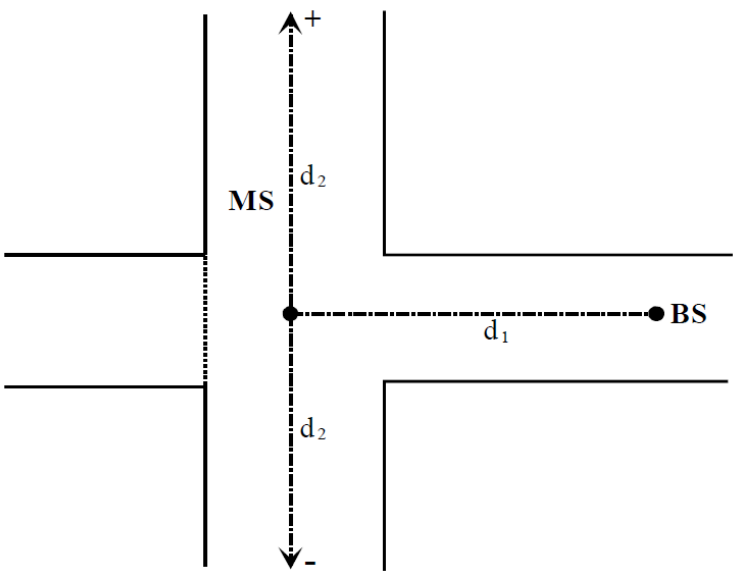

Figure 2.5: Geometry for d1 and d2 in NLOS Path Loss models. [10]

$$10\,m \leq d_1 < 5\,km$$
$$w/2 \leq d_2 < 2\,km$$
$$w = 20\,m$$
$$h_{RN} = 10\,m$$
$$h_{UE} = 1.5\,m$$

$$PL_{NLOS} = min\,(PL_f(d_1, d_2), PL_f(d_2, d_1)) \tag{2.39}$$

$$PL_f(d_k, d_i) = PL_{LOS}(d_k) + 20 - 12.5 \cdot n_k + 10 \cdot n_k \, log_{10}\left(\frac{d_i}{m}\right) + \\ +3 \, log_{10}\left(\frac{f/GHz}{5}\right) \tag{2.40}$$

$$n_k = max(2.8 - 0.0024 \cdot d_k, 1.84) \tag{2.41}$$

LOS/NLOS

As other models before, it is possible to define a joint model for LOS/NLOS condition in terms of LOS propability and distance. The function relating LOS probability and distance for this model is defined in Equation 2.42 and is compared with other models in Figure 2.4.

$$prob(LOS) = min\left(\frac{18}{d/m}, 1\right)\left(1 - e^{-\frac{d/m}{36}}\right) + e^{-\frac{d/m}{36}} \tag{2.42}$$

2.2.4 3GPP TR 36.814 V9.0.0

The 3GPP TR 36.814 V9.0.0, Release 9, covers advancements for E-UTRA physical layer aspects. In the document, there are defined specific outdoor relay models for macrocell environments. The models are specified for a frequency of 2 GHz in urban (Case 1) and suburban/rural environments (Case 3) [11]. In this report, only the models for Case 3 will be summarized. All of them are set up for specific heights of the Base Station ($h_{BS} = 32\,m$), Relay Node ($h_{RN} = 5\,m$) and user Equipment ($h_{UE} = 1.5\,m$).

PARAMETER	DESCRIPTION
d	Distance [km]

Table 2.4: Parameters in 3GPP models.

All of the 3GPP models detailed below are described in terms of distance for LOS, NLOS and combined LOS/NLOS conditions. As before, the LOS probability can be compared with other models in Figure 2.4.

Macro to UE

This model describes the path loss for the direct link between base station and user equipment:

$$f = 2\,GHz$$
$$h_{BS} = 32\,m$$
$$h_{UE} = 1.5\,m$$

LOS

$$PL_{LOS} = 103.4 + 24.2\,log_{10}\left(\frac{d}{km}\right) \tag{2.43}$$

NLOS

$$PL_{NLOS} = 131.1 + 42.8\,log_{10}\left(\frac{d}{km}\right) \tag{2.44}$$

LOS/NLOS

$$prob(LOS) = e^{-\frac{d/km-0.01}{0.2}} \tag{2.45}$$

Macro to Relay

For the link between base station and relay node:

$$f = 2\,GHz$$
$$h_{BS} = 32\,m$$
$$h_{RN} = 5\,m$$

LOS

$$PL_{LOS} = 100.7 + 23.5\,log_{10}\left(\frac{d}{km}\right) \tag{2.46}$$

NLOS

$$PL_{NLOS} = 125.2 + 36.3\, log_{10}\left(\frac{d}{km}\right) \tag{2.47}$$

LOS/NLOS

$$prob(LOS) = e^{-\frac{d/km - 0.01}{0.23}} \tag{2.48}$$

Relay to UE

The path loss in the access link (relay node to user equipment) is defined for an IN-BAND situation (the base station uses the same carrier frequency in the backhaul link (base station to relay node) and in the access link) [11]:

$$f = 2\, GHz \text{ (INBAND)}$$
$$h_{RN} = 5\, m$$
$$h_{UE} = 1.5\, m$$

LOS

$$PL_{LOS} = 103.8 + 20.9\, log_{10}\left(\frac{d}{km}\right) \tag{2.49}$$

NLOS

$$PL_{NLOS} = 145.4 + 37.5\, log_{10}\left(\frac{d}{km}\right) \tag{2.50}$$

LOS/NLOS

$$prob(LOS) = 0.5 - min\left(0.5, e^{-\frac{3}{d/km}}\right) + min\left(0.5, 3 \cdot e^{-\frac{d/km}{0.095}}\right) \tag{2.51}$$

2.2.5 IEEE 802.16j

The IEEE 802.6j (WiMAX - Multihop relay systems) standard contains some basic path loss models valid in different conditions (indoor or outdoor, urban or suburban, LOS or NLOS, above or below rooftops). [12]

PARAMETER	DESCRIPTION
f	Frequency [MHz]
d	Distance [m]
h_{BS}	BS height [m]
h_{RN}	RN height [m]
h_{UE}	UE height [m]
φ	Road orientation respect to the direct radio path [°]

Table 2.5: Parameters in IEEE 802.16j models.

Type B

This model is applied in the direct link between base station and user equipment. It is valid for suburban environments and considers the typical transmission where the base station antenna is placed above rooftops while the user equipment antenna is below rooftops [12]. The model is defined according to different clutter densities, and for these analysis it has been chosen to be intermediate path loss condition. It is a two-slope model, and for short distances it follows the free space model.

It is restricted to:

$$d > d_0 = 100\,m$$
$$10\,m \leq h_{BS} \leq 80\,m$$
$$2\,m \leq h_{UE} \leq 10\,m$$

$$PL = \left\{ \begin{array}{cc} 20\,log_{10}\left(\frac{4\pi\,d/m}{\lambda}\right) & d \leq d'_0 \\ A + 10 \cdot \gamma\,log_{10}\left(\frac{d/m}{100}\right) + \Delta PL_f + \Delta PL_h & d > d'_0 \end{array} \right\} \tag{2.52}$$

$$d'_0 = d_0 \cdot 10^{\left(-\frac{\Delta PL_f + \Delta PL_h}{\lambda}\right)} \tag{2.53}$$

$$A = 20\,log_{10}\left(\frac{4\pi\,d_0/m}{\lambda}\right) \tag{2.54}$$

$$\gamma = 4 - 0.0065 h_{BS} + \frac{17.1}{h_{BS}} \tag{2.55}$$

$$\Delta PL_f = 6\, log_{10}\left(\frac{f/_{MHz}}{2000}\right) \tag{2.56}$$

$$\Delta PL_h = \begin{Bmatrix} -10\, log_{10}\left(\frac{h_{UE}/m}{3}\right) & h_{UE} \leq 3\, m \\ -20\, log_{10}\left(\frac{h_{UE}/m}{3}\right) & h_{UE} > 3\, m \end{Bmatrix} \tag{2.57}$$

Type E

For the backhaul link in urban NLOS conditions where the base station is placed above rooftops and the relay node is placed below rooftops and in a different street as shown in Figure 2.6), the IEEE 802.16j standard concludes that this link should be well characterized with the COST-WI model defined in Section 2.2.2.

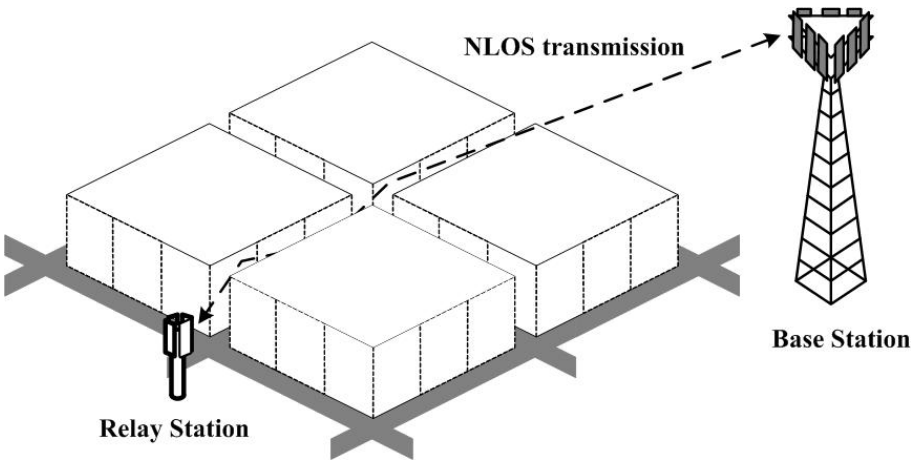

Figure 2.6: NLOS backhaul link definition in IEEE 802.16j - Type E model. [12]

Type F

This model is used in both urban and suburban environments. It defines the access link supposing the relay node and the User Equipment antennas below rooftops. Both LOS and NLOS models are provided separately for this case. [12]

This model is applicable for distances longer than 10 m. For shorter distances, the free space model defined in Equation 2.3 should be applied.

$$d > 10\,m$$

LOS

The LOS definition assumes both antennas located on the same street (see Figure 2.7).

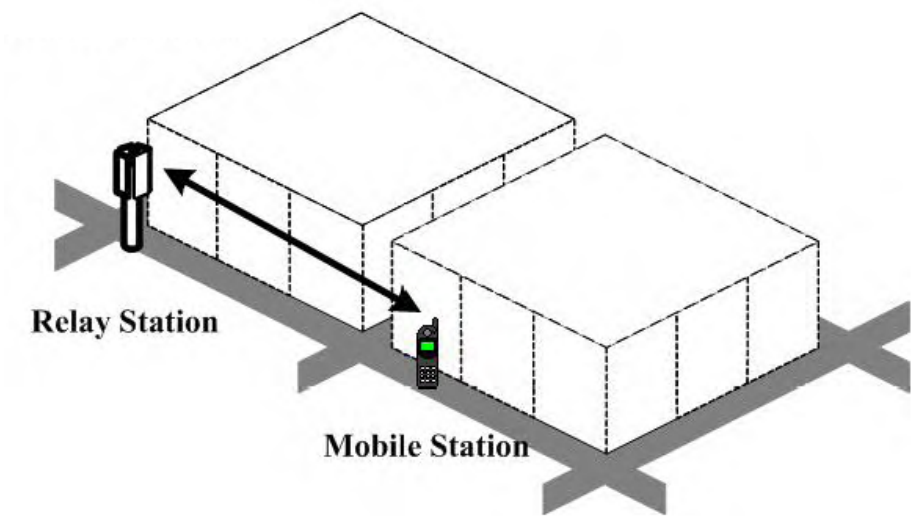

Figure 2.7: LOS access link definition in IEEE 802.16j - Type F model. [12]

This is an advanced two-slope model. The effect of traffic is taken into account by defining an effective road height, which reduces the relay node and user equipment heights. In addition, a visibility factor is included which reduces the path loss further as distance increases, and this factor accounts for the fact that LOS decreases with distance along a street. [12]

$$PL_{LOS} = 20\,log_{10}\left(\frac{e^{0.002\,d}\cdot 4\pi\,(d/m)\,D(d)}{\lambda}\right) \tag{2.58}$$

$$D(d) = \begin{Bmatrix} 1 & d \leq d_{BP} \\ d/d_{BP} & d > d_{BP} \end{Bmatrix} \tag{2.59}$$

$$d_{BP} = 4\, h'_{RN}\, h'_{UE} \frac{f_c}{c} \tag{2.60}$$

$$h'_{RN} = h_{RN} - 1.0\, m \tag{2.61}$$

$$h'_{UE} = h_{UE} - 1.0\, m \tag{2.62}$$

NLOS

In this case, the NLOS condition supposes the relay node and the user equipment antennas places in different streets. So as in WINNER II - B1 NLOS model, distances along the main street (d_1) and along the perpendicular streets (d_2) come out for a detailed analysis.

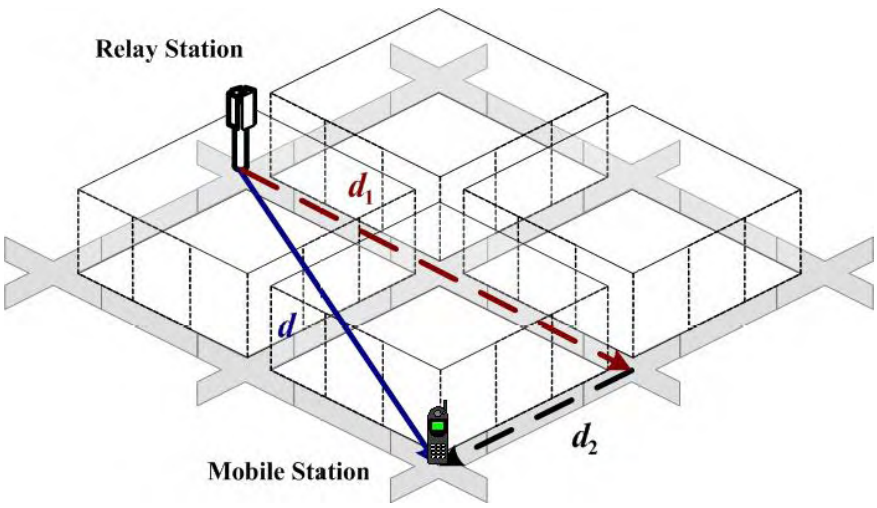

Figure 2.8: NLOS access link definition in IEEE 802.16j - Type F model. [12]

For this case, the model takes the minimum of an over-the-rooftop component and a round-the streets component (calculated with a model by Berg). The model includes a visibility factor (as previously in LOS conditions) and effective road height to give the correct breakpoint in the first street section. [12]

$$PL_{NLOS} = min(PL_{Berg}, PL_{over\,rooftop}) \tag{2.63}$$

$$PL_{over\,rooftop} = 24 + 45\,log_{10}\left(\frac{d}{m}\right) \tag{2.64}$$

$$PL_{over\,rooftop} = 20\,log_{10}\left(\frac{4\pi \cdot d_n \cdot D(R)\prod_{j=1}^{n}\left(e^{0.002\,r_{j-1}}\right)}{\lambda}\right) \tag{2.65}$$

$$r_{bp} = \begin{Bmatrix} r_0 & r_0 \leq d_{BP} \\ d_{BP} & r_0 > d_{BP} \end{Bmatrix} \tag{2.66}$$

$$R = \sum_{j=1}^{n} r_{j-1} \tag{2.67}$$

$$D(R) = \begin{Bmatrix} 1 & R \leq r_{BP} \\ R/r_{bp} & R > r_{BP} \end{Bmatrix} \tag{2.68}$$

$$k_j = k_{j-1} + d_{j-1}q_{j-1} \tag{2.69}$$

$$d_j = k_j r_{j-1} + d_{j-1} \tag{2.70}$$

$$k_0 = 0,\ d_0 = 0 \tag{2.71}$$

$$q_j = \left(\varphi_j \frac{0.5}{90}\right)^{1.5} \tag{2.72}$$

LOS/NLOS

Once again, as in this model, the radio link can be either LOS or NLOS, it is possible to define a LOS probability in terms of distance to combine both models in a joint LOS/NLOS model. The comparison between LOS probability functions for the models can be seen in Figure 2.4.

$$prob(LOS) = 1 - \left(1 - (1.56 - 0.48\, log_{10}(d))^3\right)^{1/3} \tag{2.73}$$

2.3 Comparative

The first main objective in this report is to compare the different path loss models applicable for the different links. After studying carefully the different models explained in the previous sections (in terms of frequencies, situation and height range of the terminals and environment conditions) it is possible to do the next classification:

- **Direct link (BS to UE)**: COST-HATA, COST-WI, WINNER II - C1, 3GPP - Macro to UE and 802.16j - Type B.
- **Backhaul link (BS to RN)**: COST-HATA, COST-WI, WINNER II - C1, WINNER II - B5c, 3GPP - Macro to Relay and 802.16j - Type E.
- **Access link (RN to UE)**: COST-HATA, COST-WI, WINNER II - B1, 3GPP - Relay to UE and 802.16j - Type F.

2.3.1 Base Station to User Equipment (BS to UE - direct link)

The comparison for this link is performed at two different frequencies (800 MHz and 2 GHz). The main reason to do this is compare the path loss influence for 'old' technologies (i.e. GSM) working at low frequencies and the new 3G and 4G technologies (i.e. UMTS and the future 3GPP LTE-Advanced) working over 2 GHz.

As it can be seen in the previous sections, the only models valid for frequencies lower than 2 GHz are the COST-HATA model and the COST-WI model. To compare this models for the direct link, a BS height of 32 m and a UE height of 5 m are considered. COST-WI needs to specify some other parameters and building average height (15 m), separation between buildings ($b = 20m$), road width ($w = 10m$) and road orientation ($\varphi = 90°$). The comparison for this two models at 800 MHz can be seen in Figure 2.9.

For frequencies over 2 GHz, specific models for this link are defined in the 3GPP and 802.16j standards. WINNER II proposes the model C1, but it is defined for a chosen BS height of 25 m. Also 802.16j - Type B proposes a different approach with an UE height of 2 m. The comparison between this models and COST-HATA and COST-WI can be seen in Figure 2.10.

Macro to UE @ 800 MHz				
MODEL	**CONDITIONS**	**BS**	**UE**	**NOTE**
COST-HATA	ART-BRT	32 m	1.5 m	
COST-WI	ART-BRT LOS/NLOS	32 m	1.5 m	$h_{roof} = 15\,m$, $b = 20\,m$, $w = 10\,m$, $\varphi = 90°$

Table 2.6: Summary of the models described for the direct link (BS to UE) at 800 MHz.

Macro to UE @ 2 GHz				
MODEL	**CONDITIONS**	**BS**	**UE**	**NOTE**
COST-HATA	ART-BRT	32 m	1.5 m	
COST-WI	ART-BRT LOS/NLOS	32 m	1.5 m	$h_{roof} = 15\,m$, $b = 20\,m$, $w = 10\,m$, $\varphi = 90°$
WINNER II - C1	ART-STL LOS/NLOS	25 m	1.5 m	
3GPP - Macro to UE	ART-STL LOS/NLOS	32 m	1.5 m	
802.16j - Type B	ART-STL LOS/NLOS	32 m	2 m	

Table 2.7: Summary of the models described for the direct link (BS to UE) at 2 GHz.

These models have different distance application ranges, COST-HATA is only valid from 1 km. but, normally, it is also used to predict path loss for shorter distances despite it is not totally correct.[2].

[2] All of the path loss model comparisons performed in this chapter are done for the range between 50 m and 5 km.

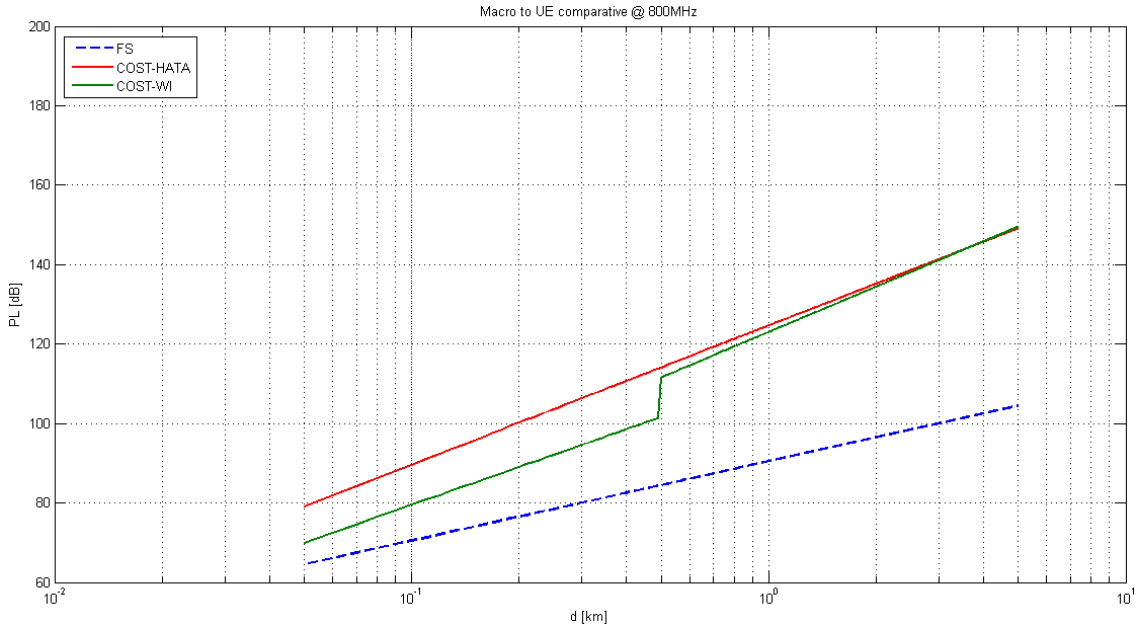

Figure 2.9: Path Loss models for the direct link (BS to UE) at 800 MHz.

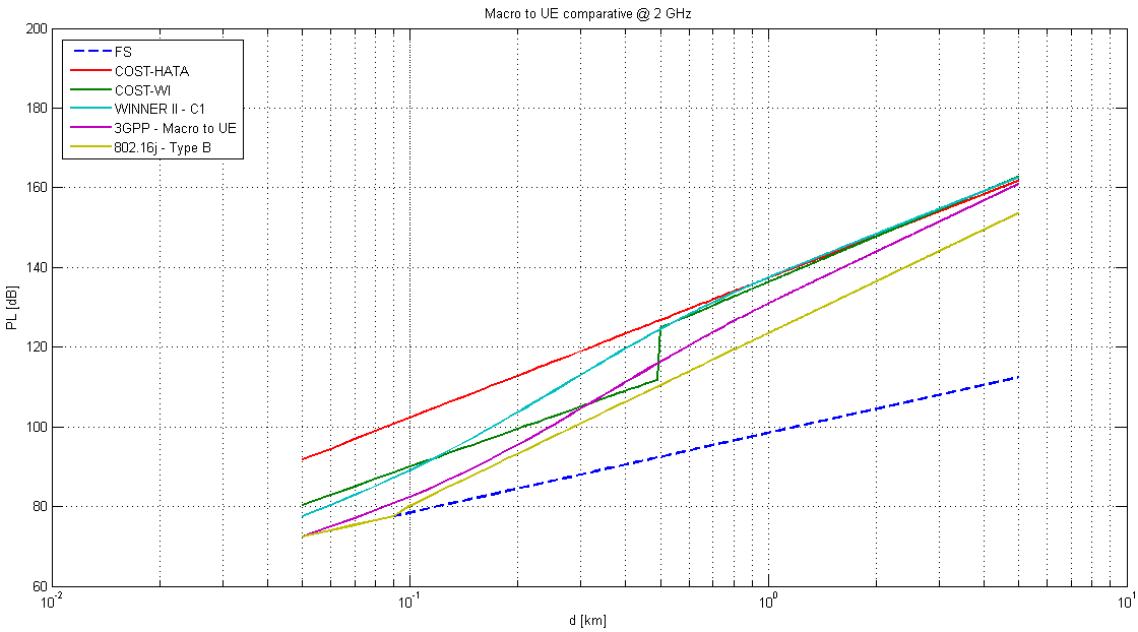

Figure 2.10: Path Loss models for the direct link (BS to UE) at 2 GHz.

As it can be seen comparing Figures 2.9 and 2.10, path loss is higher at 2 GHz. It is clear that path loss is frequency dependent since it is a rate between transmitted and received power which encapsulated two effects: spreading out of electromagnetic energy in free space and receiver antenna aperture.

COST-HATA and COST-WI have very similar slopes (approximately 34 dB/dec), higher than the FS model taken as reference (20 dB/dec). The level of the second part of the COST-WI model, for distances higher than 500 m (NLOS), is function of the BS and the UE heights as well as the height of the buildings. In this particular case, the edge of both models is barely the same, but in environments with higher buildings, COST-WI takes a higher level (severe NLOS condition). The level of the first part (LOS) predicts an intermediate level between FS and COST-HATA. This is similar for both frequencies.

Focusing now on the analysis at 2 GHz, it is possible to see in 2.10, that WINNER II - C1 is very similar to COST-WI (but it is necessary to remember that this model lies on very specific terminal heights. See Table 2.7).

The 3GPP - Macro to UE model, at the beginning, follows the FS model. It presents a similar tendency to the WINNER II - C1 model with an initial difference (LOS) of 6 dB. At the edge (NLOS) both models reach COST-HATA.

With respect to 802.16j - Type B model, it is possible to say that the first slope (LOS) follows FS, and the second slope after 100 m is approximately 43 dB/dec. For the range of distances considered in the analysis, this model gives the lowest Path Loss prediction.

2.3.2 Base Station to Relay Node (BS to RN - backhaul link)

Again for this link, the analysis is done for 800 MHz and 2 GHz. Now, the situation changes because the heights of the terminals are different to the previous case. In this link, a RN height of 5 m is considered.

At 800 MHz, in Figure 2.11 comparing COST-HATA and COST-WI it is possible to see that the second part of the COST-WI model has the edge over COST-HATA. This is due to the commented change of one of the terminals from (UE) 1.5 m in the direct link to (RN) 5 m in the backhaul link. It is possible to take a look into Equation 2.11 and see that the higher the RN antenna is placed, the higher the path loss prediction in COST-WI will be.

Macro to Relay @ 800 MHz				
MODEL	**CONDITIONS**	**BS**	**UE**	**NOTE**
COST-HATA	ART-BRT	32 m	5 m	
COST-WI	ART-BRT LOS/NLOS	32 m	5 m	$h_{roof} = 15\,m$, $b = 20\,m$, $w = 10\,m$, $\varphi = 90°$

Table 2.8: Summary of the models described for the backhaul link (BS to RN) at 800 MHz.

Macro to Relay @ 2 GHz				
MODEL	**CONDITIONS**	**BS**	**UE**	**NOTE**
COST-HATA	ART-BRT	32 m	5 m	
COST-WI	ART-BRT LOS/NLOS	32 m	5 m	$h_{roof} = 15\,m$, $b = 20\,m$, $w = 10\,m$, $\varphi = 90°$
WINNER II - C1	ART-STL LOS/NLOS	25 m	1.5 m	
WINNER II - B5c	BRT-STL LOS	10 m	5 m	
3GPP - Macro to Relay	ART-BRT LOS/NLOS	32 m	5 m	

Table 2.9: Summary of the models described for the backhaul link (BS to RN) at 2 GHz.

It can be also seen in Figure 2.11, that COST-HATA could be the prediction of COST-WI in an intermediate shadowed environment (Equation 2.21 with $prob(LOS) = prob(NLOS) = 0.5$).

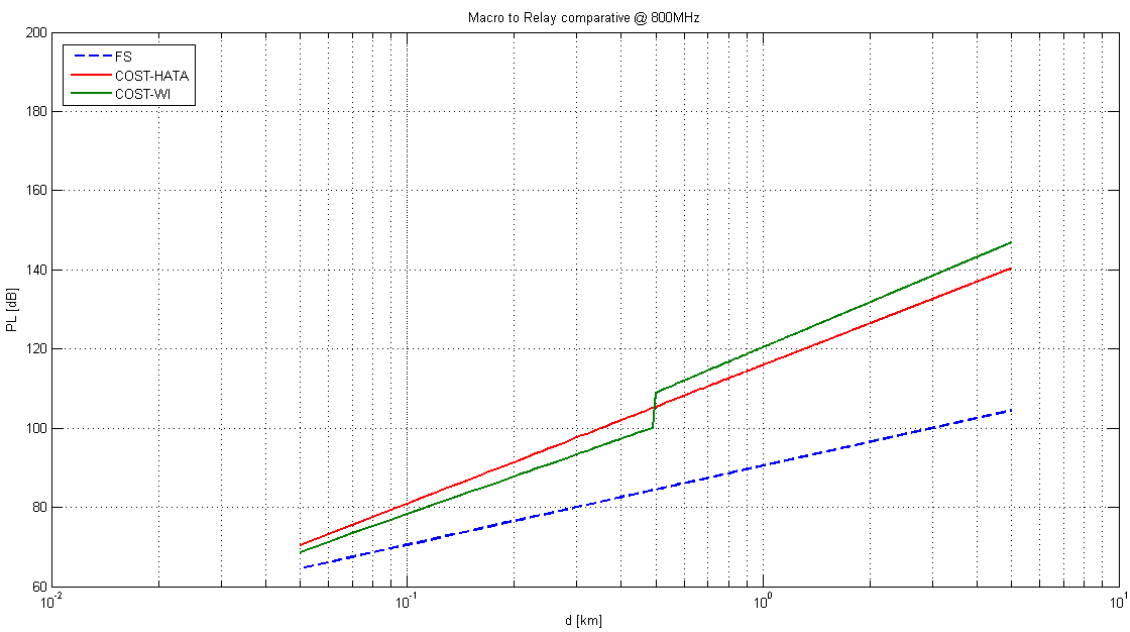

Figure 2.11: Path Loss models for the backhaul link (BS to RN) at 800 MHz.

In this case, at 2 GHz (see Figure 2.12), it is necessary to remember that the 802.16j standard in the Type E model for this backhaul link recommends to use COST-WI for

the path loss calculation.

WINNER II - C1 is similar to the case in the direct link (Figure 2.10). This is due to that there is no change in the parameters (same frequency, same specific terminal heights). WINNER II - B5c is giving the lowest Path Loss estimation. As WINNER II - C1, this model considers specific conditions (a BS height of 10 m and a RN height of 5 m). Until 1 km, it follows FS (slope of 20 dB/dec) and after the slope changes to approximately 40 dB/dec.

The 3GPP - Macro to Relay model does something similar to the 3GPP - Macro to UE model in Figure 2.10. It goes from FS (10 dB under COST-HATA) at the beginning to COST-HATA at the edge.

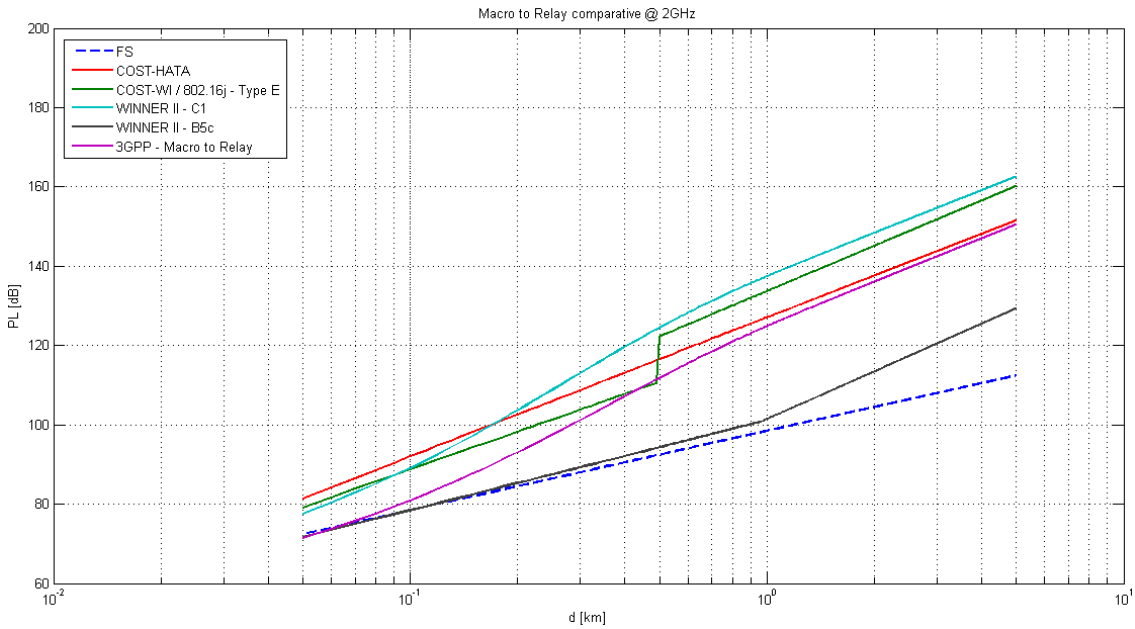

Figure 2.12: Path Loss models for the backhaul link (BS to RN) at 2 GHz.

2.3.3 Relay Node to User Equipment (RN to UE - access link)

For the access link, it is only considered a frequency of 2 GHz (this fits with the supposition of a relay working in IN-BAND mode as explained in Section 1.2). WINNER II - C1 and 802.6j - Type F models are quite specific as they consider distances along main street (d_1) and perpendicular street (d_2). For this analysis it was taken into account a diagonal with $d1 = d2$.

It can be seen in Figure 2.13 that for this link, COST-HATA and COST-WI are very similar with a deviation of only ±3 dB. This is due to the small difference between the RN height (5 m) and UE height (1.5 m) as well as the building height (15 m) which leads into a highly NLOS condition.

WINNER II - C1 model starts between FS and COST-HATA but increases rapidly its Path Loss prediction reaching 23 dB over COST-HATA edge at 5 km.

Relay to UE @ 2 GHz				
MODEL	**CONDITIONS**	**BS**	**UE**	**NOTE**
COST-HATA	ART-BRT	5 m	1.5 m	
COST-WI	ART-BRT LOS/NLOS	5 m	1.5 m	$h_{roof} = 15\,m$, $b = 20\,m$, $w = 10\,m$, $\varphi = 90°$
WINNER II - B1	BRT-STL LOS/NLOS	10 m	5 m	d_1, d_2
3GPP - Relay to UE	BRT-STL LOS/NLOS	5 m	1.5 m	
802.16j - Type F	ART-STL LOS/NLOS	32 m	2 m	d_1, d_2

Table 2.10: Summary of the models described for the access link (RN to UE) at 2 GHz.

Again, as in the direct link and the backhaul link, the 3GPP model - Relay to UE goes from FS (in this case 4 dB higher) at the beginnig to COST-HATA at the edge.

Finally, 802.16j - Type F model gives the highest Path Loss prediction, fitting COST-HATA model at the beginning but with a slope of 40 dB/dec. Probably, it is relevant to highlight that this model matches WINNER II - B1 at 1 km distance.

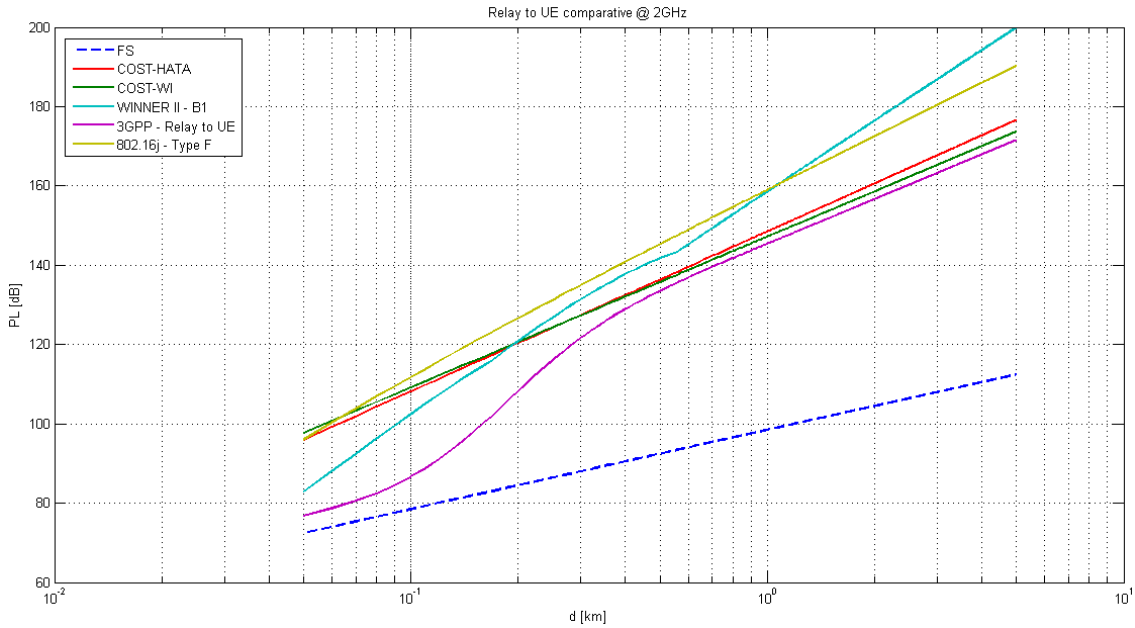

Figure 2.13: Path Loss models for the access link (RN to UE) at 2 GHz.

2.4 Main conclusions on Path Loss

Taking a look to the graphics and comments in Section 2.3, it is clear to conclude that the Path Loss models studied are very different between them. It depends on the parameters included in the model and the environment they are considering. All of them are based on measurements, so it is quite difficult they could match perfectly Path Loss in many different conditions.

As main conclusions about the selected Path Loss models (apart from the differences described in the previous sections):

- The most complete model is COST-WI, which takes into account a lot of parameters, but it is poor when the heights of the BS and the buildings are similar or even the BS is lower than the buildings. Also, its definition for LOS probability in terms of distance is not very accurate.
- WINNER II models are defined for very specific parameters and conditions, so, in principle, they could work for Path Loss in similar conditions to the specified ones.
- 3GPP models are clearly related to FS for shorter distances and COST-HATA for longer distances.
- 802.16j models are quite different from the others (except model E which recommends to follow COST-WI prediction). This is due to that they are WiMAX-based models,

normally design from measurements at frequencies higher than 2 GHz (typically 5.25 GHz).

2.5 Path loss system level effects

It is clearly seen that the selection of an appropriate propagation model determines how many base stations are required to provide a particular coverage for a network. The more precise the model is, the better the network design will be done. Typically, this network design is done basing on COST-HATA model.

In order to evaluate the influence of the different models, a system level simulation was done (see Appendix A). Each model predicts different level of path loss, which has influence on the SINR calculations. SINR is directly mapped into throughput so path loss models are also straightly related to this.

The simulation was performed to analyze the complete relayed link (backhaul link and access link), but the direct link plays also an important role in the simulation since it is necessary to establish a criteria to connect the user equipment to the relay or the base station in function of the highest received power.

Chapter 3

MEASUREMENT CAMPAIGN

In order to give answer to the different issues set out in Section 1.3, a measurement campaign was executed to study the feasibility of future relay node deployment (specially, the quality of the backhaul link) in a real urban macro-cell environment. The measurements were done in collaboration with Telenor (danish telecommunication operator [13]), who provided network information (base station location, node identification and general site information).

In this chapter, all the facts related to the measurement campaign are explained. The obtained data and the digital signal processing performed in the analysis will be explained in Chapter 4.

3.1 Objectives

As explained before, it is necessary to study how the signals behave in a real urban macro-cell scenario at different heights or if we get any advantage with different types of receiving antenna. So the measurement campaign was planned to try to achieve all these objectives:

- Record similar signals with similar antennas (both omnidirectional) at two different heights to explore height gain and signal quality.
- Record similar signals from different antennas (omnidirectional, directional) at the same height to explore their influence over signal quality.
- Record signal samples to perform a path loss analysis.

3.2 Measurement conditions

Once is known what to measure, it is necessary to define the conditions in which the measurements were performed.

As the measurements should be done in a real urban macro-cell network due to interference issues, and there were no LTE nodes working in Aalborg area, Telenor provided information enough to perform the campaign over its UMTS network (3G). More details about this can be checked out in Appendix C.

The selected scenario for the measurements was the Aalborg urban city centre, where building density is homogeneous with 3-4 floors buildings (around 15 m of height). This environment can be seen in Figure 3.1.

Figure 3.1: Homogeneous building density and height in Aalborg area. [14]

Normally, in this area, base stations are located above the rooftops. The measurements were performed in-between buildings trying to explore potential relay node locations.

One of the objectives in this project is to evaluate possible relay locations at cell edge, so all the measurements were done in cell edge conditions, under the influence of several base stations (interference).

For the later analysis, it was necessary to get an idea of signal levels and interference levels, so the UMTS recorded parameters recorded were: RSCP (received signal code power), ISCP (interference signal code power) and SIR (signal to interference ratio). A deeper explanation about this is given in Appendix C.

3.3 Measurement performance

To record all the expected data, the measurement plan was done in two different ways: routes and static spots.

The purpose on the routes was to record information from the omnidirectional antennas at different heights (2.4 m and 5.0 m) and take samples for a future path loss analysis. The static spot were designed to evaluate the difference from using an omnidirectional antenna or a directional antenna at the same height (5.0 m).

Figure 3.2 and Figure 3.3 illustrate how the measurements were done. Detailed information about the equipment used and the setup performed can be found in Appendix B.

Figure 3.2: Measurement campaign: routes setup.

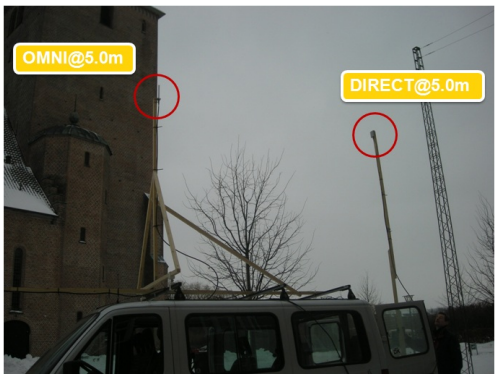

Figure 3.3: Measurement campaign: static spot setup.

3.3.1 Routes: Omnidirectional at 5.0 m vs. Omnidirectional at 2.4 m

The main objective here is to obtain as many samples as possible just in order to compare the signal at different heights and extract samples for the path loss analysis. Several routes with a length between 600 m and 1 km were planned in areas with influence of several base stations.

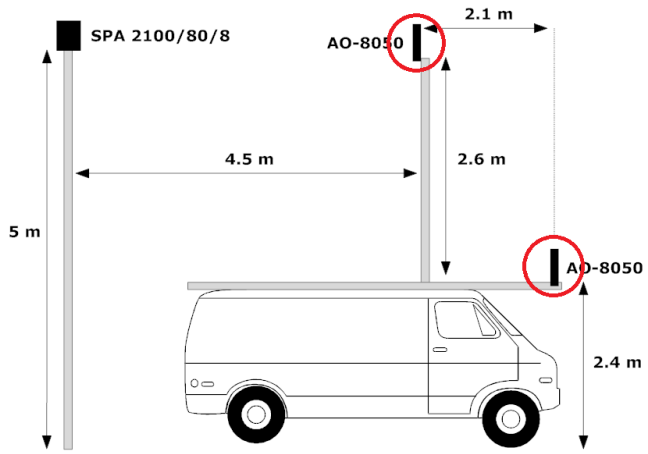

Figure 3.4: Omnidirectional antennas at different heights (5.0 m and 2.4 m).

To perform these measurements, each of the omnidirectional antennas was connected to a different scanner. In this case, the omnidirectional at 5.0 m was connected to the TSMU scanner, and the omnidirectional at 2.4 m was connected to INPUT1 in the TSMW scanner. In order to perform the subsequent analysis, a GPS position was attached to the measurements in the TSMW scanner. The scanners were configured to record 20 $^{samples}/_{s}$.

SIGNAL	DEVICE	DETAILS
Omnidirectional 5.0 m	TSMU	20 $^{samples}/_{s}$
Omnidirectional 2.4 m	INPUT1 TSMW	20 $^{samples}/_{s}$, GPS info

Table 3.1: Route measurement performance.

The different routes were driven at a calculated average speed of 13.18 $^{km}/_{h}$.

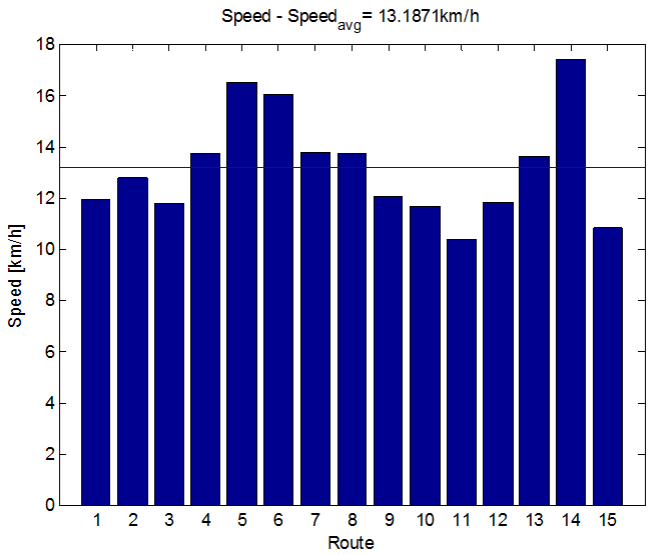

Figure 3.5: Calculated average for all the routes.

3.3.2 Static spots: Directional at 5.0 m vs. Directional at 5.0 m

In this case, the objective is to explore potential relay node locations and analyze if there is any advantage from using a directional antenna instead an omnidirectional antenna at the same height (5.0 m) in the relay part of the backhaul link.

To do this, signals were recorded in static positions with the omnidirectional antenna at 5.0 m connected to the TSMU scanner and with the directional antenna placed on a mast also at 5.0 m connected to INPUT2 in the TSMW scanner. The directional antenna was placed at 4.5 m from the omnidirectional as it can be seen in Figure 3.6.

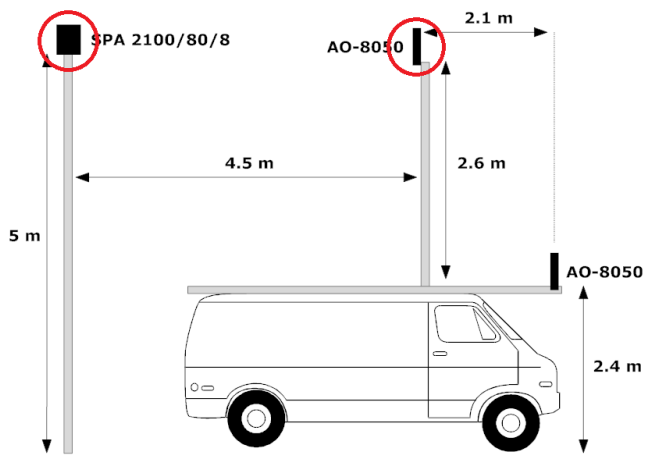

Figure 3.6: Directional and omnidirectional antenna at 5.0 m height.

The directional measurements were done by pointing the antenna to a desired base station. In this case, it was supposed that the most probable donor should be the surrounding base station with highest power. In order to avoid possible signal fades in this static measurements, the signal was sampled over 5 points on a 0.5 m x 0.5 m grid. This grid can be seen in Figure 3.7.

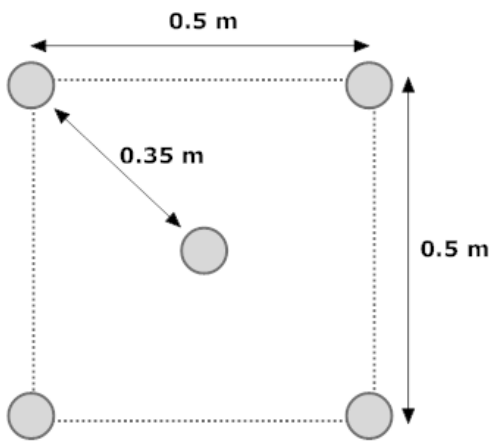

Figure 3.7: 5 different measuring points in static to avoid possible signal fades.

The signals were recorded during 50 s, so the directional antenna mast was placed at each point of the sampling grid during 10 $^{s}/_{point}$.

SIGNAL	DEVICE	DETAILS
Directional 5.0 m	INPUT2 TSMW	20 $^{samples}/_{s}$, sampling grid: 10 $^{s}/_{point}$
Omnidirectional 5.0 m	TSMU	20 $^{samples}/_{s}$

Table 3.2: Static spot measurement performance.

3.4 Campaign Execution

Finally, the measurement campaign took place on Thursday 17th and Friday 18th of February 2011. It was a challenge to perform the measurements with all the city covered by the snow and an average of -2°C. These two days, 15 routes and 15 static points were measured. Some problems were found related to some incomplete network information from Telenor, but it was possible to solve them after studying carefully the signals recorded. Some static measurements were not right at all since the static spot was close to a wall and the directional antenna was pointed straight into it which does not make much sense.

A second measurement campaign was run on Thursday 12th of May 2011 to record some extra (better planned) static spots. The weather was much better than in the previous measurements (cloudy and 16°C) so it was much easier to work in these conditions. In this occasion, each static spot was planned carefully with visual references.

3.5 Results

After both measurement campaigns, 15 routes and 25 static spots were recorded.

To analyze the routes, the complete signals along the routes should be compared, sample by sample. For the static spots, it is just a matter of focusing on average signal level at that point.

The processing on this data is explained in the next chapter.

Chapter 4

DATA PROCESSING

This chapter summarizes the different data analysis performed based on the different measurments explained in the previous chapter.

As explained before, the project is focus on potential relay nodes where it is necessary to evaluate the quality of the link with a potential donor base station. On this purpose, it is necessary to compare the compare the signals from the omnidirectional antennas at different heights in order to explore for a height gain value. It is also necessary to analyze if there is any benefit from using a directional instead of an omnidirectional antenna.

4.1 Omnidirectional at 5.0 m vs. Omnidirectional at 2.4 m

To explore the height gain between 2.4 m and 5.0 m, 3 parameters were defined: RSCPHG, ISCPHG and SIRHG. Each of them tries to express the difference between RSCP (signal level), ISCP (interference level) and SIR (signal to interference ratio) at the different heights[1].

It was necessary to correct the measured values, translating them to just after the antenna to make them comparable due to the different attenuation of the cables connecting the antennas and the scanners. This is shown in Figure 4.1.

$$SIGNAL_{xxx} = MEASURED\_SIGNAL_{xxx} + L_{cable,xxx} \tag{4.1}$$

[1]From now on, and to make the equations clear, the subindex 500 refers to 5.0 m height and the subindex 240 refers to 2.4 m. height

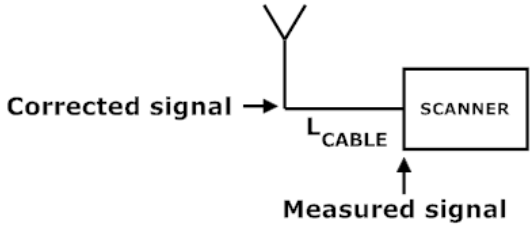

Figure 4.1: Correction factor to obtain comparable signals.

The correction factors in this case are $L_{cable,500} = 2.02\,dB$ and $L_{cable,240} = 1.92\,dB$. It is trivial to see that they should be applied only to RSCP and ISCP and not to SIR, since this is a quotient between RSCP and ISCP in linear units. It is possible to read more about these parameters in Appendix C.

PARAMETER	NAME
$RSCPHG$	Received Signal Power Height Gain [dB]
$ISCPHG$	Interference Signal Power Height Gain [dB]
$SIRHG$	Signal to Interference Ratio Height Gain [dB]

Table 4.1: Parameters defined to study height gain.

RSCPHG expresses the power gain from 2.4 m to 5.0 m. It is the most important parameter in this analysis. It can be valid to be applied as height factor in a future path loss model.

$$RSCPHG = RSCP_{omnidirectional500} - RSCP_{omnidirectional240} \tag{4.2}$$

ISCPHG expresses the ratio of interference from 2.4 m to 5.0 m.

$$ISCPHG = ISCP_{omnidirectional500} - ISCP_{omnidirectional240} \tag{4.3}$$

SIRHG summarizes the gain in quality signal from 2.4 m to 5.0 m.

$$SIRHG = SIR_{omnidirectional500} - SIR_{omnidirectional240} \tag{4.4}$$

These 3 parameters were calculated for every single route, comparing samples at the same position. This process is explained with more detail in Appendix D. An average was extracted for each single route based on all the samples recorded in that route.

The summary for each parameter can be seen in Figure 4.2 for RSCPHG, Figure 4.3 for ISCPHG and Figure 4.4 for SIRHG.

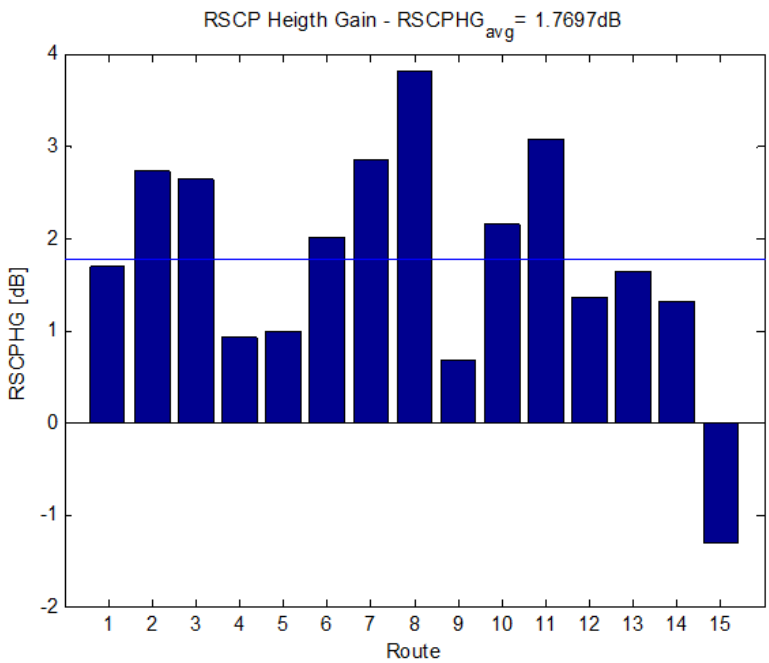

Figure 4.2: Average RSCPHG along all the routes.

As it can be seen in Figure 4.2, in average, the signal at 5.0 m is 1.77 dB higher than at 2.4 m. This result agrees with the conclusion in [15]. It is not clear why route 15 presents a higher value of RSCP at 2.4 m than at 5.0 m. With respect to this route it is possible to say that half of it was recorded in-between buildings and the other half in a LOS situation.

Figure 4.3 shows that, in average, the interference level is 3.60 dB higher at 5.0 m than at 2.4 m. With respect to SIR (Figure 4.4), it is 1.84 dB better at 2.4 m than at 5.0 m.

The explanation on why is happening this should be simple. In this urban macro-cell environment, the base stations are situated above rooftops so, since 5.0 m is higher than 2.4 m, it is easier to receive more signal higher up. The same reason can explain why the inference is higher at 5.0m; the signal travels above rooftops easier than in-between buildings so signals from other base stations (interference) are easier to be received at 5.0 m.

There is not so much difference in received power (only to 1.77 dB) at 5.0 m and 2.4 m, but the interference is 3.60 dB higher at 5.0 m, that is why the SIR is better ($3.60\,dB - 1.77\,dB = 1.84\,dB$) at 2.4 m.

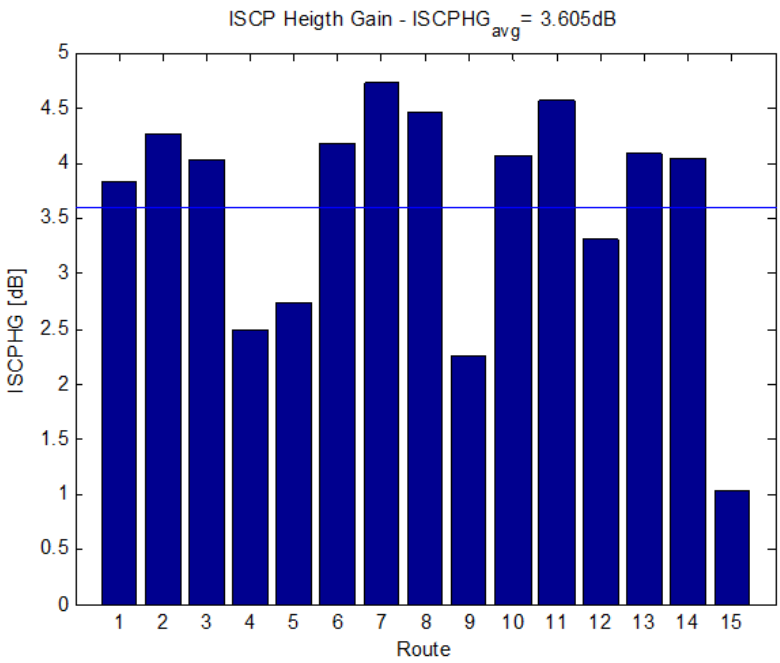

Figure 4.3: Average ISCPHG along all the routes.

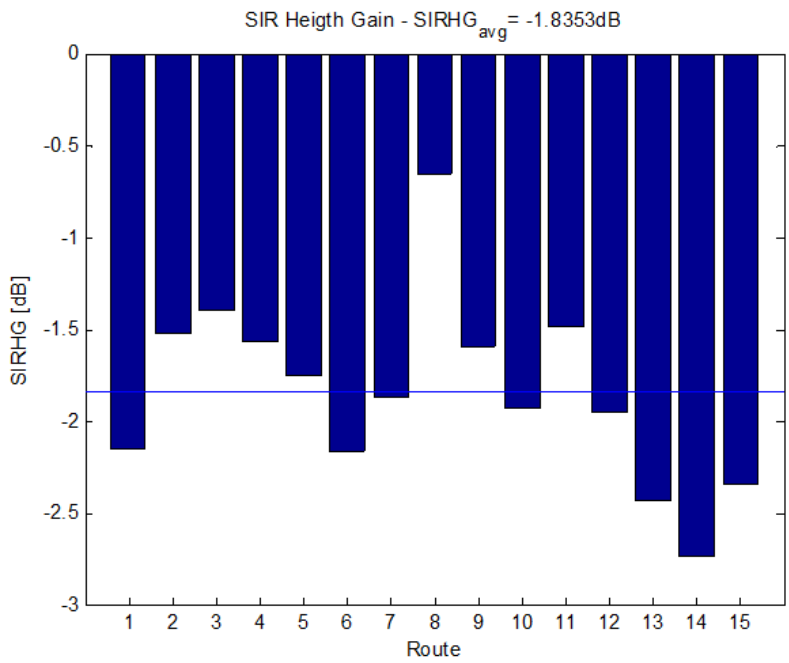

Figure 4.4: Average SIRHG along all the routes.

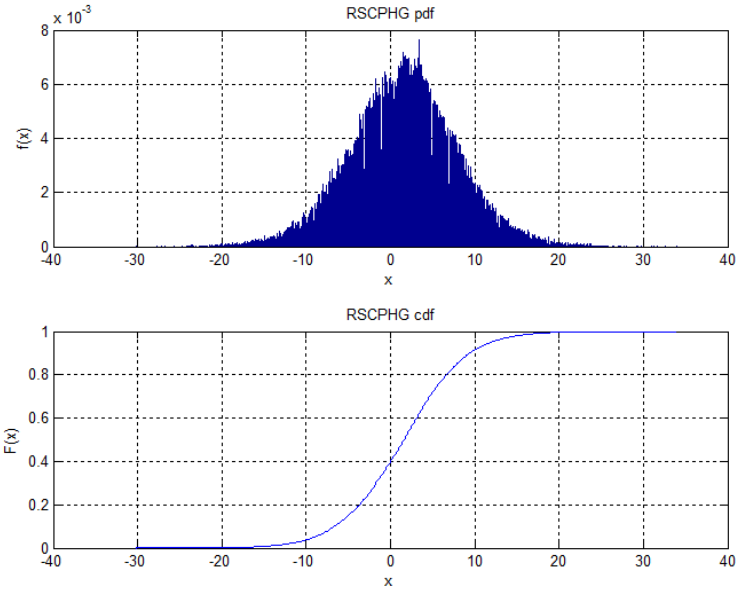

Figure 4.5: RSCPHG distribution calculated with all the samples.

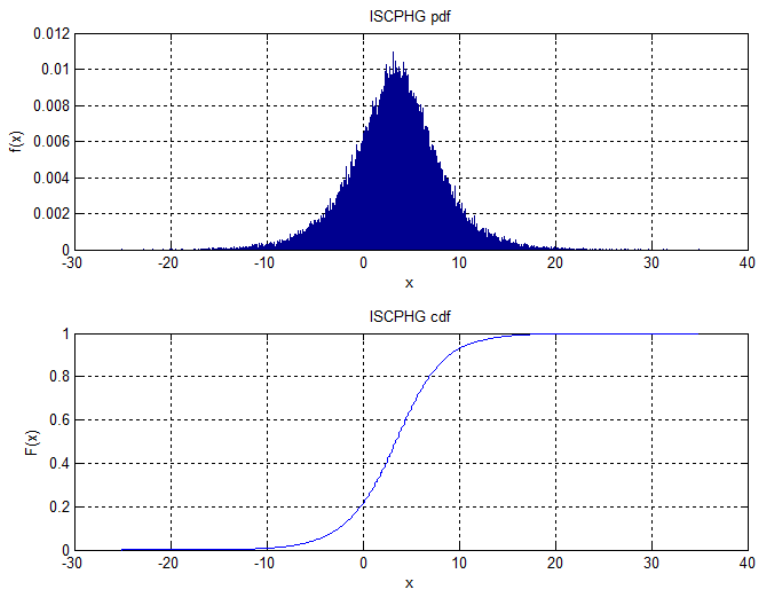

Figure 4.6: ISCPHG distribution calculated with all the samples.

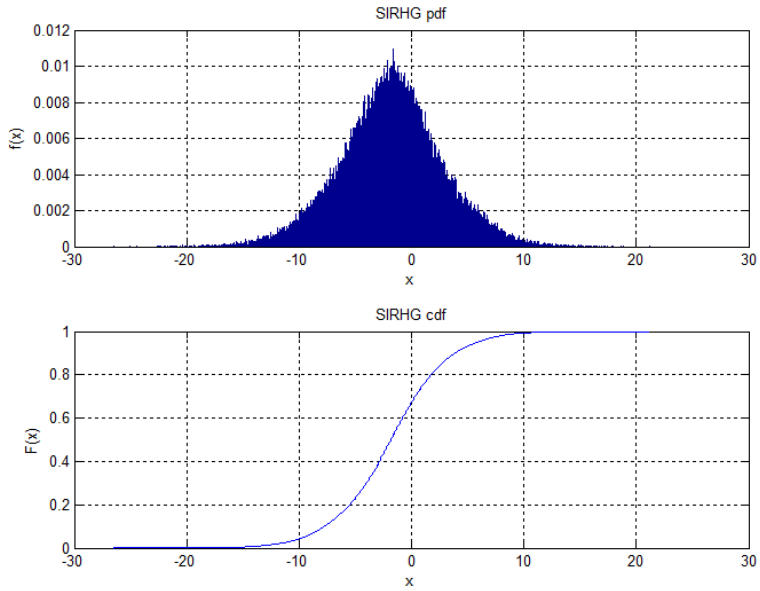

Figure 4.7: SIRHG distribution calculated with all the samples.

The different parameters distributions were calculated just to get an idea of the deviation (68% of the maximum) from the average obtained values. In the case of the RSCPHG, the deviation is $\pm 6.43\,dB$. For the ISCPHG, $\pm 4.81\,dB$ and $\pm 4.64\,dB$ for the SIRHG.

4.2 Directional at 5.0 m and Omnidirectional at 5.0 m

To evaluate the difference from using a directional antenna or an omnidirectional antenna at 5.0 m, 3 parameters were defined: RSCPTG, ISCPTG and SIRTG. Each of them tries to express the gain in RSCP (signal level), ISCP (interference level) and SIR (signal to interference ratio) between the omnidirectional antenna at 5.0 m and the directional at 5.0 m.

It is necessary to clear that the signals are compared after the antenna (see previous Figure 4.1), so the effect of the antenna is taken into account. In ideal conditions, the directional antenna should get higher RSCP and lower ISCP than the omnidirectional, since it should filter interference[2]. The directional antenna should exploit the higher gain and the narrower beamwidth.

[2]RSCPTG and ISCTG should lead to the difference of gains only when both antennas are similar which is not the case in this particular study.

As it was done in the previous section, it was necessary to correct the measured value to make them comparable (see Figure 4.1 and Equation 4.1). In this case, the correction factors are $L_{cable,directional} = 5.01\,dB$ and $L_{cable,omnidirectional} = 2.02\,dB$.

PARAMETER	NAME
$RSCPTG$	Received Signal Power Type Gain [dB]
$ISCPTG$	Interference Signal Power Type Gain [dB]
$SIRTG$	Signal to Interference Ratio Type Gain [dB]

Table 4.2: Parameters defined to study antenna type gain.

RSCPTG indicates the difference in received power from the directional antenna with respect to the omnidirectional.

$$RSCPTG = RSCP_{directional500} - RSCP_{omnidirectional500} \tag{4.5}$$

ISCPTG expresses the interference ratio filtered by the directional antenna with respect to the omnidirectional.

$$ISCPTG = ISCP_{directional500} - ISCP_{omnidirectional500} \tag{4.6}$$

SIRTG is the most important parameter in this analysis. It gives an idea of the overall performance (quality of the potential relay node backhaul link) using a directional antennna instead of an omnidirectional.

$$SIRTG = SIR_{directional500} - SIR_{omnidirectional500} \tag{4.7}$$

The 3 parameters were calculated for every single static spot, comparing average signal levels at the same position. This process is explained with more detail in Appendix D.

In this analysis, the static spots can be categorized according to the different environment conditions. It is possible to distinguish 6 different conditions in this study:

- LOS conditions: total or partial vision over the direct signal from the donor base station.
  - Close to main street. Almost LOS: the directional antenna is pointing along a main street illuminated by a base station, so the signal propagates easily along this street.
  - Clear LOS: direct vision. There is no obstacle between the directional antenna and the donor base station. See Figure 4.8.

Figure 4.8: LOS condition.

  - Clear LOS, but pointing to incorrect donor BS (interference from correct donor BS): this is an special situation in which the directional antenna is pointing to the closest base station (supposed donor), but it exist other further base station pointing straight to the spot introducing a high interference.

- IN-BETWEEN BUILDINGS (most relevant case)
  - Open space or pointing along street towards donor BS: this is the most probable location for a relay node deployment (typical pedestrian street, commercial areas, squares...). The directional antenna can be pointed to the desired donor base station. See Figure 4.9.

Figure 4.9: Typical in-between buildings situation. Good location for a relay node.

  - Directional pointing to a wall: the directional antenna should be oriented to the donor base station, but there is a high building between.
  - Very closed environment: small street with high buildings surrounding. See Figure 4.10.

Figure 4.10: Closed environment. Small street surrounded by tall buildings.

In clear LOS conditions, as it can be seen in Figure 4.11, the directional antenna receives much more power from the desired donor base station than the omnidirectional. In this example, the directional does not perform so good with respect to interference as expected, maybe because the interferer base stations were LOS also. The overall performance of the directional antenna is much better than the omnidirectional (the directional antenna is 8.69 dB better in SIR than the omnidirectional).

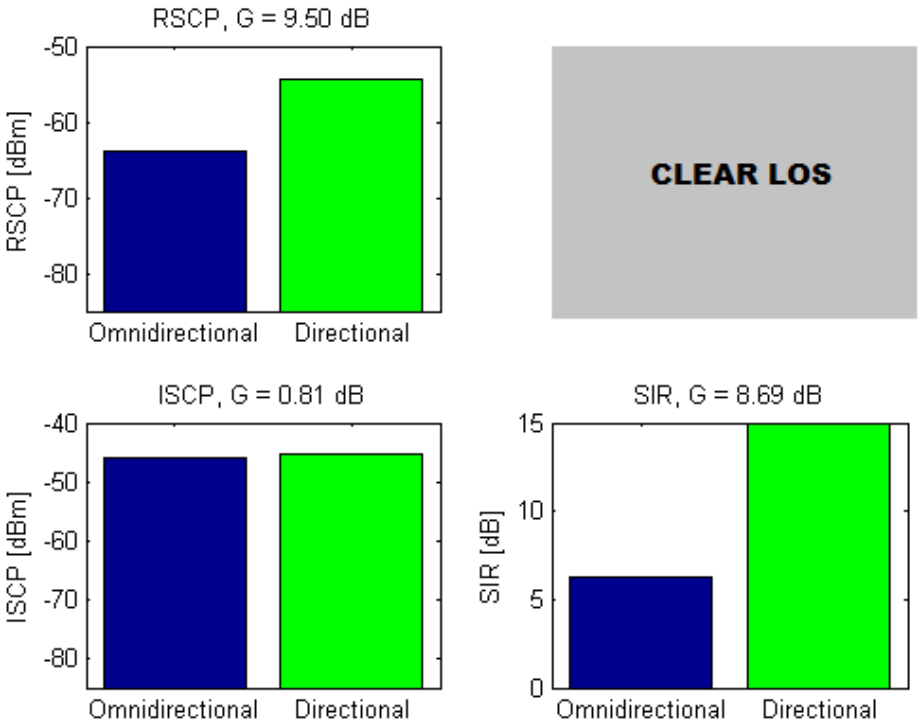

Figure 4.11: Potential relay node location: clear LOS.

Figure 4.12 shows an example of almost LOS conditions. In this case, it can be seen how the directional antenna still performs better than the omnidirectional ($SIRHG = 5.70\,dB$). The directional antenna receives more power than the omnidirectional but this time, the directional is filtering interference as expected (the interference level is 2.29 dB lower in the directional).

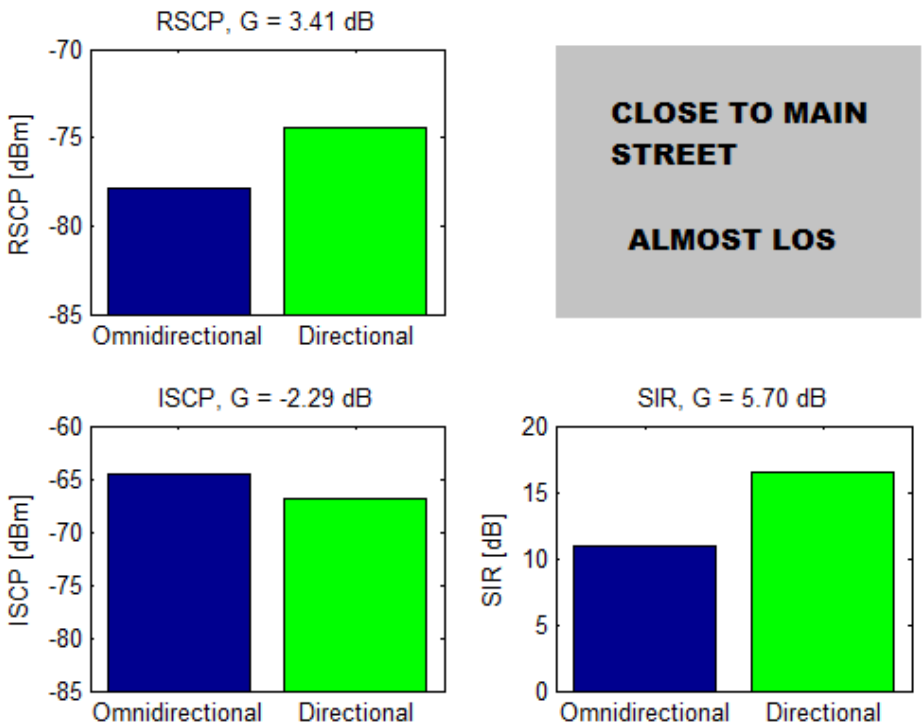

Figure 4.12: Potential relay node location: almost LOS.

To illustrate what happen when the directional antenna is pointing to an incorrect donor (Figure 4.13), it is possible to think about two possible base stations at similar distance, but the directional antenna is pointing to the base station with the lowest received power, so the higher power from the other base station is acting as interference. In this case, there is no gain from using the directional antenna instead of the directional antenna.

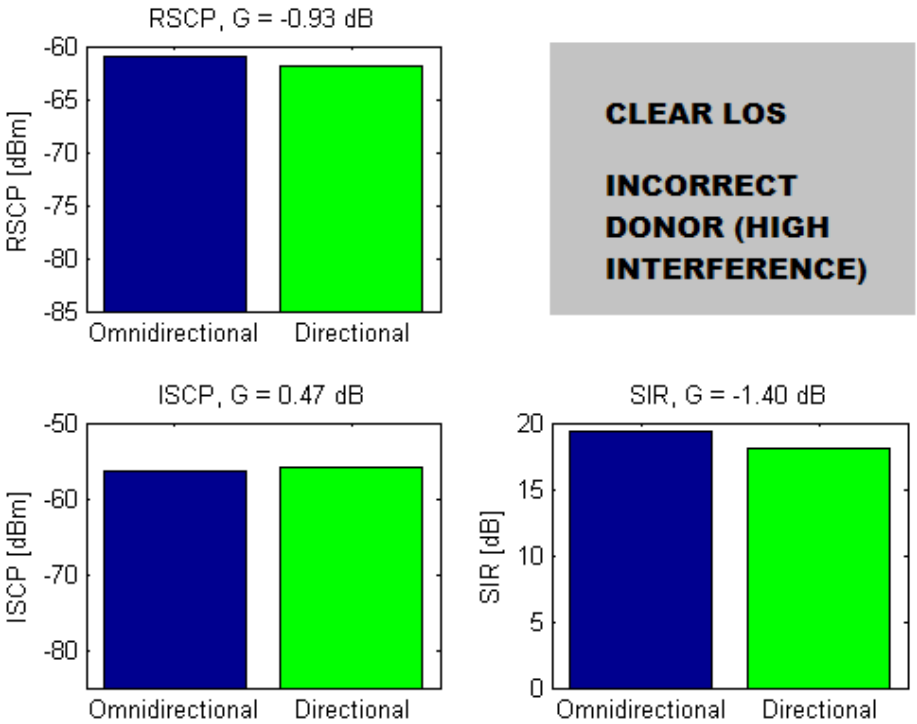

Figure 4.13: Potential relay node location: clear LOS but incorrect donor.

Now focusing on more realistic potential relay node locations, in a typical in-between buildings situation, with a well-pointed directional antenna, more power than in the omnidirectional is received, and also more interference, but still more power, so the SIR improves with respect to the omnidirectional.

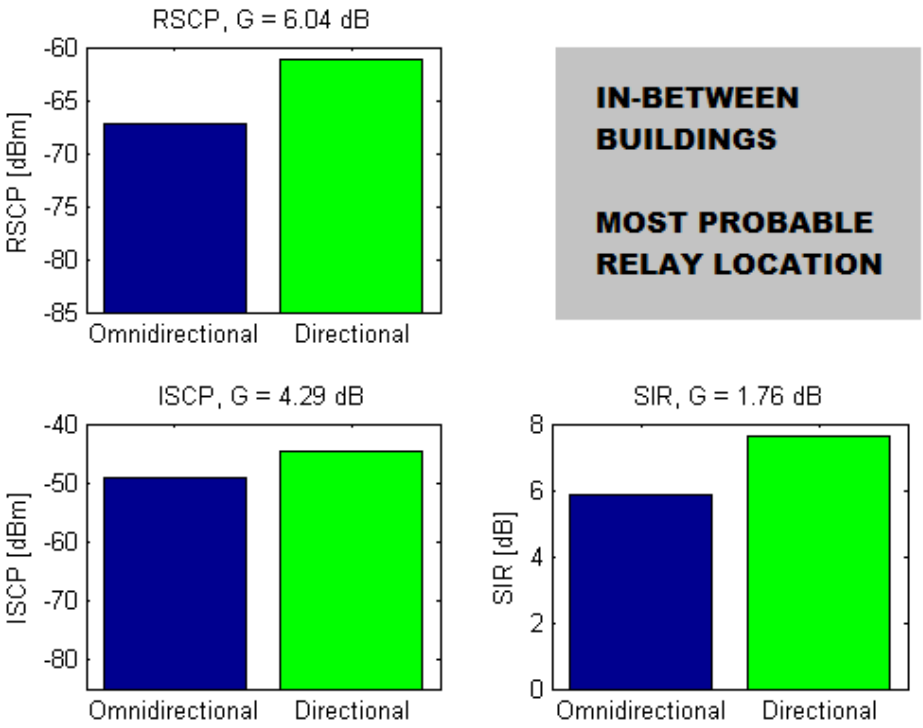

Figure 4.14: Potential relay node location: in-between buildings.

The next example, is just to show what happen in a bad planned location, when the directional antenna is pointing into a building between the spot and the desired donor base station (Figure 4.15). In this particular case, there is no benefit from using the directional antenna instead of the omnidirectional since it is impossible to get a direct signal in this way.

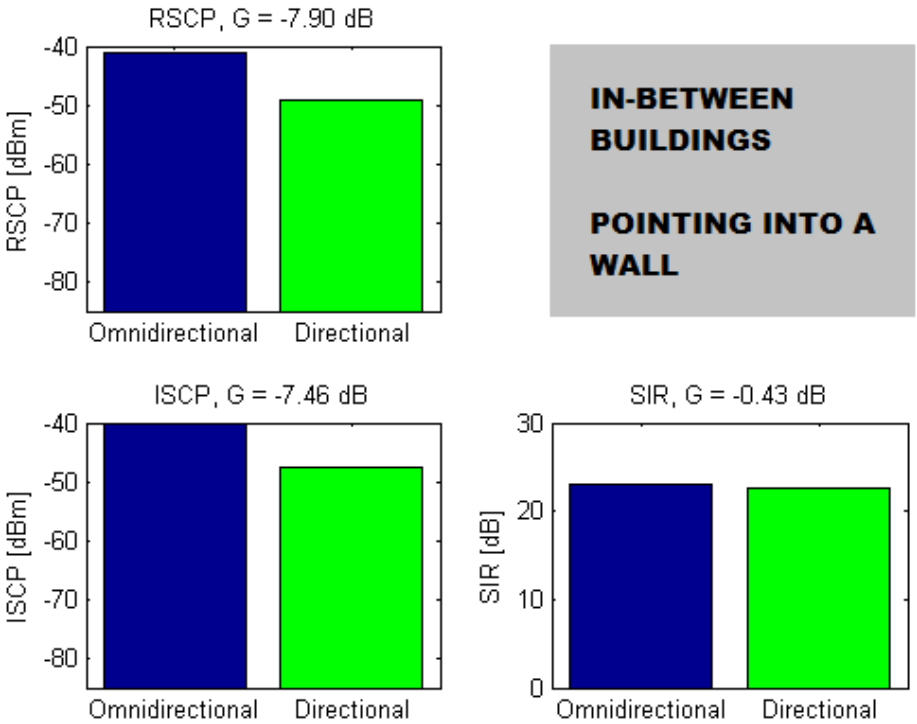

Figure 4.15: Potential relay node location: in-between buildings but pointing into a wall.

Finally, in very closed environments (Figure 4.16) with high buildings it is very difficult to get a good location to point the directional antenna correctly, so as in the previous example, there is no benefit from using the directional antenna. The omnidirectional performs a bit better maybe because it is capable to receive more reflections of the desired signal in this closed environment.

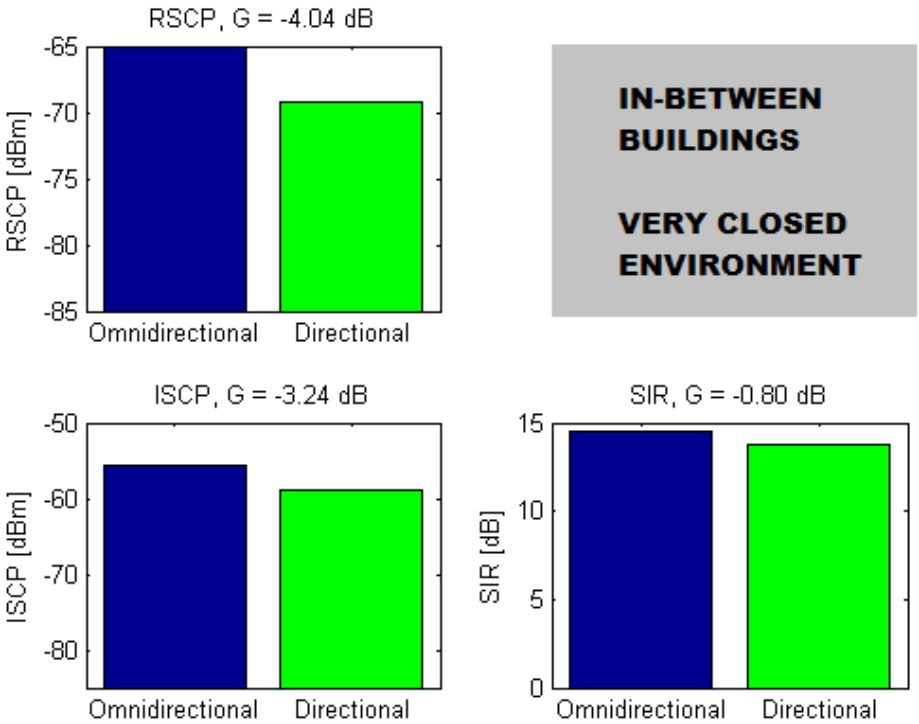

Figure 4.16: Potential relay node location: in-between buildings and very closed environment.

From now on, clear LOS and almost LOS will be grouped in LOS (green data); the most probable relay node locations in-between buildings are grouped in IN-BB (yellow data); and finally, pointing to an incorrect donor (high interference), pointing to a wall or closed environments are classified as OTHER (red data).

Figure 4.17 summarizes RSCPTG for all the static spots measured. Figure 4.18 does the same but with ISCPTG.

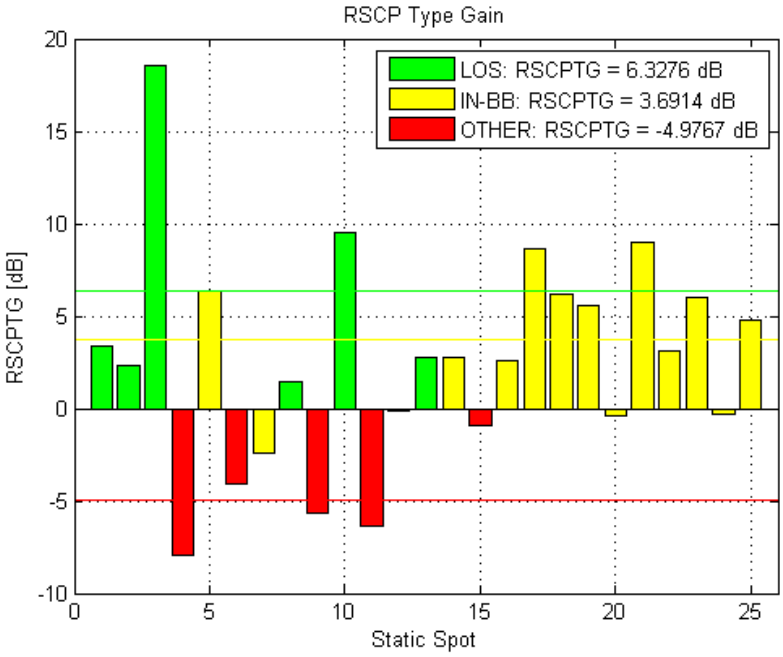

Figure 4.17: Average RSCPTG for the different static spots.

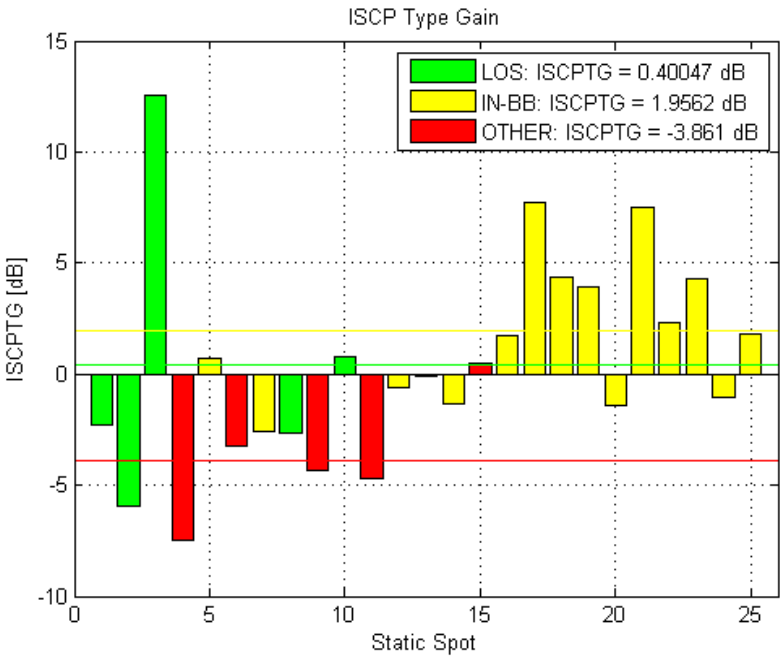

Figure 4.18: Average ISCPTG for the different static spots.

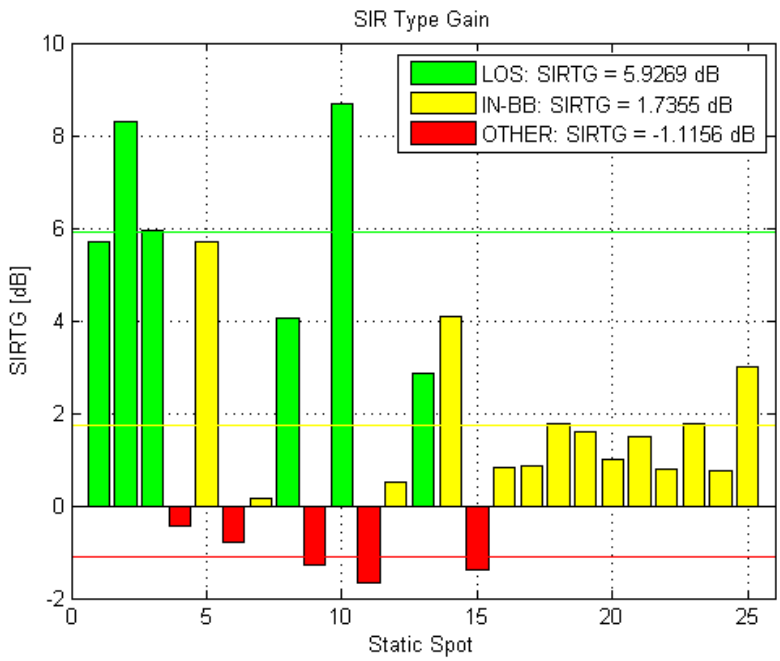

Figure 4.19: Average SIRTG for the different static spots.

Focusing on the most probable future relay location in-between buildings, as it can be seen in Figure 4.19, in average, the SIR obtained with the directional antenna is 1.73 dB better than the SIR obtained with the omnidirectional antenna.This means that, at least under the conditions specified in the previous chapters, the quality of the potential backhaul link is improved by using a directional antenna. This improvement is even better in LOS conditions.

Chapter 5

PATH LOSS ANALYSIS

From the previous measurements performed at different heights, path loss is calculated. In order to do this, a detailed link budget equation is calculated taking into account as many parameters as is possible to control; in this case, transmitted and received power, antenna gains (only vertical) and cable losses.

The analysis on the calculated path loss is done for different receiver antenna heights (2.4 m and 5.0 m) and separating signals from base stations at different heights (17 m, 19 m, 21 m, 23 m, 25 m, 27 m and 34 m).

At the end of the chapter a small comparison of the calculated path loss with existing models is done.

5.1 Link budget

Through a simple link budget equation it is possible to estimate the received signal level at the receiver.

$$P_{rx} = P_{tx} - L_{feeder} + G_{tx} - PL + G_{rx} - L_{cable} \tag{5.1}$$

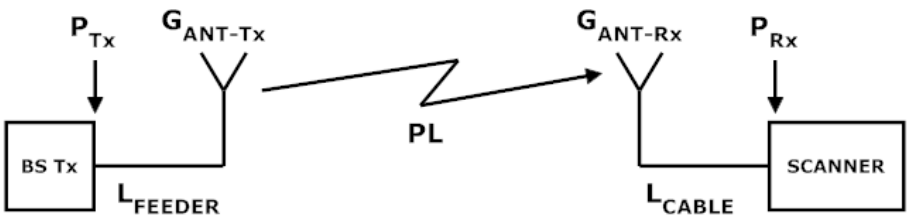

Figure 5.1: Definition of path loss in the system.

As the received power is known (measured in the scanner), an estimation of the path loss can be done just by reordering the terms in the last equation:

$$PL = P_{tx} - L_{feeder} + G_{tx} + G_{rx} - L_{cable} - P_{rx} \tag{5.2}$$

Translating the last expression into UMTS terms, according to the facts explained in Appendix C, it is possible to calculate the measured path loss as indicated in Equation 5.3.

$$PL = P_{P-CPICH} - L_{feeder} + G_{tx} - PL + G_{rx} - L_{cable} - RSCP \tag{5.3}$$

It is difficult to select the correct base station gain, so it has been approximated by the gain seen over a 15 m building (see Appendix E). This approximation supposes the signal from the base station propagating over the buildings until the street where the measurement is being recorded.

5.2 Measured path loss

In order to extract path loss samples from the route measurements explained in Section 3.3.1, the different received signals (RSCP) were averaged over 2 m length every 5 m distance (see Figure 5.2).

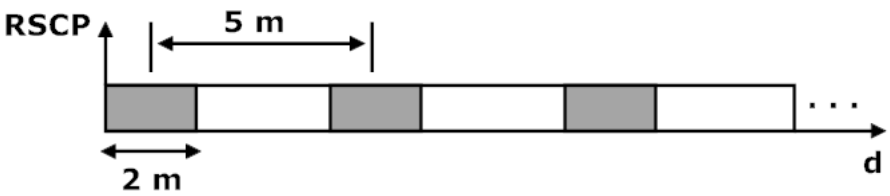

Figure 5.2: Sampling intervals over distance for path loss calculation.

It has been been checked that averaging the signal like this does not change anything with respect to the original trends calculated without averaging the signal over a certain distance.

The different calculated path loss samples are plotted against distance and compared with the different models seen in Chapter 2. As an example, Figure 5.3 shows the measured path loss for a signal received at 2.4 m from a base station placed at 34 m height. The rest of the graphics can be seen in Appendix D, Section D.3.

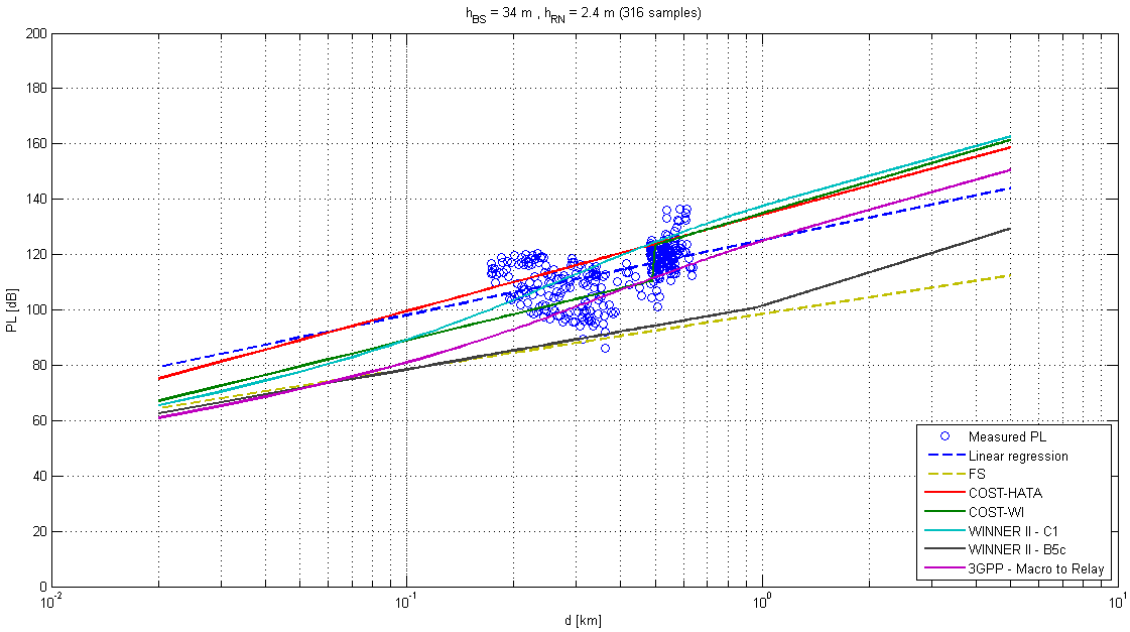

Figure 5.3: Measured path loss at 2.4 m from a base station at 34 m height.

The dashed blue line in the graphic shows the linear regression calculated over the samples. This means that an expression similar to Equation 5.4 relating path loss and distance can be obtained for each group of samples.

$$PL_{linear\,regression} = k_0 + k_1 \cdot d \tag{5.4}$$

With this linear regression, it is possible to get an idea of the trend followed by path loss. The slope k_1 $[^{dB}/_{dec}]$ can be seen as a propagation coefficient giving an estimation on how the path loss grows with distance.

The next sections summarize this linear regression calculated for the different groups of samples according to the different base station and receiver antenna heights. A comparative between path loss measured at different receiver antenna heights is done. Also a general comparative with the existing models is conducted.

5.2.1 Receiver antenna at 2.4 m

Table 5.1 collects the different constant and slope from the linear regression of the path loss calculated with the receiver antenna at 2.4 m height.

BASE STATION HEIGHT	CONSTANT, $k_0[dB]$	SLOPE, $k_1[^{dB}/_{dec}]$
17 m	121.36	10.58
19 m	110.91	30.99
21 m	114.36	0.54
23 m	125.52	35.58
25 m	109.28	7.19
27 m	113.15	12.55
34 m	125.15	26.99

Table 5.1: Measured path loss trends with receiver antenna at 2.4 m.

The calculated constant term varies from 109.28 dB and 125.52 dB (16.24 dB). The slope shows a big variation from 0.54 dB/dec to 35.99 dB/dec (35.45 dB/dec). This is due to the fact that not so many samples are considered in this analysis. To get believable slopes it is necessary to obtain samples in a bigger range of distances (in this study, with the measurements performed, almost all the samples are recorded at a distance between 200 m and 1 km as it can be seen in Figure 5.3, which is not enough to trust the calculated slope because samples outside this range can change it significantly.). This is happening also for the samples measured at 5.0 m showed in the next subsection.

5.2.2 Receiver antenna at 5.0 m

Table 5.2 collects the different constant and slope from the linear regression of the path loss calculated with the receiver antenna at 5.0 m height. This time, the constant term varies from 106.43 dB to 130.51 dB (24.08 dB) and the calculated slope from -2.34 dB/dec (this is not a possible value since it means that path loss decreases with distance, so the power is not being attenuated with distance, it is received higher power than the transmitted power) to 45.61 dB/dec (47.95 dB/dec).

BASE STATION HEIGHT	CONSTANT, $k_0[dB]$	SLOPE, $k_1[^{dB}/_{dec}]$
17 m	114.14	5.97
19 m	110.64	38.41
21 m	107.14	-2.34
23 m	130.51	45.61
25 m	106.43	9.06
27 m	111.45	16.12
34 m	119.01	22.80

Table 5.2: Measured path loss trends with receiver antenna at 5.0 m.

5.2.3 Comparative between path loss at 2.4 m and path loss at 5.0 m

To get an idea of how the constant term in the measured path loss grows with base station height (the highest the base station is, the longest the path covered by the signal is, so path loss increases with base station height), a linear regression is made. Figure 5.4 and Figure 5.5 illustrate this fact.

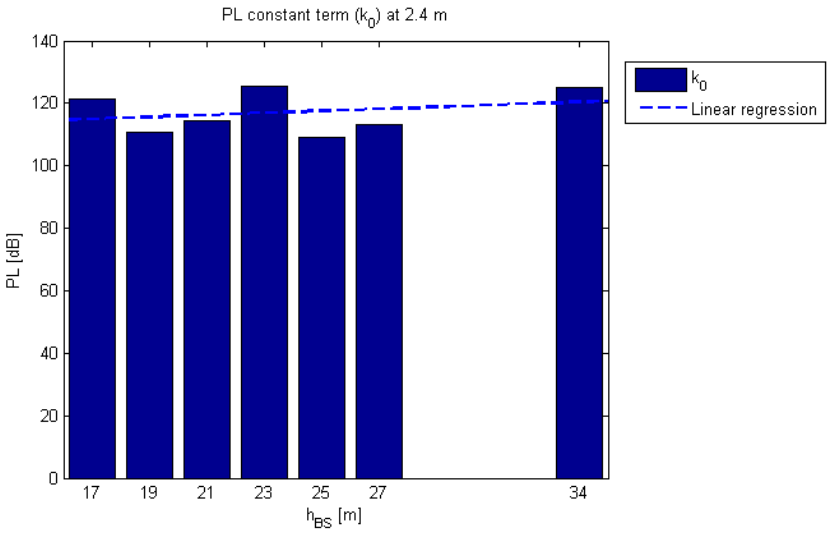

Figure 5.4: Path loss at 2.4 m constant term with respect to base station height.

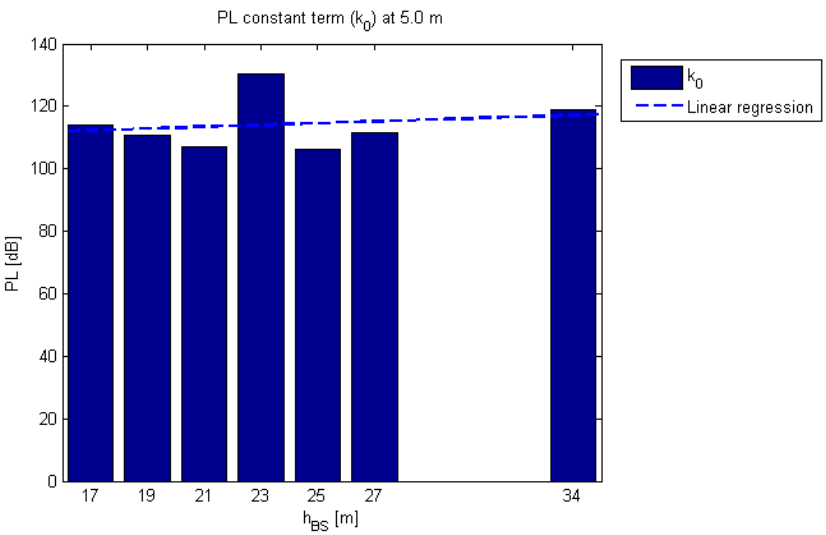

Figure 5.5: Path loss at 5.0 m constant term with respect to base station height.

Since the path loss compared with base station height shows the same trend for the receiver at 2.4 m and 5.0 m it is possible to get an estimation of how much is the difference in measured path loss at these two heights. For this purpose, MPLHG is defined.

PARAMETER	NAME
$MPLHG$	Measured Path Loss Height Gain [dB]

Table 5.3: Parameter defined to study measured path loss height gain.

$$MPLHG = PL_{measured240} - PL_{measured500} = 2.10\,dB \tag{5.5}$$

MPLHG indicates that the measured path loss is 2.10 dB higher with the receiver antenna at 2.4 m that an 5.0 m. In other words, the highest the antenna, the lowest the path loss (the path covered by the signal should be shorter).

5.2.4 Comparative with existing models

A visual comparison between the measured path loss, the linear regression calculated and the existing path loss models can be seen for each group of recorded samples in Appendix D.

It is difficult to make a conclusion about which model fits better the measured path loss since it exists a great variation in level, and the samples are concentrated at very similar distances.

This high variation in path loss for similar distances can be explained by the difficulty of including the horizontal gain of the base station in the analysis (as the measurements were done in an urban macro-cell environment, it is not realistic to consider the direct ray from the base station antenna to the receiver, and the fact of recording the samples on the move can introduce big changes in the horizontal gain since bearing is changing at every moment. [1])

[1]The worst situation possible is think about describing a circle with constant radio around a base station. Ahead of it, a lot of power is received. On the sides, less power. And at the back, since the signal proceeds from the backside lobe, the received power is even lower. When computing the measured path loss as explained before, this power levels belong to a same distance, but the level variation is enormous.

Chapter 6

CONCLUSIONS AND FUTURE WORK

After the different results obtained from the simulations and real measurements in an urban macro-cell environment, it is clear to conclude that the use of relay nodes is beneficial to enhance cell edge coverage and capacity.

6.1 Conclusions on path loss models

After the research on different path loss models, the comparative between them and the system level simulation, it is clear the importance of the path loss models in the design of cellular systems. Theoretically from the simulation, it is possible to see how the overall SINR and throughput of the network improves when introducing a relay placed at cell edge.

6.2 Conclusions on relay deployment

When measuring at two different heights (2.4 m and 5.0 m) it was found that the signal quality was better at 2.4 m. More power was received at 5.0 m but also more interference. This was due to fact of the signal propagation over the buildings.

When comparing two different types of antenna (directional and omnidirectional) at the same height (5.0 m) it was found that the result depended on the situation. Considering a probable relay node location placed in an urban area, in-between buildings it was possible to see how the directional antenna performed better filtering interference and increasing the quality of the potential backhaul link, so in principle, a directional antenna at the relay side of the backhaul link should be better.

Considering LOS conditions, the gain of using a directional antenna is even higher. For closed environments with small streets and high buildings were it is very difficult to point well the directional antenna towards the desired donor, the omnidirectional antenna could perform better since it is easier to catch more reflections of the desired signal on the buildings.

6.3 Future work

The next step on this project should be to extract a realistic empirical path loss model based on measurements. To achieve this, it is necessary to plan the measurement campaign in a different way as done in this project. It is not so easy to take samples to analyze signal quality in interference conditions and path loss at the same time.

It is necessary to be very specific with the measurement conditions fixing as many aspects as possible (i.e. measure in clear LOS or NLOS, keeping always within the main lobe influence). Also a long range of distances should be measured to evaluate reliable trends.

References

[1] Steven W. Peters, Ali Y. Panah, Kien T. Truong, and Robert W. Heath. Relay Architectures for 3GPP LTE-Advanced. *URASIP Journal on Wireless Communications and Networking*, 2009.

[2] T. Beniero, S. Redana, J. Hamalainen, and B. Raaf. Effect of Relaying on Coverage in 3GPP LTE-Advanced. *Vehicular Technology Conference. IEEE*, 2009.

[3] E. Lang, S. Redana, and B. Raaf. Business Impact of Relay Deployment for Coverage Extension in 3GPP LTE-Advanced. *Communications Workshops. ICC. IEEE International Conference*, 2009.

[4] Takehiro Nakamura. Proposal for Candidate Radio Interface Technologies for IMT-Advanced Based on LTE Release 10 and Beyond (LTE-Advanced). *3GPP. Mobile ITU-R WP 5D 3rd Workshop on IMT-Advanced*, 2009.

[5] Vijay K. Garg. *Wireless Communications and Networking*. Elsevier Inc., 2007.

[6] S. T. Rapaport. *Wireless Communications - Principles and Practice*. Prentice Hall Communications Engineering and Emerging Technologies Series, 2002.

[7] Y. Okumura, E. Ohmori, T. Kawano, and K. Fukuda. Field Strength and its Variability in VHF and UHF Land-Mobile Radio Service. *Review of the Electrical Communication Laboratory*, 16, 1968.

[8] COST 231. Evolution of Land Mobile Radio, 1999. Final Report, Path Loss Models.

[9] COST 259. Wireless Flexible Personalized Communications, 2001. Final Report, Directional Channel Models.

[10] IST-4-027756 WINNER II D1.1.2 V1.2, 2008. Channel Models.

[11] 3GPP TR 36.814 V9.0.0 (2010-03), 2010. Technical Specification - Group Radio Access Network. Further advancements for E-UTRA Physical Layer Aspects (Release 9).

[12] IEEE 802.16j - 06/013r3, 2007. Multi-hop Relay System Evaluation Methodology (Channel Model and Performance Metric).

[13] Telenor. `http://www.telenor.dk/english/index.aspx`. Accessed on 25th of May 2011.

[14] Maria Morari. Best Tourism, Aalborg. `http://www.bestourism.com/items/di/1103?title=Aalborg&b=174`. Accessed on 25th of May 2011.

[15] Quang Hien Chu, Jean-Marc Conrat, and Jean-Christophe Cousin. On the Impact of Receive Antenna Height in a LTE-Advanced Relaying Scenario. *Proceedings of the 3rd European Wireless Technology Conference*, 2010.

[16] Jens Zander, Seong-Lyun Kim, Magnus Almgren, and Olav Queseth. *Radio Resource Management for Wireless Networks.* Artech House Publishers, 2001.

[17] Preben Mogensen, Wei Na, Istvan Z. Kovacs, Frank Frederiksen, Akhilesh Pokhariyal, Klaus I. Pedersen, Troels Kolding, Klaus Hugl, and Markku Kussela. LTE Capacity compared to the Shannon Bound. *IEEE*, 2007.

[18] RHODE & SCHWARZ radio network analyzers TSMU,TSMW. `http://www2.rohde-schwarz.com/en/products/test_and_measurement/Drive_Test_Tools/`. Accessed on 27th of May 2011.

[19] Dansk Microbølge Teknik ApS. `http://www.dmtonline.dk`. Accessed on 27th of May 2011.

[20] Huber+Shuner. `http://www.hubersuhner.com`. Accessed on 27th of May 2011.

[21] Electronic Communications Committee (ECC) within the European Conference of Postal and Telecommunications Administrations (CEPT). *UMTS Coverage Measurements*, 2007.

[22] 3GPP TS 25.211 (2010-09), 2010. Physical channels and mapping of transport channels onto physical channels (FDD).

[23] Henrik Asplund, Jan-Erik Berg, and Troels B. Sørensen. The Influence of a Base Station Antenna Tilt on Path Loss. *Antennen och dess Omvä rld, Kopplingen mellan Antenn och Radiosystem*, 1999.

Appendix A

SYSTEM LEVEL SIMULATION

As explained in Chapter 2, propagation path loss models play an important role in design of cellular systems. In this appendix, it will be investigated the influence of using different path loss models on network system level design.

A.1 Simulation

RUNE (Rudimentary Network Emulator) is a set of MATLAB functions designed to provide the necessary tools for simulating cellular systems. This functions handle various aspects of a cellular system such as mobiles, base stations, connectivity, propagation loss, interference, ... [16]

With the help of RUNE functions, and some modifications, a relay simulation is performed. The main objective is to investigate the influence of a relay inside a network besides of the importance of the path loss calculation on network planning.

A.1.1 Scenario

The simulation is considering 4 sites with 3 base stations each. Cells are distributed following the typical hexagonal pattern where base stations are placed at the vertex of each cell as indicated in Figure A.1. This fact implies using sectorial antennas covering 120° each.

For the analysis, two different inter-site distances are taken into account (ISD=500 m and ISD=1732 m) according to the 3GPP specifications [11] for urban (case 1) and suburban (case 3) macro cellular environments.

Only one relay is considered and it is placed in the middle of several base stations (in

order to evaluate it in a high interference condition). The distance imposed between the base station and the relay node is 0.7R.

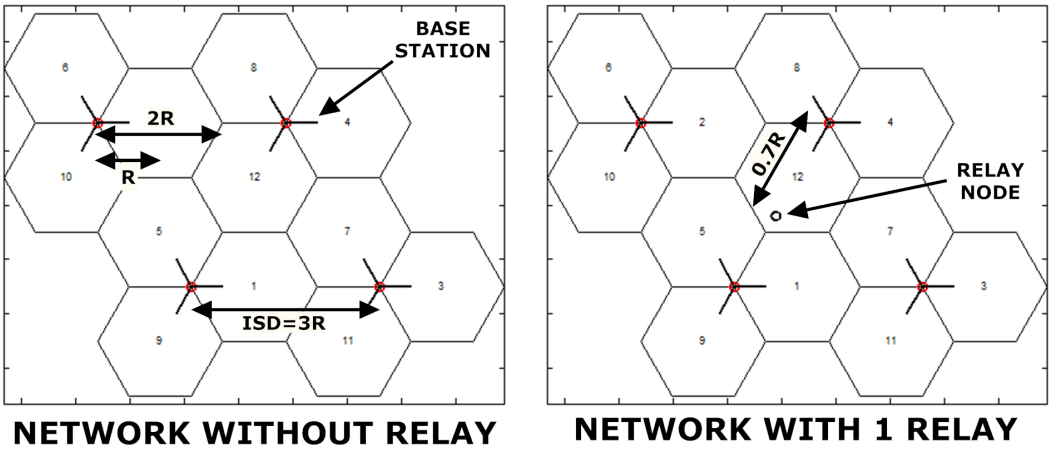

Figure A.1: BS and RN disposition and cell distribution for the network simulation.

A.1.2 Parameters

The simulation is performed at a frequency of 2 GHz, supposing a signal bandwidth of 10 MHz. To include noise, a power spectral density of -174 dBm/Hz is selected.

An in-band situation is analyzed, so also the link between relay node and user equipment is considered at 2 GHz.

GENERAL	
PARAMETER	**VALUE**
ISD	500 m / 1732 m
f_c	2 GHz
BW	10 MHz
Noise PSD	-174 dBm/Hz

Table A.1: Summary of the general parameters in the simulation.

Each base station is supposed at 32 m height and transmits 46 dBm. The antenna in a base station is considered to be directional with a gain of 14 dBi. The pattern for this antenna can be seen in Table A.2.

As it can be seen in Figure A.1, each site counts on 3 different base stations, pointing to different directions. This direction is indicated in the figure with a black line coming out from the red point.

BASE STATION (BS)	
PARAMETER	**VALUE**
P_{tx}	46 dBm
h_{BS}	32 m
G_{BS}	14 dBi
Antenna Pattern	$A(\theta) = -min\left(12\left(\frac{\theta}{70}\right)^{2.25}\right)\ dB$
NF	5 dB

Table A.2: Summary of the parameters for the BS in the simulation.

The relay node connected to base station in cell 12 (see Figure A.1) is simulated at 5 m height. It uses a different antenna in reception (directional with a gain of 7 dBi) and in transmission (omnidirectional with a gain of 5 dBi). This is done in order to filter interference in the link between base station and relay node. The transmitted power from the relay is considered to be 30 dBm (lower than base station). A noise figure of 5 dB is also taken into account for the relay node.

RELAY NODE (RN)	
PARAMETER	**VALUE**
P_{tx}	30 dBm
h_{RN}	5 m
G_{RN} (RX)	7 dBi
Antenna Pattern (RX)	$A(\theta) = -min\left(12\left(\frac{\theta}{70}\right)^{2.20}\right)\ dB$
G_{RN} (TX)	5 dBi
Antenna Pattern (TX)	$A(\theta) = 0\,dB$ (omnidirectional)
NF	5 dB

Table A.3: Summary of the parameters for the RN in the simulation.

Finally, the user equipment is simulated at 1.5 m height with an omnidirectional antenna of 0 dBi and a noise figure of 9 dB.

USER EQUIPMENT (UE)	
PARAMETER	**VALUE**
h_{UE}	1.5 m
G_{UE} (RX)	0 dBi
NF	9 dB

Table A.4: Summary of the parameters for the UE in the simulation.

A.2 Performance

The objective in this simulation is to evaluate the relayed link: backhaul link and access link. To do this, the different families of path loss models will be used (see Table A.5). For each family, a model for the different links is assigned.

FAMILY	DIRECT LINK	BACKHAUL LINK	ACCESS LINK
HATA	COST-Hata	COST-Hata	COST-Hata
CWI	COST-WI	COST-WI	COST-WI
WINNER	C1	C1	B1
3GPP	Macro to UE	Macro to Relay	Relay to UE
WiMAX	B	E (CWI)	F

Table A.5: Summary of the different families of path loss models used in the simulation.

A.3 Calculations

A.3.1 Backhaul link: base station to relay node (ISD=500)

To evaluate this link for the different path loss models, signal to interference-noise ratio (SINR) and throughput (TP) are calculated. It is also evaluated the use of an omnidirectional and a directional antenna to compare the different behavior at the relay part of the link.

SINR

$$SINR_{BS-RN} = P_{rx,BS-RN} - I_{BS-RN} - N \tag{A.1}$$

$$P_{rx,BS-RN} = P_{tx,BS} + G_{BS} - PL_{BS-RN} + G_{RN} \tag{A.2}$$

$$I_{BS-RN} = 10\,log_{10}\left(\sum_{BS\neq donor} 10^{-\left(\frac{P_{rx,BS-RN}}{10}\right)}\right) \tag{A.3}$$

$$N = NPSD + 10\,log_{10}(BW) + NF \tag{A.4}$$

Figure A.2 shows the different SINR obtained with the different path loss models applied to the backhaul link and for different types on antenna in the relay part. As it can be seen, SINR is much better with the directional antenna for all the models.

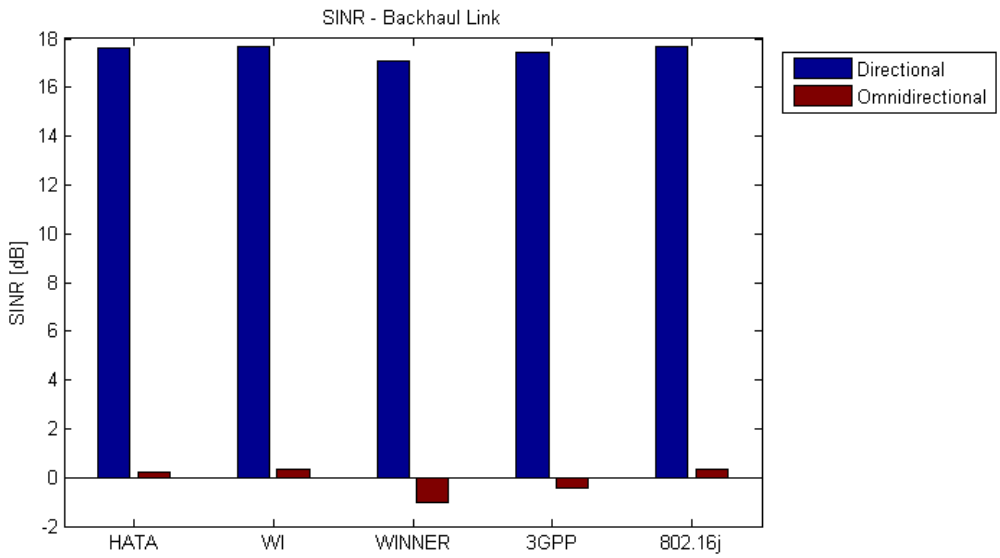

Figure A.2: SINR in the backhaul link for the different path loss models (ISD=500).

All of the models estimate a similar SINR with the directional antenna, but with the onmidirectional WINNER and 3GPP predicts the worst SINR. In the case of WINNER, this is because the WINNER C1 model applied to the backhaul link predicts the highest path loss making the desires received signal very weak in comparison with the amount of interference received.

THROUGHPUT

By simply applying Shannon's formula, it is possible to map the previous calculated SINR into throughput. [17]

$$TP_{BS-RN} \quad = \quad BW \cdot log_2\left(1 + 10^{\left(\frac{SINR_{BS-RN}}{10}\right)}\right) \tag{A.5}$$

Figure A.3 shows the calculated throughput for each different path loss model and the different antennas. As expected since throughput is a direct map of SINR, it is much

better for the directional antenna.

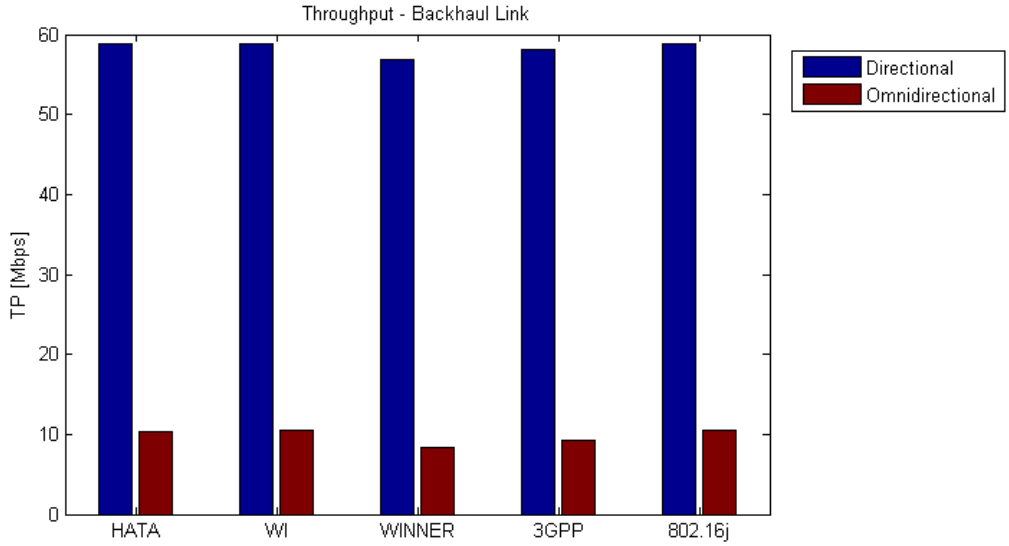

Figure A.3: TP in the backhaul link for the different path loss models (ISD=500).

To summarize what happens in this bakhaul link, it is possible to say that COST-Hata, COST-WI and WiMAX estimate a very similar behavior; and WINNER and 3GPP estimate something worse (higher interference).

A.3.2 Access link: relay node to user equipment (ISD=500)

This link is evaluated and compared for the different models calculating area covered by the relay, SINR and TP. This calculations are done by analyzing statistically what happen when a single user is in the network. To do this, a single user equipment is dropped into different points of the network (corners of 10 m x 10 m squares sampling the simulated network).

AREA COVERED

The criteria selected to calculate the area covered by the relay is highest power. This means, that when an user receives higher power from the relay node than from any other base station, it is connected to the relay. Figure A.4 shows the different cell percentage covered according to the different models.

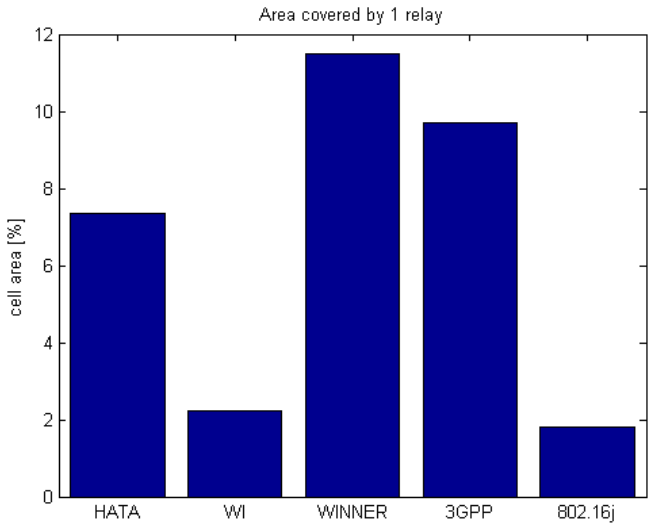

Figure A.4: Area covered by a relay calculated with the different path loss models (ISD=500).

Just to illustrate this a little bit more, Figure A.5 shows the area covered in dark red calculated with WINNER path loss models. It predicts almost a 12% of the cell covered by a single relay. This is due to the great difference between the WINNER C1 model applied for the direct link and the WINNER B1 applied for the access link. WINNER B1 predicts much lower path loss for points close to the relay.

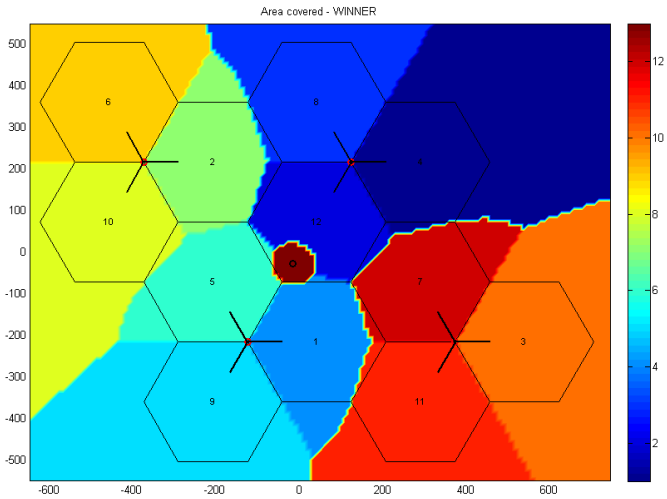

Figure A.5: Area covered by the relay calculated with WINNER path loss models (ISD=500).

SINR

$$SINR_{RN-UE}(x,y) = P_{rx,RN-UE}(x,y) - I_{BS-UE}(x,y) - N \tag{A.6}$$

$$P_{rx,RN-UE}(x,y) = P_{tx,RN} + G_{RN} - PL_{RN-UE}(x,y) + G_{UE} \tag{A.7}$$

$$I_{BS-UE}(x,y) = 10\,log_{10}\left(\sum_{BS} 10^{-\left(\frac{P_{rx,BS-UE}(x,y)}{10}\right)}\right) \tag{A.8}$$

$$N = NPSD + 10\,log_{10}(BW) + NF \tag{A.9}$$

Calculating SINR for all the points of the grid covered by the relay, Figure A.6 is obtained.

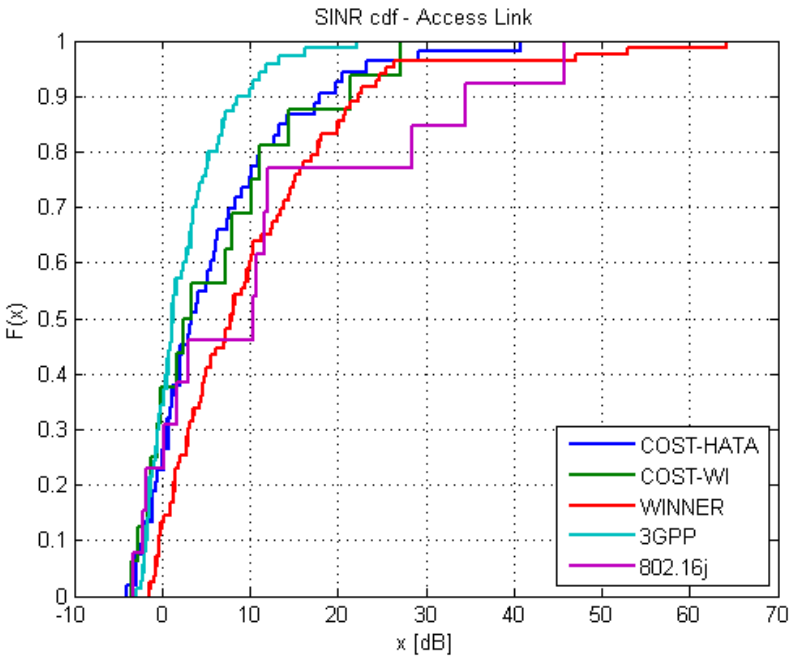

Figure A.6: SINR in the access link for the different path loss models (ISD=500).

As expected from the covered area calculations, WINNER presents the best performance (higest area covered implies also highest power at further points, so probably also highest SINR). The model that presents the worst estimation of SINR is 3GPP.

THROUGHPUT

In a similar way as done for the backhaul link, the SINR of the access link can be mapped into TP by applying Shannon's formula.

$$TP_{RN-UE}(x,y) \quad = \quad BW \cdot log_2\left(1 + 10^{\left(\frac{SINR_{RN-UE}(x,y)}{10}\right)}\right) \tag{A.10}$$

Figure A.7 shows the calculated throughput for all of the points of the grid covered by the relay. Again, as it happened in SINR, WINNER estimates the best throughput and 3GPP the worst.

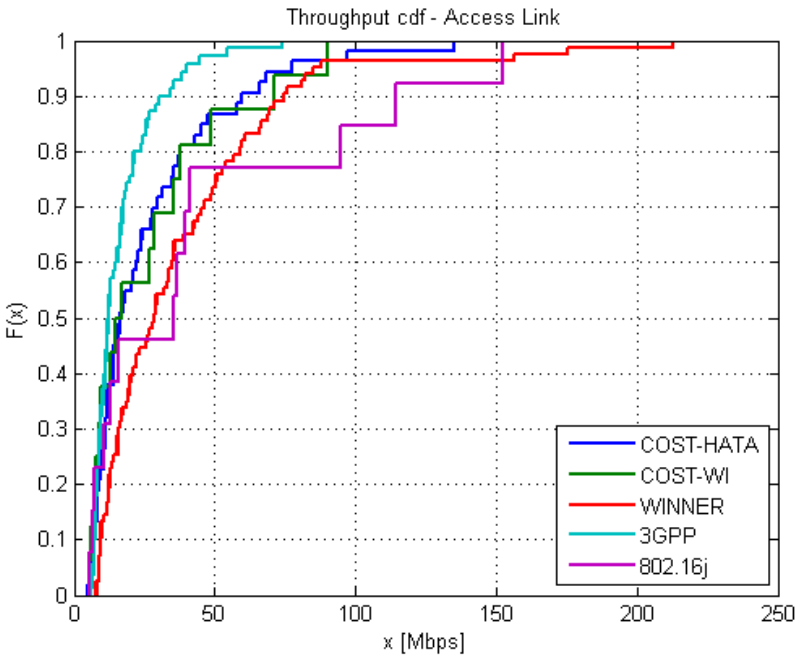

Figure A.7: TP in the access link for the different path loss models (ISD=500).

A.3.3 Overall link: backhaul + access (ISD=500)

To evaluate the different path loss models over the total link between base station - relay node - user equipment, the throughput over the 2 hops is calculated and combined to get the overall throughput. The effective throughput is the throughput that a single user equipment experiences from a two-hop transmission when that user is alone in the network.

OVERALL THROUGHPUT

$$TP_{2hops}(x,y) \quad = \quad min\,(TP_{BS-RN}, TP_{RN-UE}(x,y)) \tag{A.11}$$

Figure A.8 shows the overall throughput over 2 hops calculated for the different models and compared with the case of no relay. It is clearly seen how the throughput is much better when a relay is included in the network. This time, the quality of the backhaul link is very important and that is why COST-WI offers the best performance.

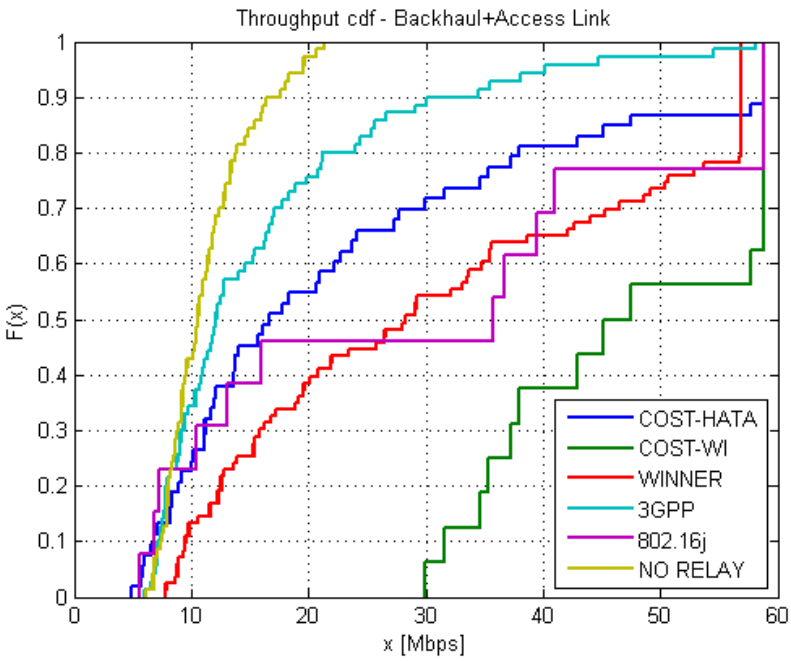

Figure A.8: TP in the overall link (backhaul+access) for the different path loss models (ISD=500).

EFFECTIVE THROUGHPUT

The effective throughput is calculated assuming an inband relay working in half-duplex mode. t_r represents the part of the time used in the backhaul transmission and (1-t_r) the part used in the access transmission.

$$TP_{eff}(x,y) \quad = \quad t \cdot TP_{BS-RN} \tag{A.12}$$

$$t_r \cdot TP_{BS-RN} = (1 - t_r) \cdot TP_{RN-UE}(x, y) \tag{A.13}$$

$$t_r = \frac{TP_{RN-UE}(x, y)}{TP_{RN-UE}(x, y) + TP_{BS-RN}} \tag{A.14}$$

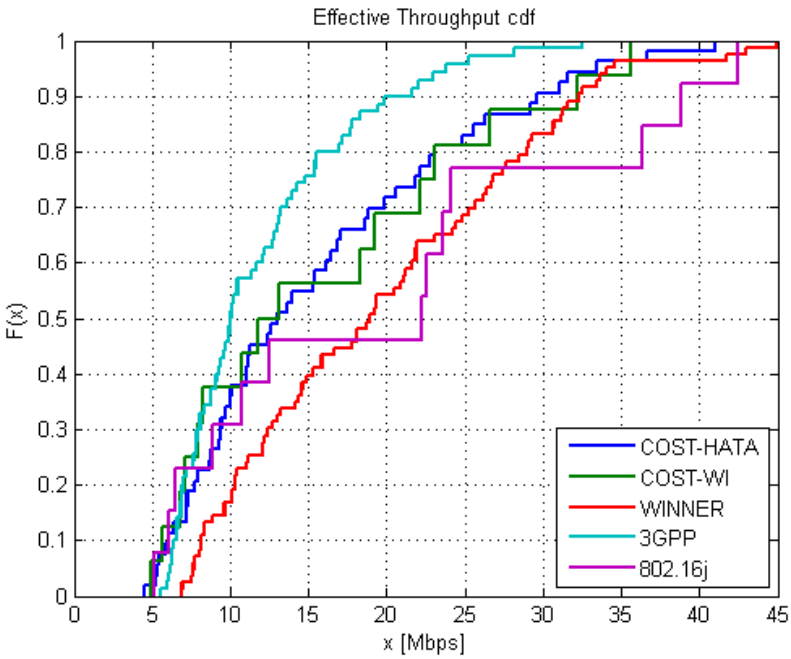

Figure A.9: Effective TP for the different path loss models (ISD=500).

As it can be seen in Figure A.9, WINNER estimates the best effective throughput, COST-Hata and COST-WI perform very similar and the worst estimation belongs to 3GPP.

A.4 Other representations (ISD=500)

Other maps like RSSI (Received Signal Strength) or SINR over the total network area were also calculated for all the models. Figure A.10 and A.11 show an example of the calculations with the 3GPP models.

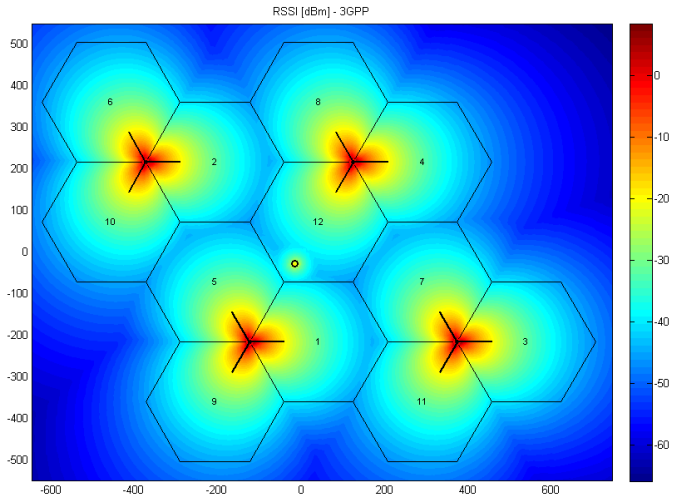

Figure A.10: RSSI calculated with the 3GPP path loss models (ISD=500).

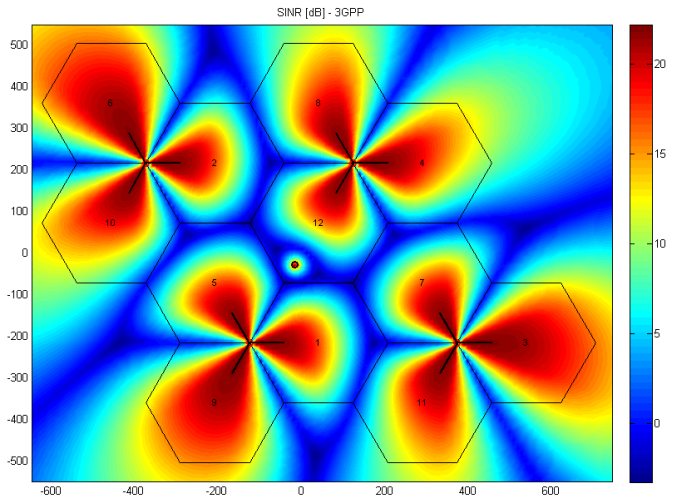

Figure A.11: SINR calculated with the 3GPP path loss models (ISD=500).

A.4.1 Backhaul link: base station to relay node (ISD=1732)

In the same way as as done for ISD=500, for ISD=1732 it is possible to evaluate the backhaul link for the different models by calculating SINR and TP. Once again, it is compared the use of a directional antenna or a directional anntena ath the relay side.The expressions remain similar as before, the only change is the distance between nodes, which is higher in this case.

SINR

Figure A.12 shows the different SINR obtained with the different path loss models applied to the backhaul link and for different types on antenna in the relay part. As it can be seen, SINR is much better with the directional antenna for all the models.

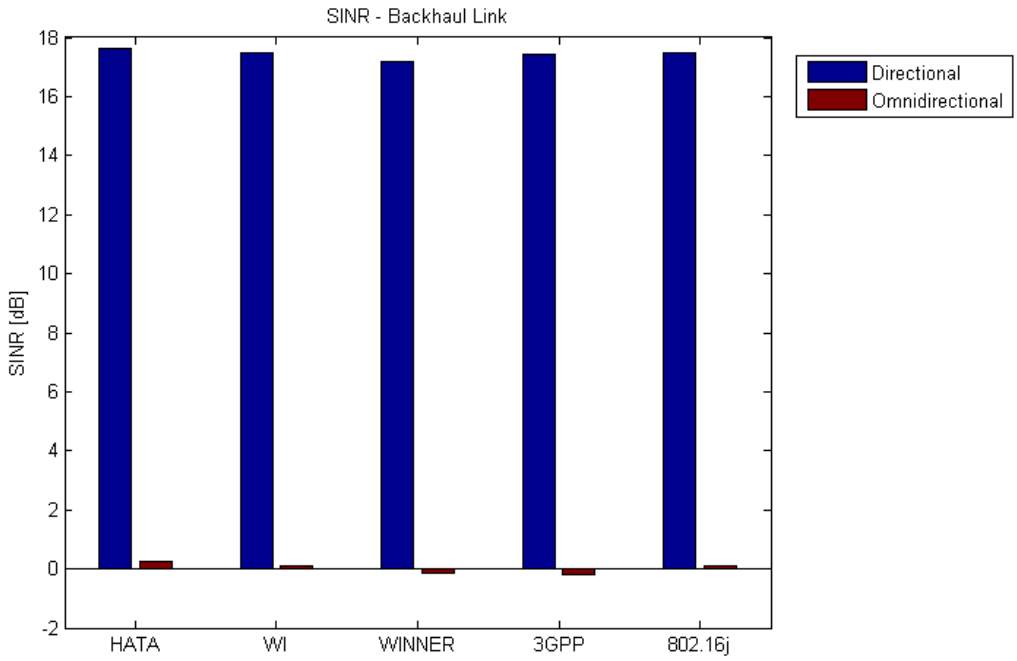

Figure A.12: SINR in the backhaul link for the different path loss models (ISD=1732).

All of the models estimate a similar SINR with the directional antenna. The same happens with the omnidirectional, this time there is not so much difference between the models. This means that at long distances all of the models perform very similar.

THROUGHPUT

Figure A.13 shows the calculated throughput for each different path loss model and the different antennas. As expected since throughput is a direct map of SINR, it is much better for the directional antenna.

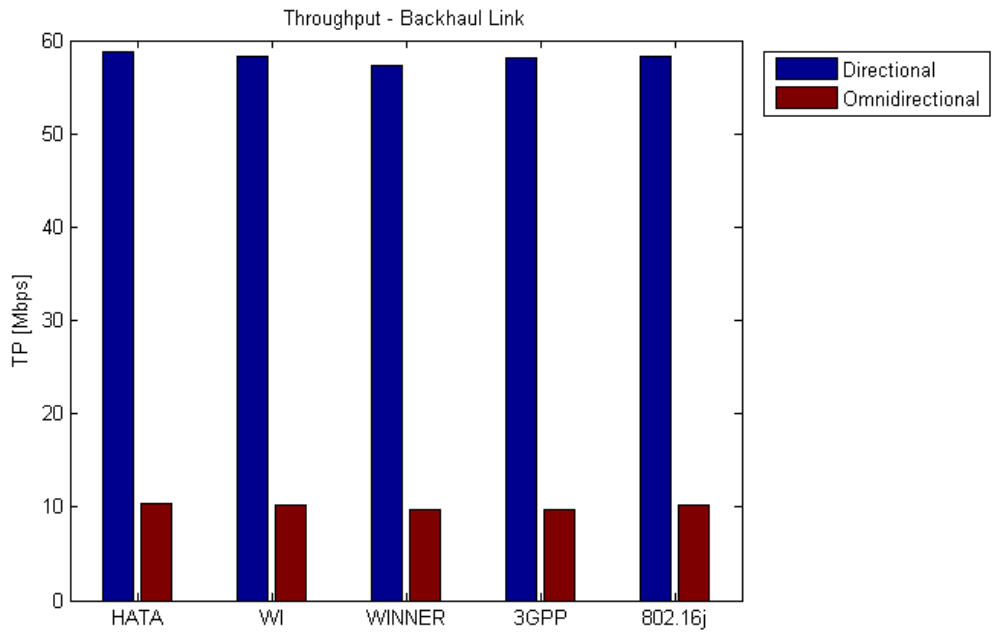

Figure A.13: TP in the backhaul link for the different path loss models (ISD=1732).

A.4.2 Access link: relay node to user equipment (ISD=1732)

For ISD=1732 also area covered by the relay, SINR and TP are calculated.

AREA COVERED

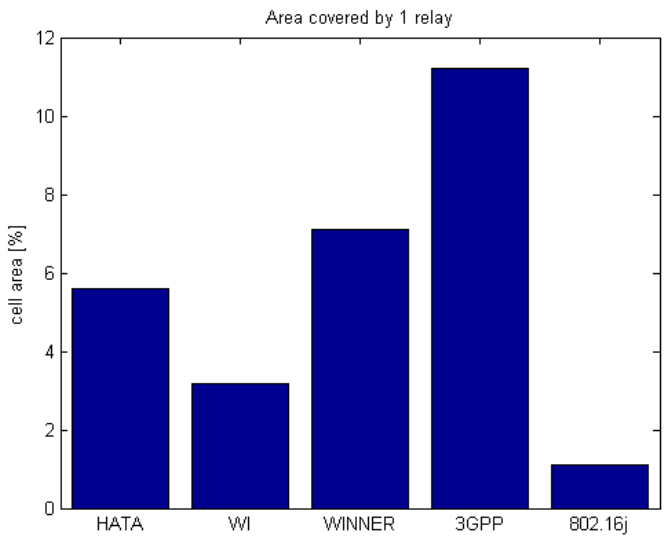

Figure A.14: Area covered by a relay calculated with the different path loss models (ISD=1732).

This time is the 3GPP model the one that estimates a larger area covered by the relay (almost 12% of the cell). WiMAX predicts the smaller area covered (1%).

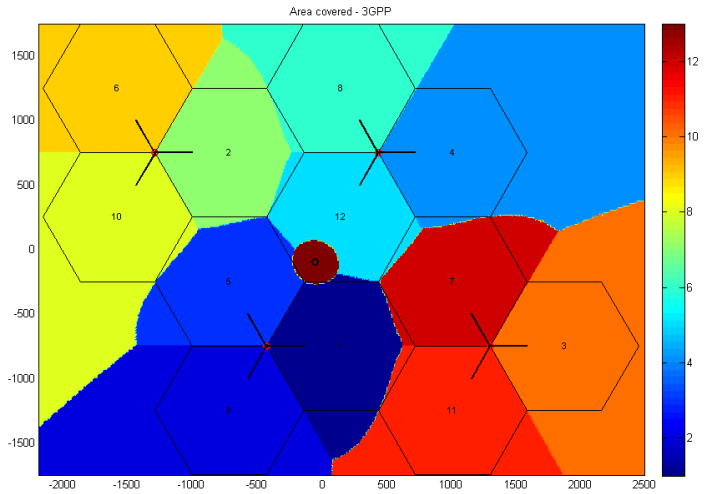

Figure A.15: Area covered by the relay calculated with 3GPP path loss models (ISD=1732).

SINR

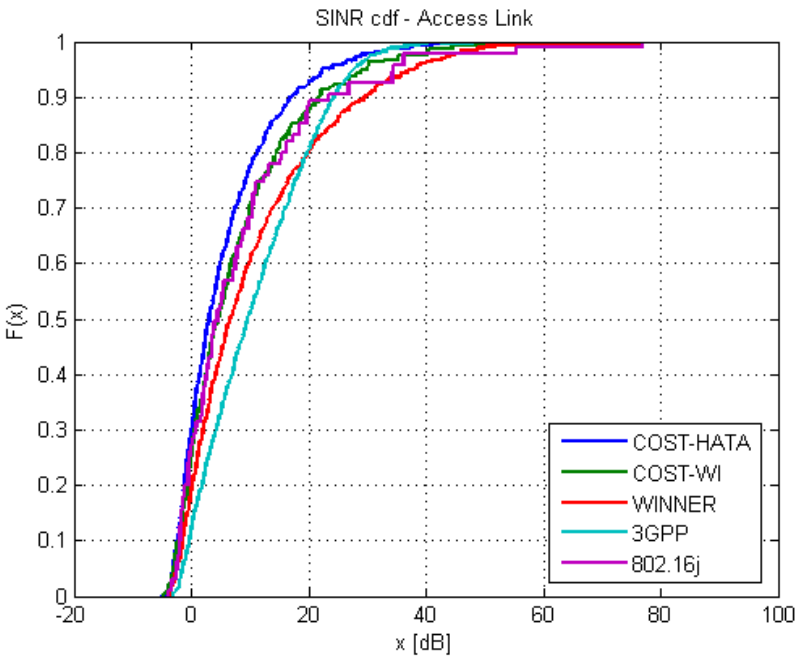

Figure A.16: SINR in the access link for the different path loss models (ISD=1732).

Figure A.16 shows the calculated SINR in the access link for the different path loss models. WINNER estimates the best SINR while COST-Hata estimates the worst SINR. This is exactly what will happen in Figure A.17 with the throughput in the access link for this ISD=1732. Anyway, all the models perform very similar, there are not big differences as with ISD=500.

THROUGHPUT

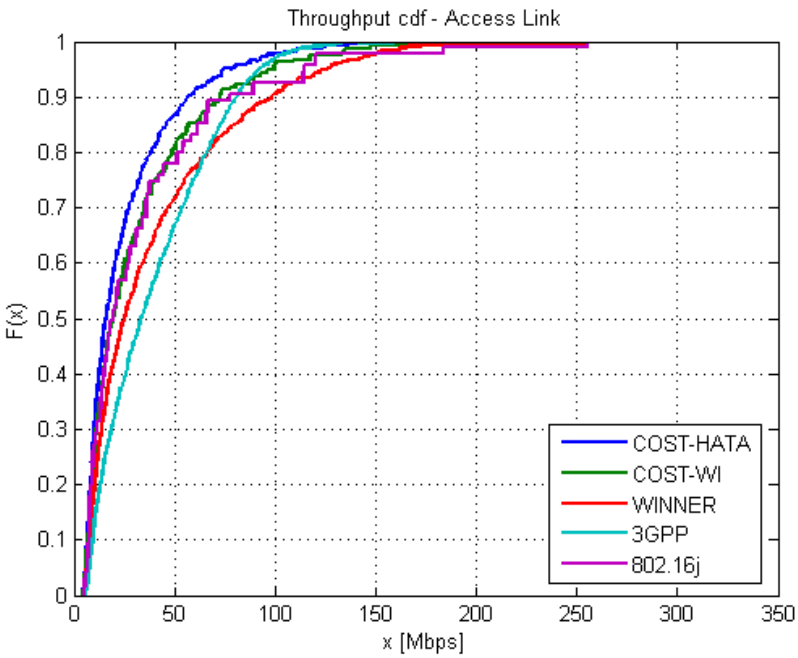

Figure A.17: TP in the access link for the different path loss models (ISD=1732).

A.4.3 Overall link: backhaul + access (ISD=1732)

Similarly to ISD=500, this total link connecting base station - relay node - user equipment can be analyzed by calculating the overall throughput over the 2 hops and the effective throughput.

OVERALL THROUGHPUT

Figure A.18 shows the overall throughput over 2 hops calculated for the different models and compared with the case of no relay. It is clearly seen how the throughput is much better when a relay is included in the network. 3GPP offers the most optimistic estimation.

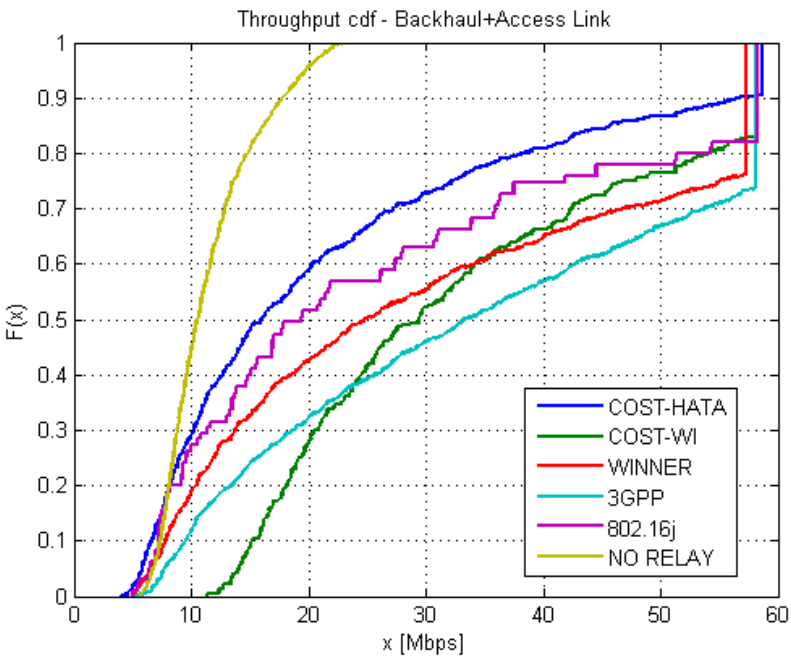

Figure A.18: TP in the overall link (backhaul+access) for the different path loss models (ISD=1732).

EFFECTIVE THROUGHPUT

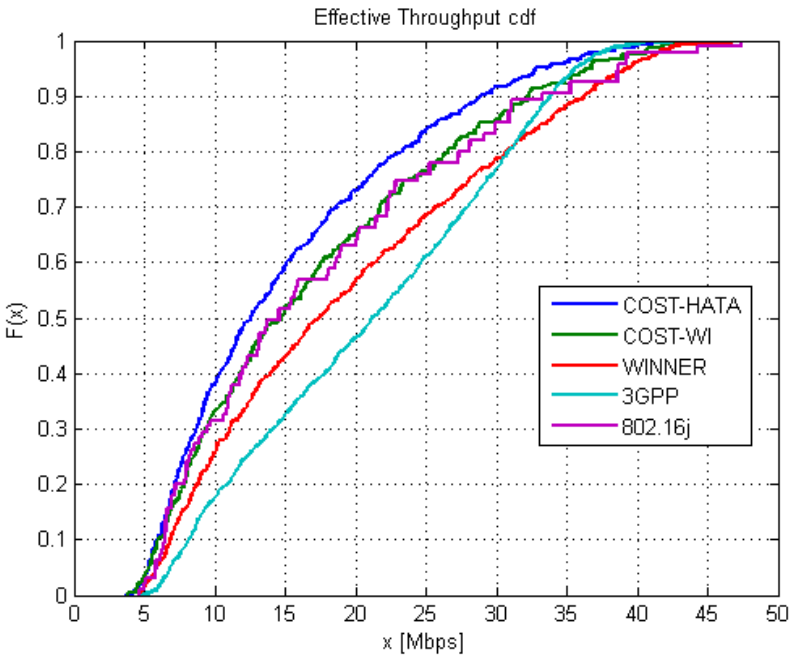

Figure A.19: Effective TP for the different path loss models (ISD=1732).

With respect to the effective throughput shown in Figure A.19, all of the models perform very similar.

A.5 Other representations (ISD=1732)

Other maps like RSSI (Received Signal Strength) or SINR over the total network area were also calculated for this ISD for all the models. Figure A.20 and A.21 show an example of the calculations with the COST-Hata models.

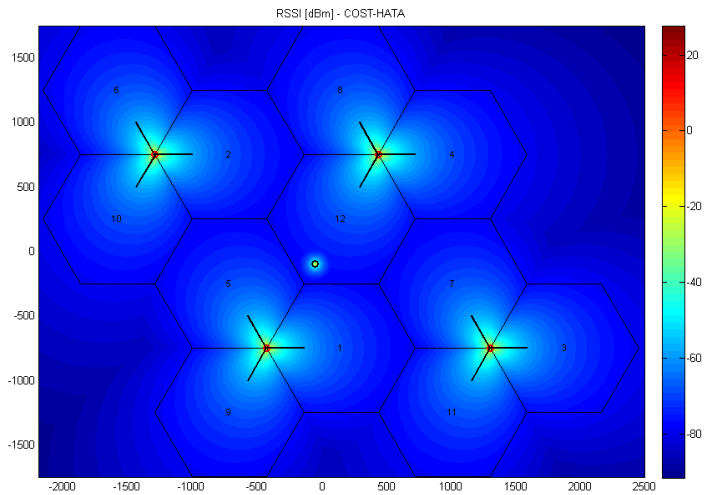

Figure A.20: RSSI calculated with the COST-Hata model (ISD=1732).

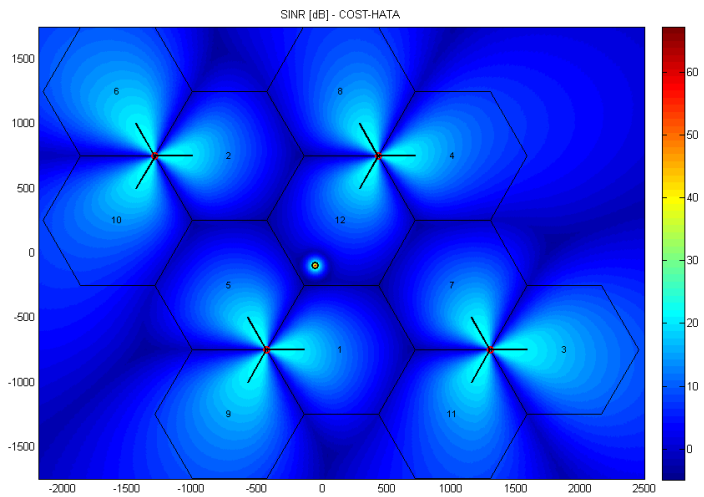

Figure A.21: SINR calculated with the COST-Hata model (ISD=1732).

A.6 Main conclusions on User Experience

For ISD=500, some of the models (WINNER) are more optimistic than other while predicting SINR, TP or area covered. With ISD=1732, all the models make very similar predictions.

It is clear that there is an advantage from using the directional antenna at the relay side, filtering interference and increasing SINR and TP to obtain a better overall link performance.

Appendix B

EQUIPMENT INFORMATION

This appendix collects different details about the equipment used in the measurement campaign as well as the setup performed.

B.1 Measurement equipment

ITEM	DESCRIPTION
Antenna AO-8050	Omnidirectional antenna (2 dBi) at 2.4 m
Antenna AO-8050	Omnidirectional antenna (2 dBi) at 5.0 m
Antenna SPA 2100/80/8	Directional antenna (80°horizontal, 8 dBi) at 5.0 m
Omni-TSMW connection	Coaxial cable (1.92 dB attenuation)
Omni-TSMU connection	Coaxial cable (2.02 dB attenuation)
Direct-TSMW connection	Coaxial cable (5.01 dB attenuation)
R&S TSMU	Radio Network Analyzer
R&S TSMW	Radio Network Analyzer
TSMU-Laptop1 connection	IE3194 cable
TSMW-Laptop2 connection	LAN cable
Fujitsu Siemens Lifebook S7020	Laptop used to record measurements fro R&S TSMU
Fujitsu Siemens Celsius H700	Laptop used to record measurements fro R&S TSMW

Table B.1: Description of the equipment used in the measurements.

B.1.1 R&S TSMU

TSMU is a radio network analyzer manufactured by RHODE & SCHWARZ [18]. It allows to perform measurements in different technologies such as WCDMA or GSM. It is capable to demodulate 3G broadcast information.

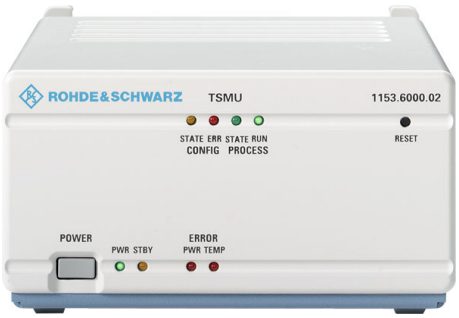

Figure B.1: TSMU radio network analyzer.

PARAMETER	VALUE
Frequency range	80 MHz - 3 GHz
Input bandwidth	4 MHz
Sampling rate	up to 20 $^{samples}/_{s}$
WCDMA sensitivity	up to -122 dBm
WCDMA dynamic range	up to 29 dB

Table B.2: TSMU specifications.

B.1.2 R&S TSMW

TSMW is the newest radio network analyzer manufactured by RHODE & SCHWARZ [18]. It is quite similar to the TSMU with the main difference that this model has two RF inputs which can be used to measure in two different technologies at the same time. With this scanner it is possible to measure LTE.

Figure B.2: TSMW radio network analyzer.

PARAMETER	VALUE
Frequency range	30 MHz - 6 GHz
Input bandwidth	20 MHz
Sampling rate	up to 200 $^{samples}/_{s}$
WCDMA sensitivity	up to -123 dBm
WCDMA dynamic range	up to 30 dB

Table B.3: TSMW specifications.

B.1.3 AO-8050

This is the omnidirectional antenna from DMT [19] selected to perform the measurements. A comparison between this antenna and the directional can be seen in Table B.4.

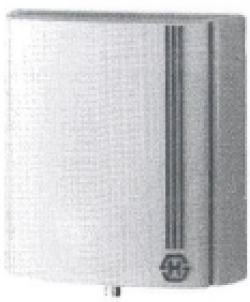

Figure B.3: Omnidirectional antenna AO-8050.

B.1.4 SPA 2100/80/8

This is the directional antenna from HUBER+SHUNER [20] selected to perform the measurements. A comparison between this antenna and the omnidirectional can be seen in Table B.4.

Figure B.4: Directional antenna SPA 2100/80/8.

PARAMETER	OMNIDIRECTIONAL	DIRECTIONAL
Model	DMT AO-8050	H+S SPA 2100/80/8
Frequency range	1710-2170 MHz	2000-2200 MHz
Impedance	50 Ω	50 Ω
VSWR	≤2.0	1.5
Polarization	linear, vertical	linear, vertical
Gain	2 dBi	8 dBi
3 dB beamwidth (V)	17.5°	60°
3 dB beamwidth (H)	360°	80°
Front-to-back ratio	-	15 dB

Table B.4: Comparative of antenna specifications.

B.1.5 Cables

All the connection cables were calibrated in the laboratory with the help of a signal generator and a spectrum analyzer, obtaining the following attenuation factors:

CABLE	ATTENUATION
Omnidirectional at 2.4 m - TSMW	1.92 dB
Omnidirectional at 5.0 m - TSMU	2.02 dB
Directional at 5.0 m - TSMW	5.01 dB

Table B.5: Attenuation in connection cables.

B.2 Measurement setup

To perform the measurements in the city, it was also necessary a van from the Center for PersonKommunikation (CPK) of Aalborg University to mount all the equipment. The deployment can be seen in Figure B.5. Notice above all antenna heights and distance between antennas.

Some pictures related to the setup can be seen at the end of this section(Figures B.7, B.8 and B.9).

With respect to the connectivity of the measurement system, it can be also seen in Figure B.6. It was necessary to use two different scanners to record signals simultaneously. Each of the scanners was operated from a different laptop.

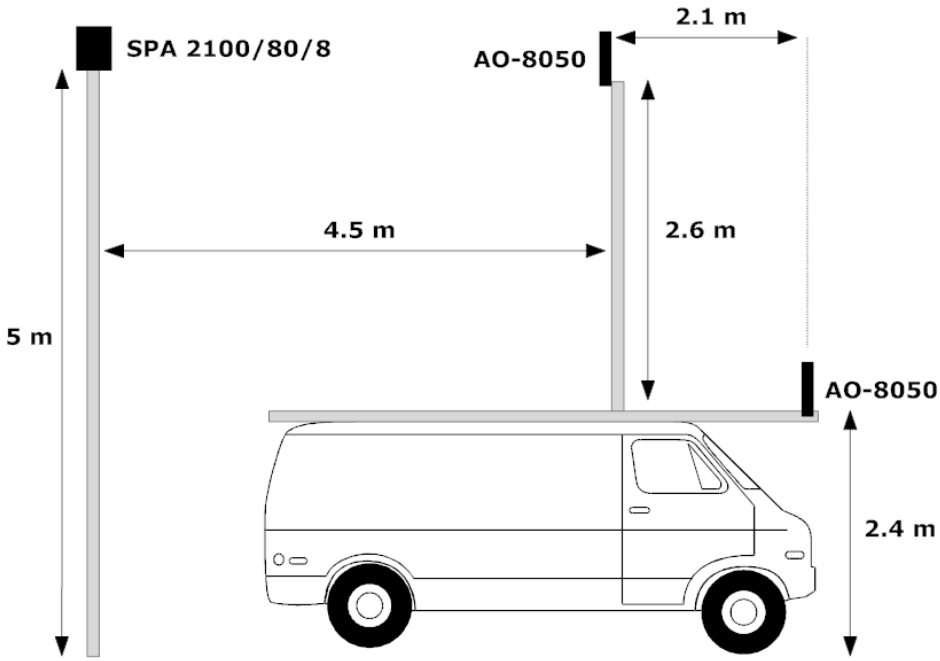

Figure B.5: Antenna layout over the van.

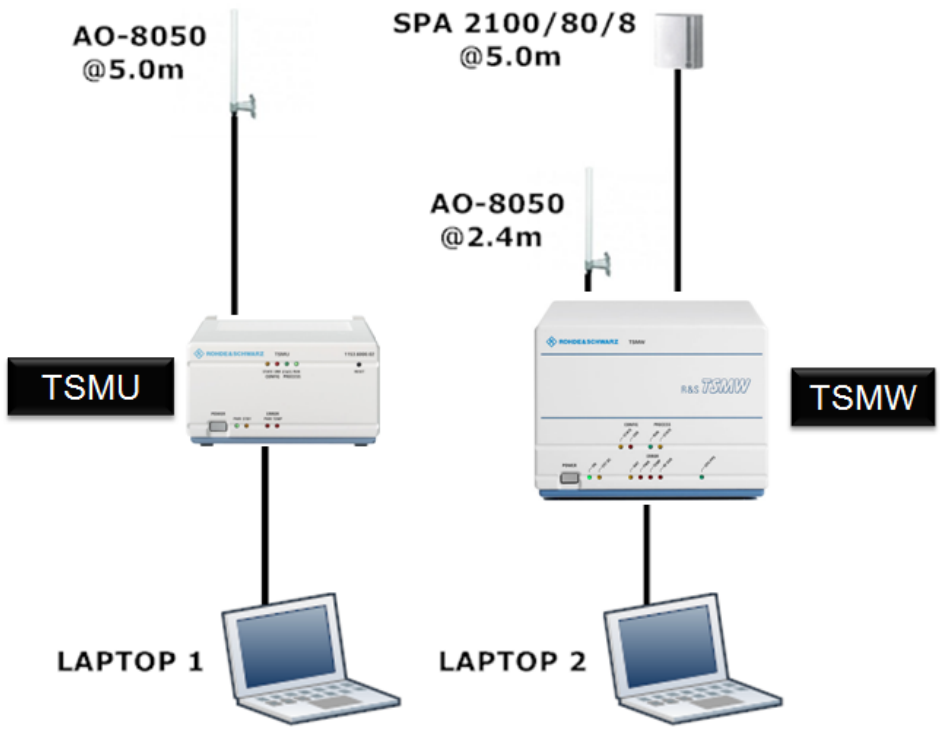

Figure B.6: Connectivity of the measurement system.

Figure B.7: CPK van used to mount the equipment.

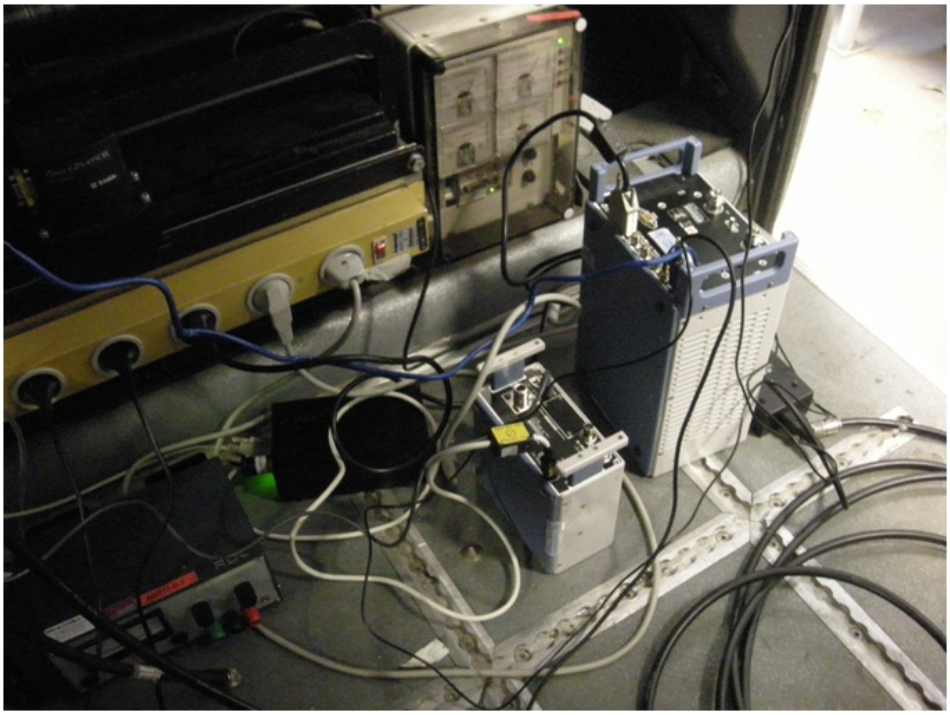

Figure B.8: Scanners mounted on the van and ready to measure.

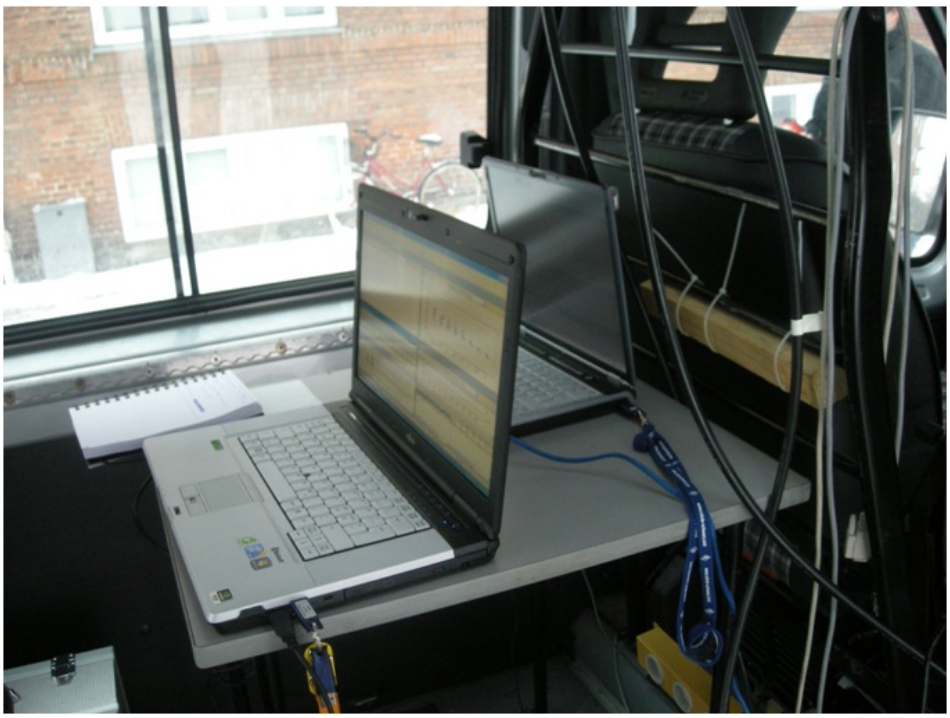

Figure B.9: Laptops mounted on the van and ready to measure.

B.3 Setup drawbacks

It is difficult to measure from two different scanners at the same time because the time stamp recorded in each laptop and the delay from driver load in each scanner is different.

It was necessary to create two different workspaces to operate the different inputs in TSMW, since it was not possible to measure both inputs in parallel at the same time.

Appendix C

MEASURED SIGNAL

C.1 Measuring LTE on UMTS

It was neccesary to run the measurement campaign in a real network to explore interference conditions in a real urban macro-cell scenario, which is the most probable scenario for the future relay nodes. There was no LTE network available in Aalborg, so a similar performance was obtained by measuring on the UMTS network.

UMTS works on the 2100 MHz band and LTE Europe will be deployed at 2600 MHz, which means that the frequency shift is not extremely large, so trends can be very similar. Results can be adapted from the measurements on UMTS to LTE with a small frequency scaling.

Of course UMTS does not fulfill the LTE peak data rates , but it is not important for this project, based more on signal propagation criteria (power and interference: signal quality) than on overall network performance.

C.2 UMTS basics

The Universal Mobile Telecommunication System (UMTS) allows multiple base stations to transmit on the same frequency at the same time while maintaining the possibility to separate the different transmissions on the receiver side (WCDMA). The user data is first modulated onto a binary code (key) and then transmitted. WCDMA applies a two-layered code structure consisting of a orthogonal spreading codes and pseudo-random scrambling codes. [21]

At the receiver, a correlation between the signal and the known code is performed (comparison of the received bits with the code). This method is highly effective even if some of the

received bits were destroyed by interferences. Physically, the RF energy spread over a wide bandwidth collected by the receiver is translated to narrow band by the correlation (descrambling process). [21]

C.3 UMTS WCDMA FDD parameters

In WCDMA FDD cellular systems, CPICH (Common Pilot Channel) is a downlink channel broadcast transmitted by the base stations with constant power and known bit sequence. Its power is usually between 5% and 15% of the total transmitted power.

This CPICH is divided into P-CPICH (Primary Common Pilot Channel) and S-CPICH (Secondary Common Pilot Channel). The P-CPICH is used by the UEs to complete the identification of the Primary Scrambling Code, while the S-CPICH can be used by other base stations. [22]

Once the scrambling code for a CPICH is known, the channel can be used for measurements of signal quality, usually with RSCP and E_c/I_o; or other as ISCP, SIR and RSSI.

A deeper explanation on RSCP, ISCP and SIR is given since these are the main measured parameters used in the project.

C.3.1 RSCP

The Received Signal Code Power (RSCP) is the received power on one code measured on the pilot bits of the primary CPICH. This means it is a parameter calculation after the descrambling proccess.

In the TMSU and TSMW scanners, RSCP is defined as the sum of the received powers of all peaks on one code, measured on the pilot bits of the P-CPICH.

C.3.2 ISCP

The Interference Signal Code Power (ISCP) is also measured on the P-CPICH after the correlation as RSCP. It makes reference to the interference on the received signal measured on the pilot bits.

In the TMSU and TSMW scanners, ISCP is taking into account both the orthogonal and the nonorthogonal parts of the interference.

C.3.3 SIR

The signal to interference ratio (SIR) can be defined basing on the two previous parameters (see Equation C.1). It is the linear ratio between RSCP and ISCP multiplied with a spreading factor (SF). When measuring on P-CPICH, SF=256.

$$SIR = \frac{RSCP}{ISCP} \cdot SF \tag{C.1}$$

C.4 TELENOR

Telenor's signal operates on UMTS2100, band I. The radio channel is 5 MHz wide. The frequency separation between transmission and reception is 190 MHz.

PARAMETER	DOWNLINK	UPLINK
$UARFCN$	10813	9863
f_c	2162.6 MHz	1972.6 MHz
f_l	2160.1 MHz	1970.1 MHz
f_h	2165.1 MHz	1975.1 MHz

Table C.1: Telenor UMTS signal parameters. UMTS2100 band I, FDD.

Appendix D

PROCESSING DETAILS

This appendix supports the different calculations specified in the main text (Chapter 4 and Chapter 5) with respect to data processing on routes, static spots and measured path loss.

Only one example of route processing and static spot processing is showed in this appendix.

It has been found relevant to include all the graphics resultants from the measured path loss calculations.

D.1 Routes processing

To calculate RSCPHG, ISCPHG and SIRHG the signals measured at different heights are aligned and compared sample by sample. Once RSCPHG, ISCPHG and SIRHG are calculated for each single sample, a simple average is calculated to summarize each route.

Figure D.1, Figure D.2 and Figure D.3 show similar signals (RSCP, ISCP and SIR) measured at 2.4 m and 5.0 m perfectly aligned and the final values of $RSCPHG = 2.15\,dB$, $ISCPHG = 4.01\,dB$ and $SIRHG = -1.93\,dB$ calculated.

A similar process was followed with all the different routes measured.

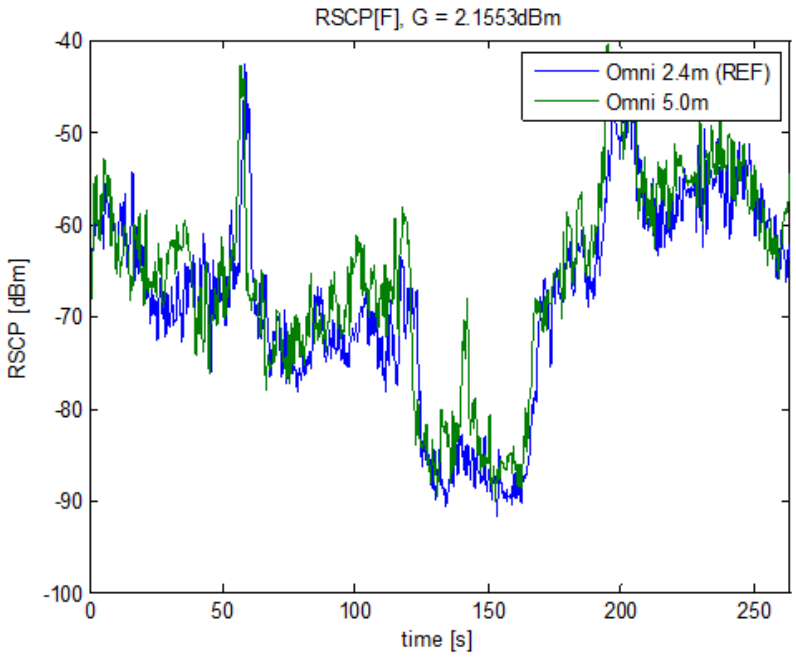

Figure D.1: Example of RSCPHG calculation for a route.

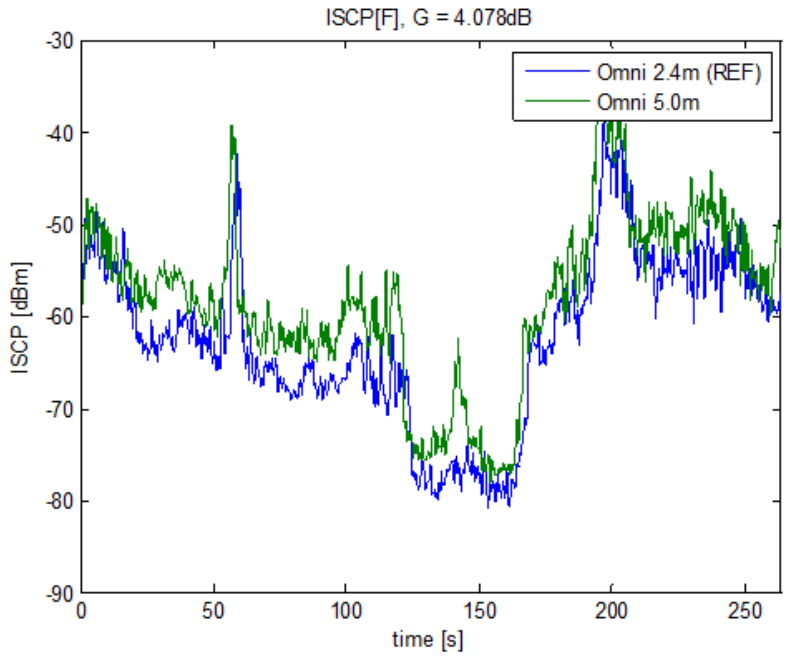

Figure D.2: Example of ISCPHG calculation for a route.

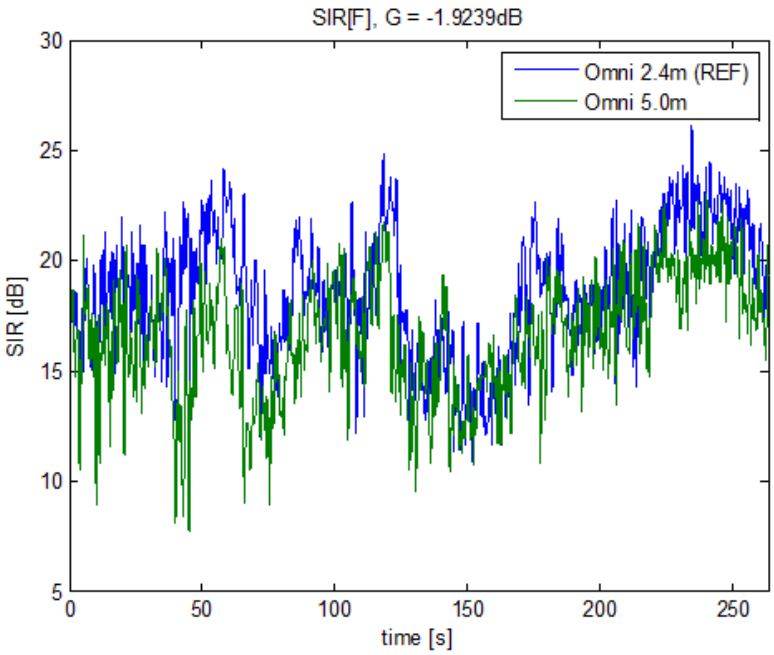

Figure D.3: Example of SIRHG calculation for a route.

D.2 Static spot processing

For the static spots no alignment is necessary for the different signals since the important fact here is average levels of RSCP, ISCP and SIR at the selected location.

Figure D.4 shows an example of RSCPTG, ISCPTG and SIRTG calculation for a static spot. The second row shows the average value calculated on the measured signals in the first row. $RSCPTG = 3.08\,dB$, $ISCPTG = 2.31\,dB$ and $SIRTG = 0.77\,dB$ is calculated by subtracting these two average values from the different antennas.

A similar process was followed with all the different static spots measured.

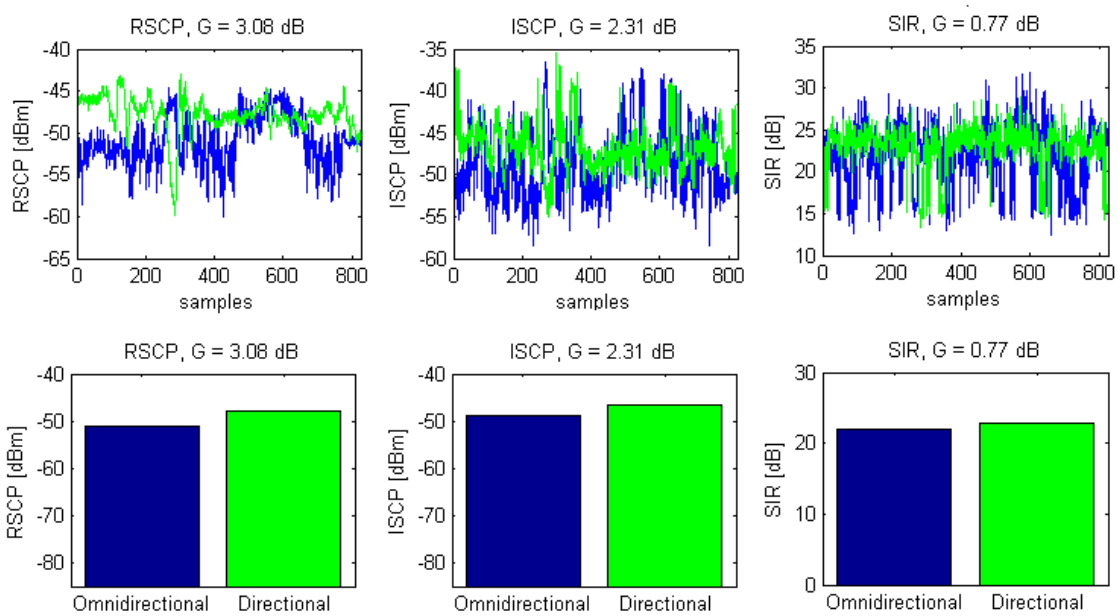

Figure D.4: Example of RSCPHG, ISCPHG and SIRHG for a static spot.

D.3 Measured path loss

Path loss is estimated from the different measurements classifying the data according to different receiver height (2.4 m and 5.0 m) and base station height (17 m, 19 m, 21 m, 23 m, 25 m, 27 m and 34 m).

This section includes all the different graphics obtained showing the measured path loss in function of distance to the base station. The linear regression calculated on the samples and the existing path loss models is also plotted.

It is necessary to notice the different slopes in the linear regression lines and the great variation in values obtained for similar distances. This facts are explained in the main text (Chapter 5).

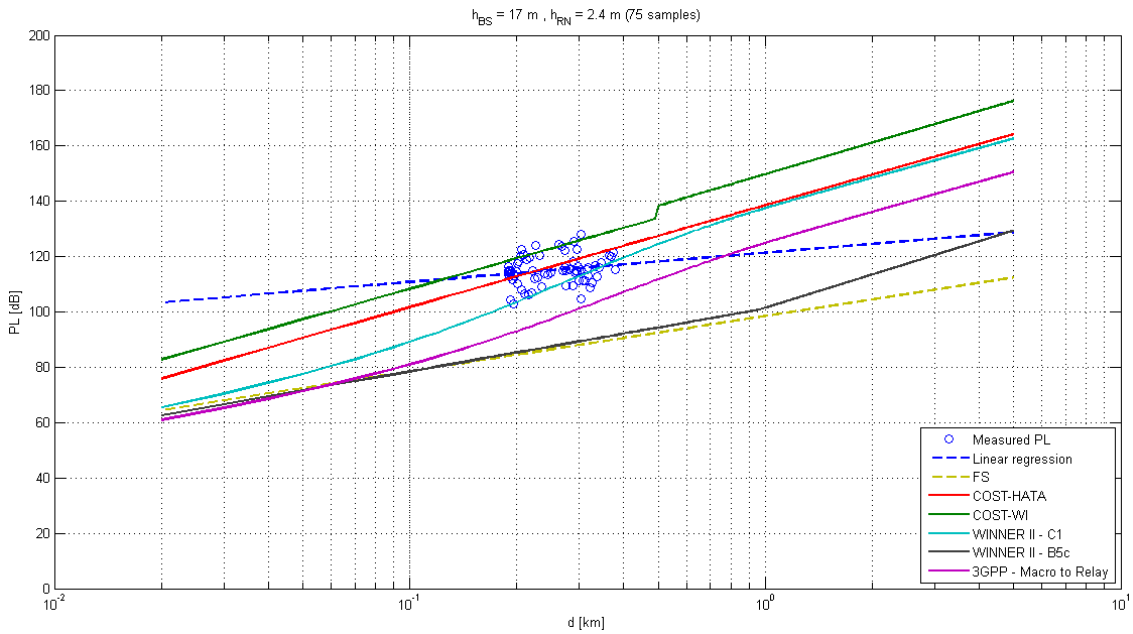

Figure D.5: Measured path loss at 2.4 m from a 17 m height base station.

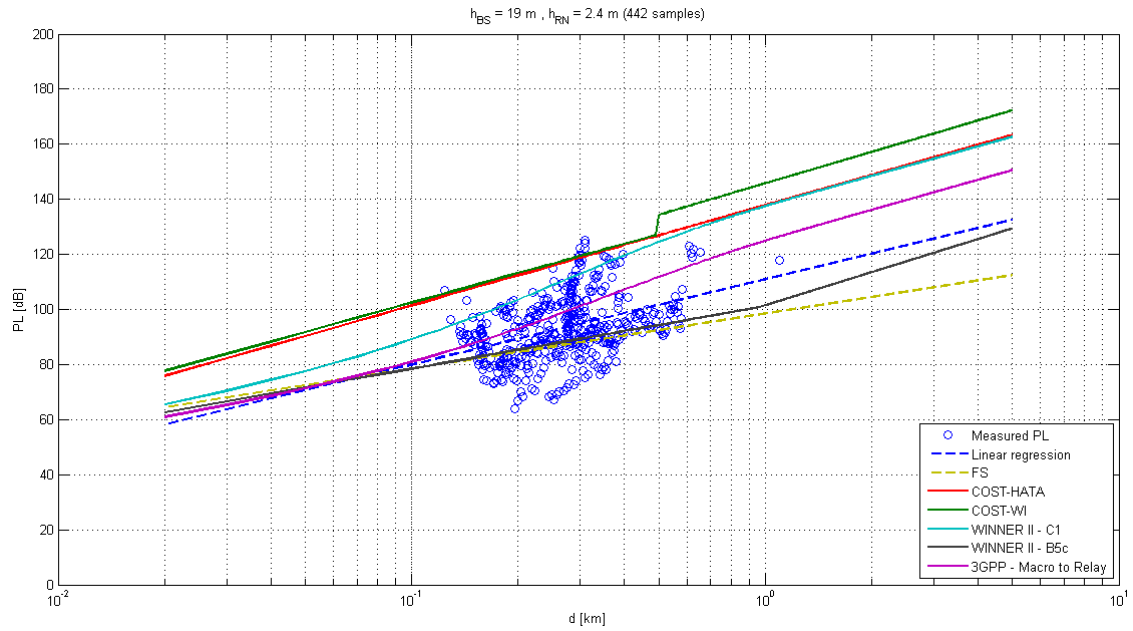

Figure D.6: Measured path loss at 2.4 m from a 19 m height base station.

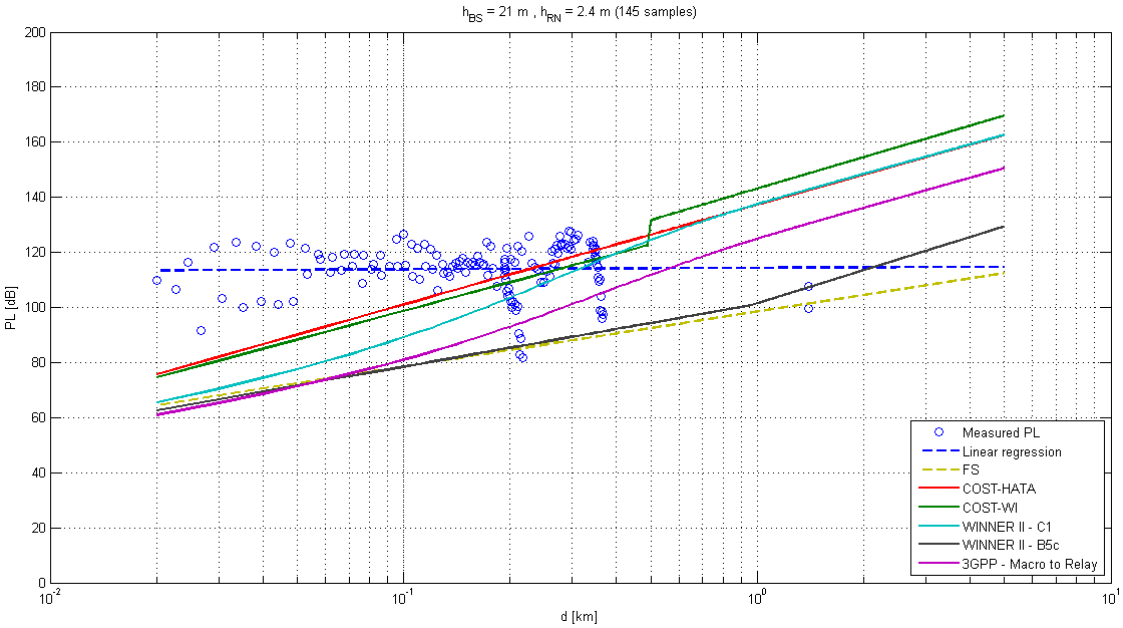

Figure D.7: Measured path loss at 2.4 m from a 21 m height base station.

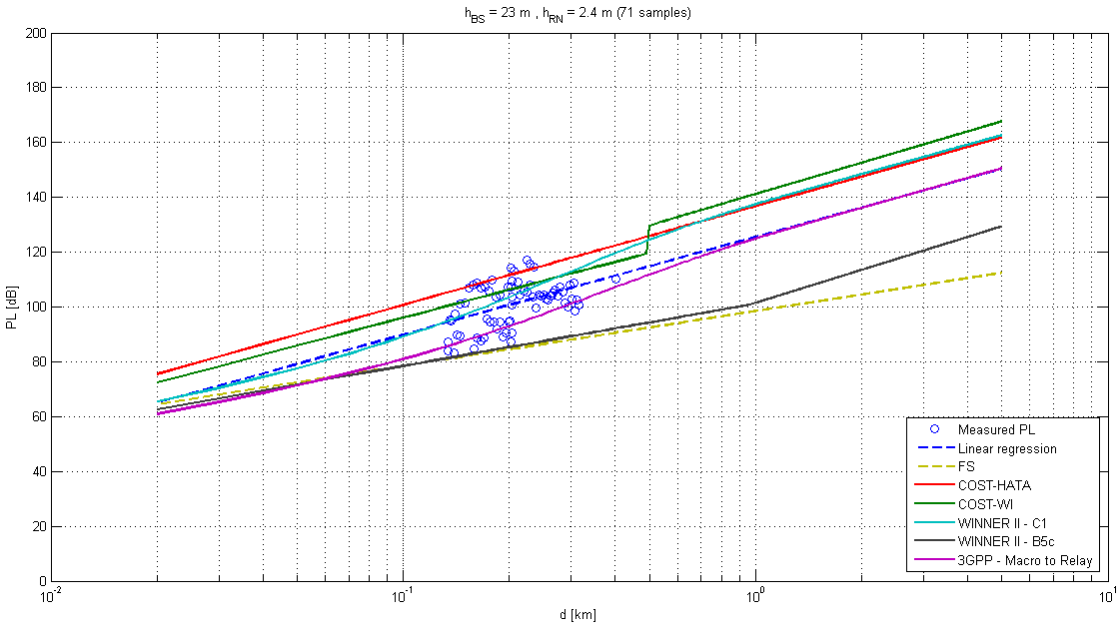

Figure D.8: Measured path loss at 2.4 m from a 23 m height base station.

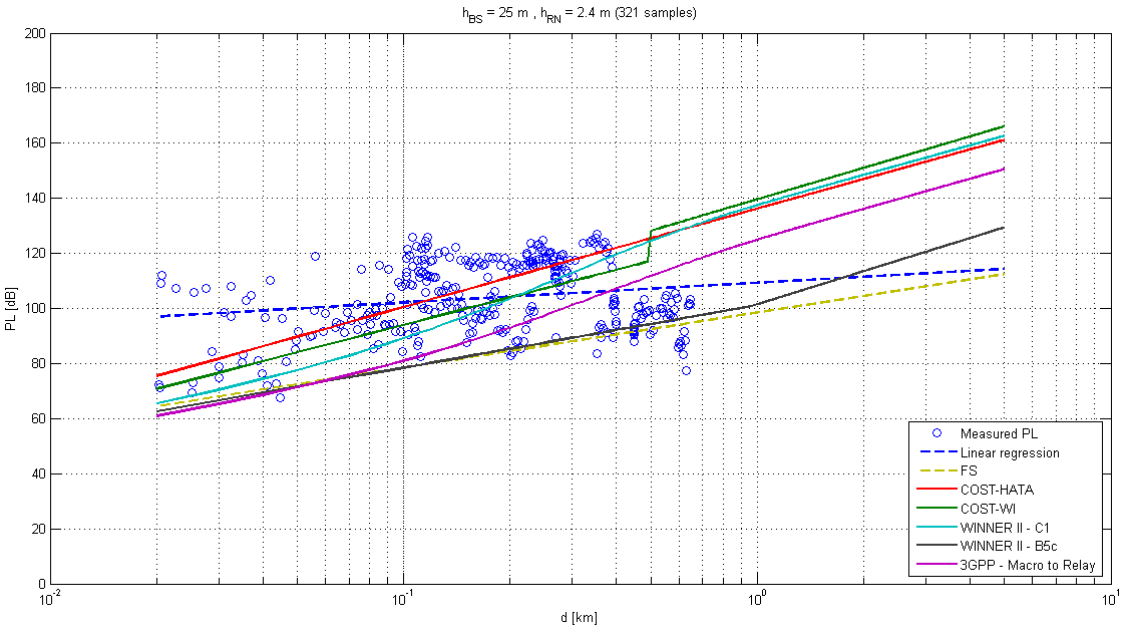

Figure D.9: Measured path loss at 2.4 m from a 25 m height base station.

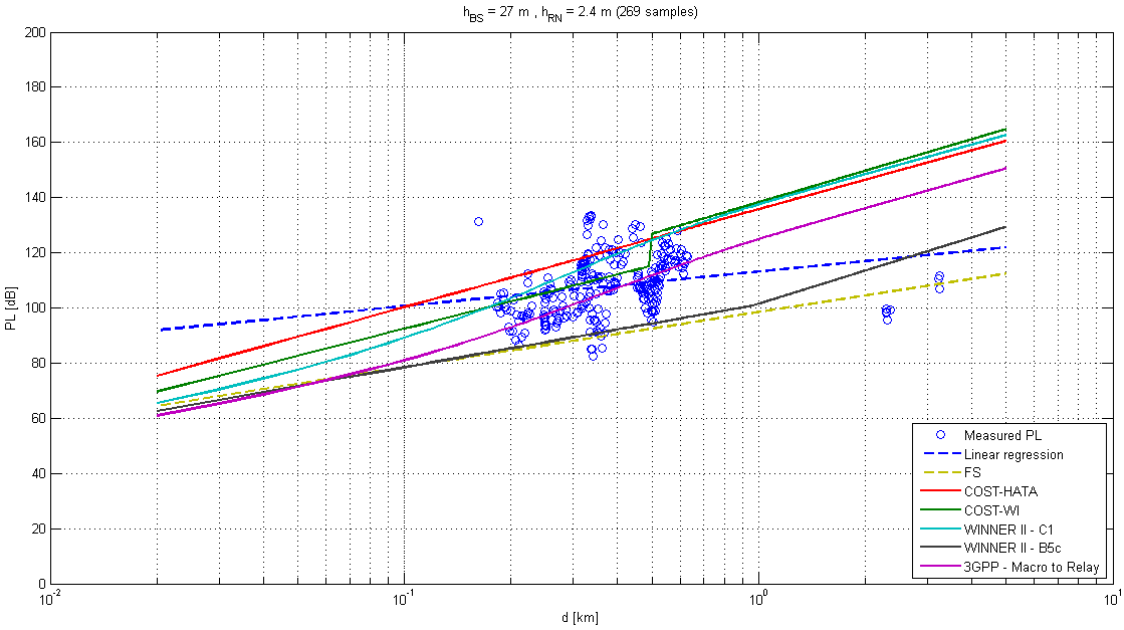

Figure D.10: Measured path loss at 2.4 m from a 27 m height base station.

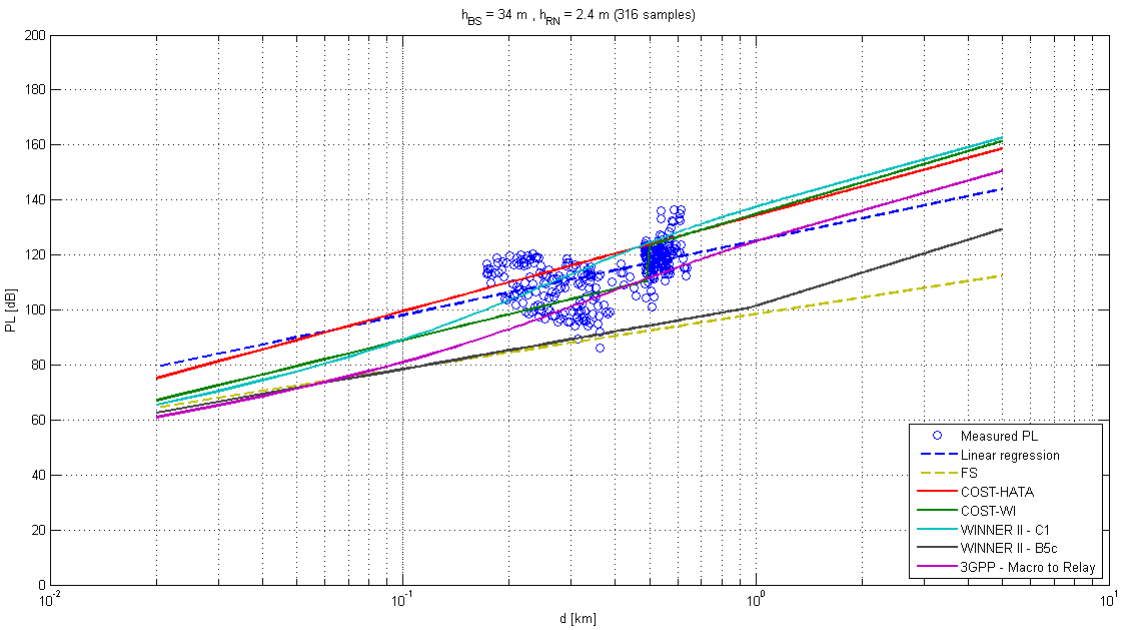

Figure D.11: Measured path loss at 2.4 m from a 34 m height base station.

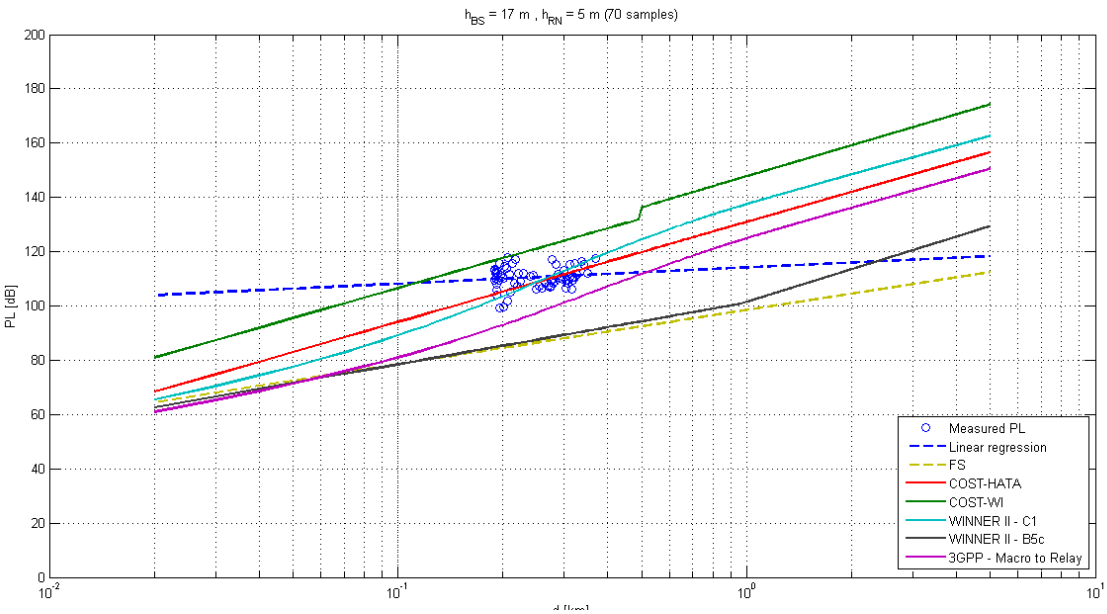

Figure D.12: Measured path loss at 5.0 m from a 17 m height base station.

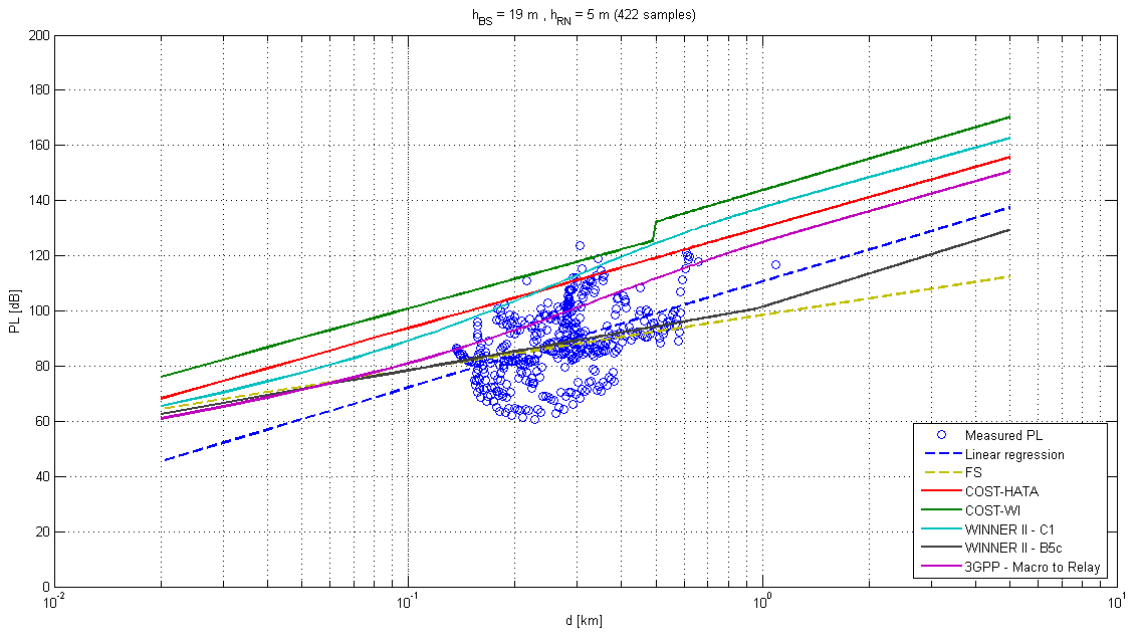

Figure D.13: Measured path loss at 5.0 m from a 19 m height base station.

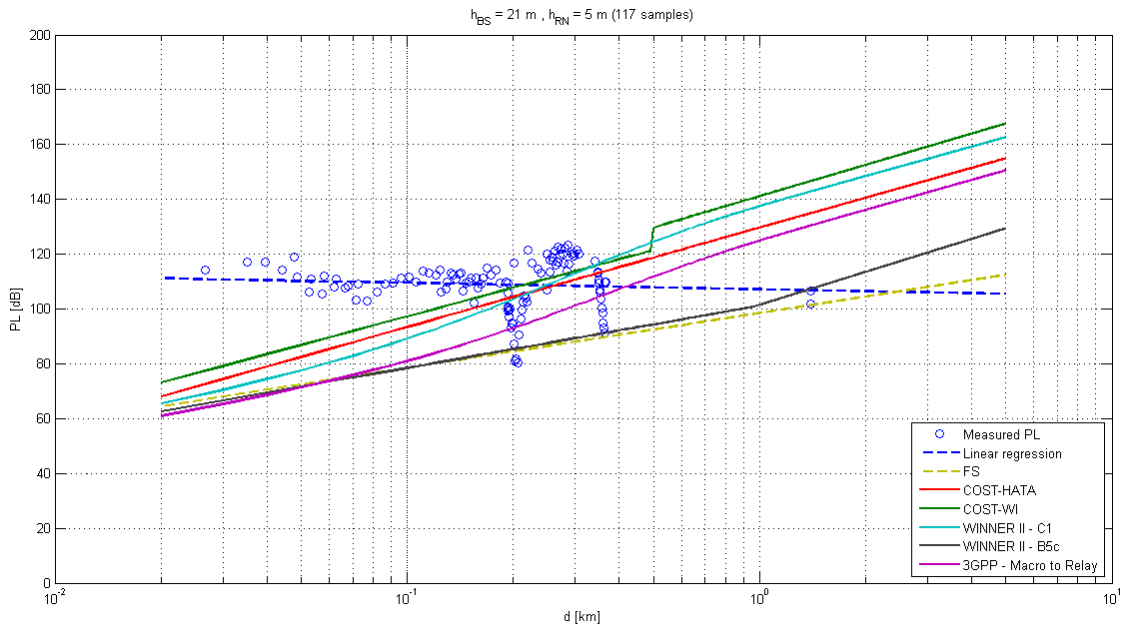

Figure D.14: Measured path loss at 5.0 m from a 21 m height base station.

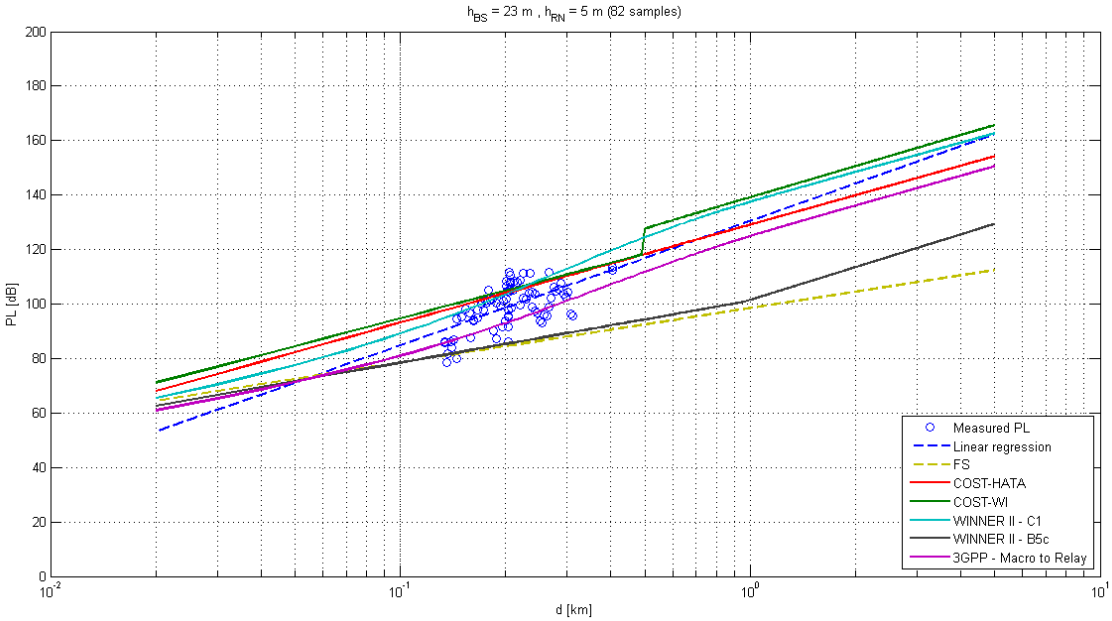

Figure D.15: Measured path loss at 5.0 m from a 23 m height base station.

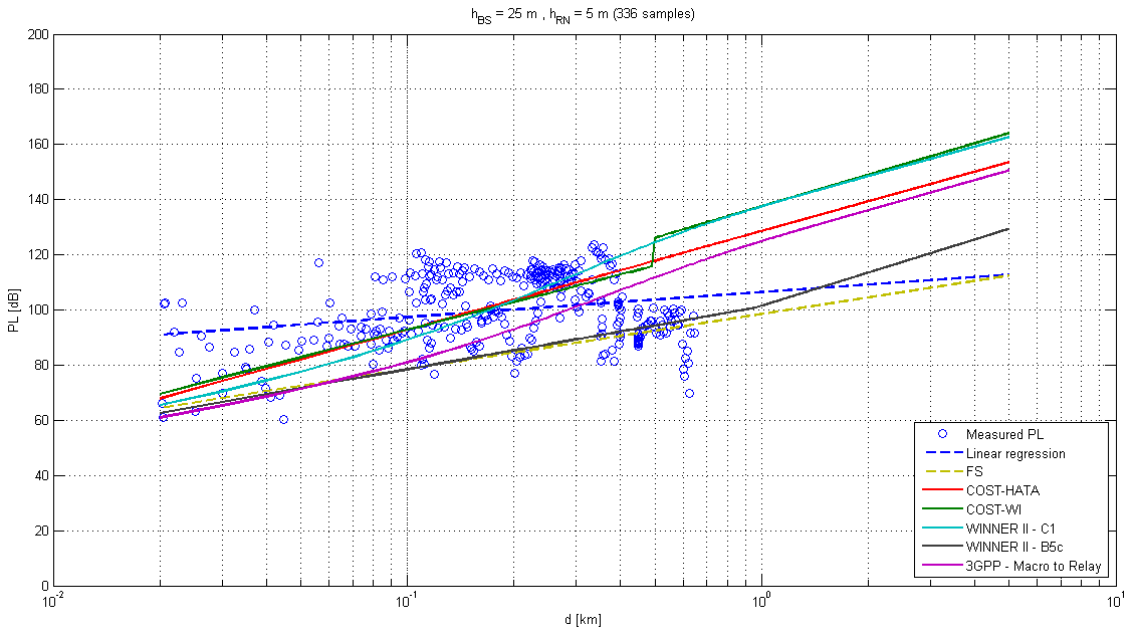

Figure D.16: Measured path loss at 5.0 m from a 25 m height base station.

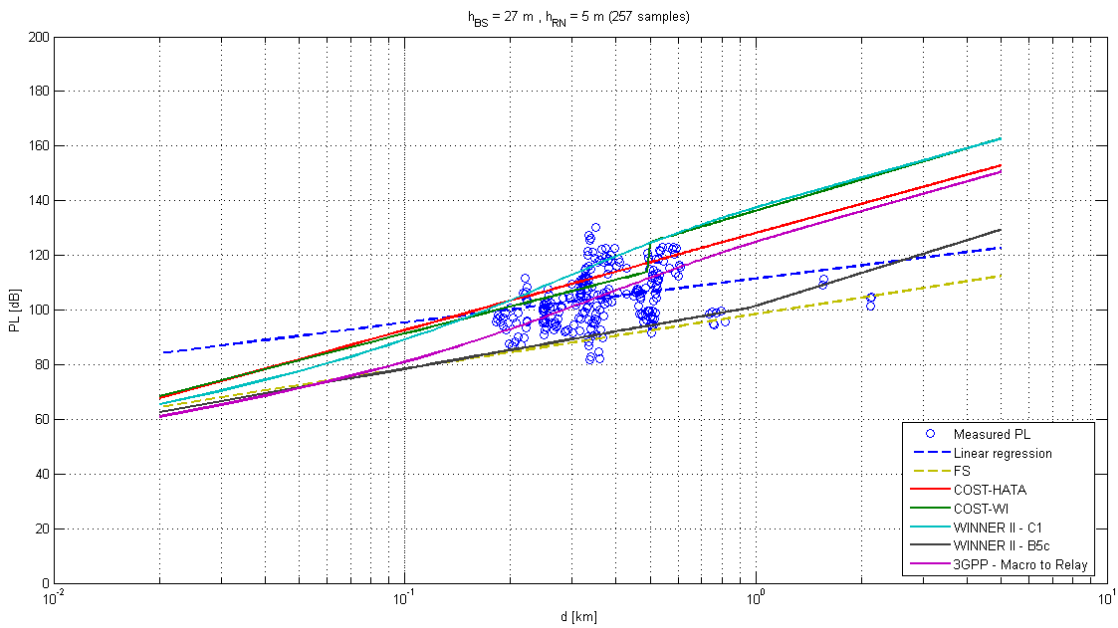

Figure D.17: Measured path loss at 5.0 m from a 27 m height base station.

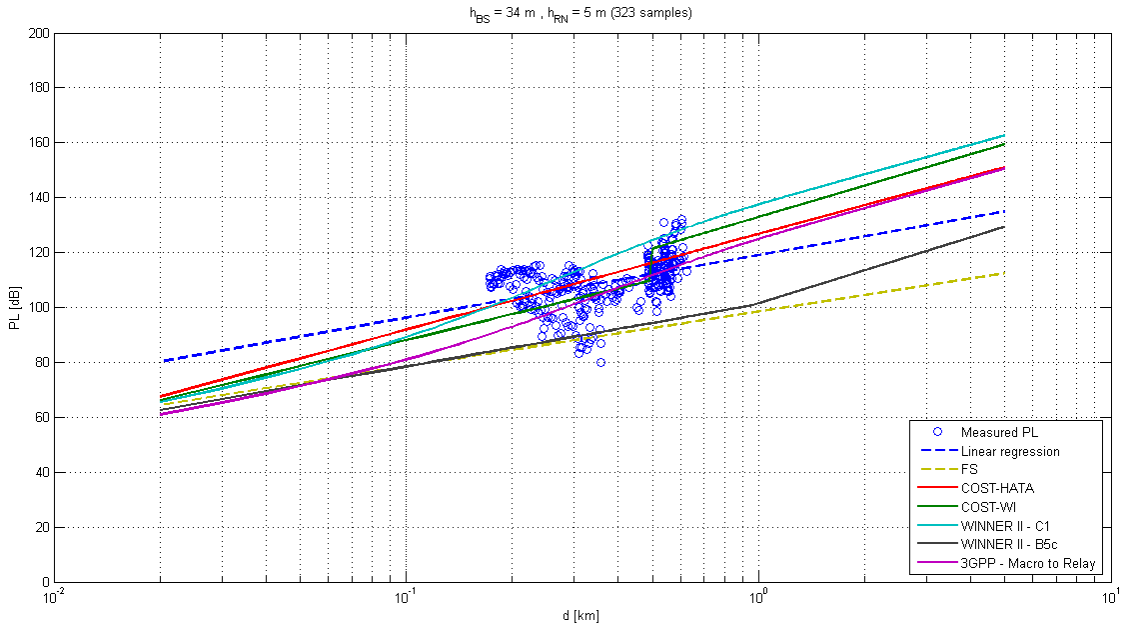

Figure D.18: Measured path loss at 5.0 m from a 34 m height base station.

Appendix E

VERTICAL GAIN CORRECTION

Since the measurements were done in an urban macro-cell scenario, when estimating the measured path loss is not realistic to suppose the gain at the base station antenna as its maximum value (only true in LOS conditions and base station antenna pointing straight into the receiver antenna).

In order to work with a base station gain value as correct as possible, it was assumed propagation over the rooftops until the street where the measurements were performed.

E.1 Vertical gain and down-tilt

It can be seen in Figure E.1 how antenna pattern becomes very important in these macro-cell situation. It is not realistic to suppose a constant gain value seen from every distance.

As explained in Chapter 5, horizontal gain is quite difficult to compute in urban macro-cell environments, but vertical gain can be approximated by assuming a constant average building height. Under this assumption, the gain value seen from a particular distance corresponds to the gain value seen from above a building at that distance.

Also the different down-tilt angles are very important, since not taking them into account can lead into an erratic path loss exponent at least within a limited distance interval when estimating it. [23]

For the measured path loss estimation performed in the main text and the previous appendix, the antenna patterns from the different base stations and the correspondent down-tilt angles were perfectly known.

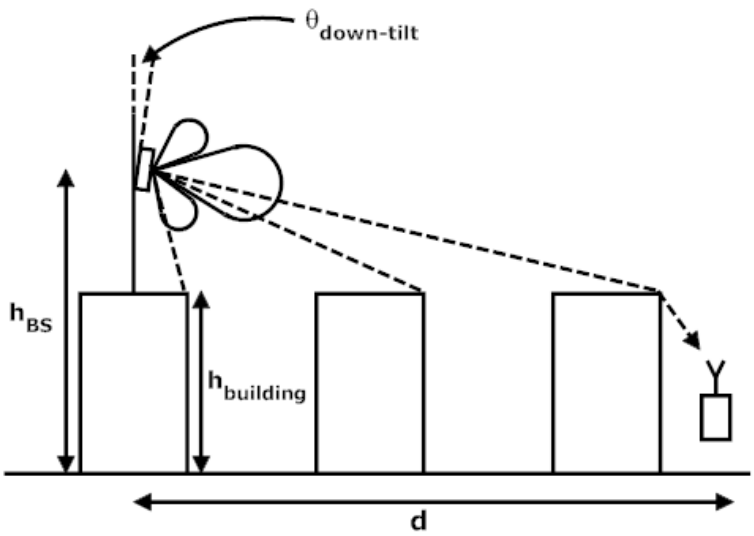

Figure E.1: Vertical gain correction.

E.2 Gain vs. distance

There is a huge difference from using a constant maximum gain or the corrected values as it can be seen in Figure E.2. This figure shows the corrected vertical gain seen at 15 m height (average building height) from a similar base station antenna but with two different down-tilt angles (0°and 6°) with respect to distance. In this case, without vertical correction a constant gain of 18 dBi would have been considered.

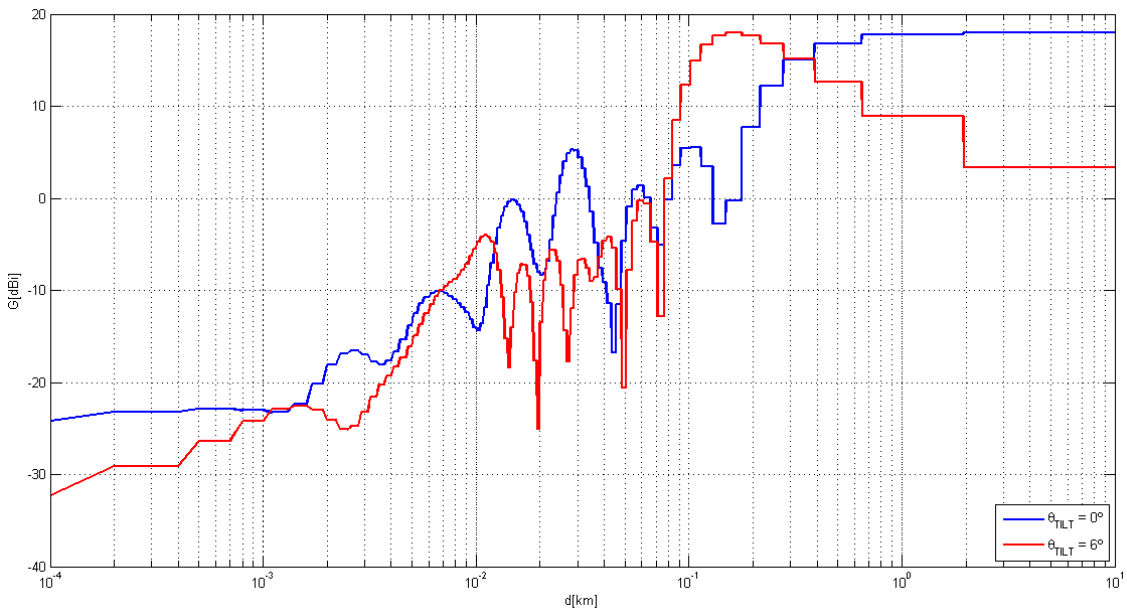

Figure E.2: Corrected vertical gain in terms of distance for two different down-tilts.